Some kinetic, equilibrium and structural studies of the reactions of 1,3,5-trinitrobenzene, 2,4,6-trinitrotoluene and 2,4,6-trinitrobenzyl chloride with nucleophiles

Brooke, David Nigel

SOME KINETIC, EQUILIBRIUM AND STRUCTURAL STUDIES OF THE REACTIONS OF 1,3,5-TRINITROBENZENE, 2,4,6-TRINITROTOLUENE AND 2,4,6-TRINITROBENZYL CHLORIDE WITH NUCLEOPHILES

by

David Nigel Brooke, B.Sc. (Durham)

(Hatfield College)

A thesis submitted for the degree of Doctor of Philosophy in the University of Durham, 1981

DECLARATION

The material in this thesis is the result of research carried out in the Department of Chemistry, University of Durham, between October 1978 and June 1981. It has not been submitted for any other degree, and is the author's own work, except where acknowledged by reference.

Some kinetic, equilibrium and structural studies of the reactions of 1,3,5-Trinitrobenzene, 2,4,6-Trinitrotoluene and 2,4,6-Trinitrobenzyl chloride with nucleophiles.

by David Nigel Brooke.

Sodium sulphite reacts with trinitrotoluene (TNT) and trinitrobenzyl chloride (TNBCl) in aqueous solution to form both mono- and di-adducts by addition at unsubstituted ring positions.

Stopped-flow measurements on the reactions of TNBCl with alkoxide ions in the corresponding alcohol reveal the presence of three processes, though only with ethoxide ion are all three observed clearly. Initial formation of an adduct by addition at C-3 is followed by addition at C-1 to give the more stable adduct. The slowest of the three processes corresponds to proton abstraction.

Kinetic measurements on the addition of methoxide ion to TNT in DMSO-methanol mixtures allow values for the kinetic and equilibrium parameters of this reaction in methanol to be obtained by extrapolation.

Studies on the reaction of sodium hypochlorite with TNT and trinitrobenzene suggest that hypochlorite ion addition to these compounds is unlikely.

TNT reacts with primary and secondary amines to give σ^{H}-complexes, probably by addition at C-3, and the trinitrobenzyl anion, the latter being the major product at equilibrium. With TNBCl, benzylamine, isopropylamine and n-butylamine give adducts by addition at C-1, which have similar stabilities to the anion formed by proton loss from the parent compound. With piperidine, addition

is thought to occur at C-3, and the major process is proton abstraction.

PUBLICATIONS

Some of the work reported in this thesis has been the subject of the following papers:

The Stabilities of Meisenheimer Complexes. Part 21. Sulphite Additions to 2,4,6-Trinitrobenzyl Chloride.
J. Chem. Soc., Perkin Trans. 2, 1980, 1850.
(With Dr. M.R. Crampton)

The Stabilities of Meisenheimer Complexes. Part 23. Rate and Equilibrium Data for the Reaction of 2,4,6-Trinitrotoluene with Sodium Methoxide.
J. Chem. Res., 1980, (s) 340, (m) 4401.
(With Dr. M.R. Crampton)

The Stabilities of Meisenheimer Complexes. Part 24. Some Reactions of 2,4,6-Trinitrotoluene and 2,4,6-Trinitrobenzyl chloride with Bases.
J. Chem. Soc. Perkin Trans. 2, 1981, 526.
(With Dr. M.R. Crampton, Dr. G.C. Corfield, Dr. P. Golding and Dr. G.F. Hayes)

The Stabilities of Meisenheimer Complexes. Part 29. The Reactions of 2,4,6-Trinitrotoluene and 2,4,6-Trinitrobenzyl chloride with Aliphatic Amines in Dimethyl Sulphoxide.
J. Chem. Soc. Perkin Trans. 2, (submitted)
(With Dr. M.R. Crampton)

ACKNOWLEDGEMENTS

I would like to thank my supervisor, Dr. M.R. Crampton, for his constant help and guidance during this work.

I would also like to thank the members of the department, academic, technical and student, who helped in any way.

Thanks are also due to the Science Research Council for the provision of a maintenance grant.

Finally, I would like to thank Helen Mc Andrew for typing this manuscript.

For my Family and Friends

CONTENTS

	Page
CHAPTER ONE : INTRODUCTION	1
1.1: The Reactions of Aromatic Nitrocompounds with Nucleophiles	2
1.2: General Aspects of Meisenheimer Complex Chemistry	4
1.2.1: Examples of Structures of σ-complexes	5
a: Complexes with oxygen bases	5
b: Complexes with nitrogen bases	7
c: Complexes with carbon bases	8
d: Complexes with sulphur bases	9
1.2.2: The Stabilities of Meisenheimer Complexes	9
a: structural effects	10
b: medium effects	12
1.3: The Reactions of 2,4,6-Trinitrotoluene with Nucleophiles	13
CHAPTER TWO : EXPERIMENTAL	26
2.1: Materials	27
2.1.1: Solvents	27
2.1.2: Substrates	27
2.1.3: Nucleophiles	28
2.1.4: Salts	29
2.2: Measurement Techniques	30
2.2.1: Rates	30
2.2.2: Equilibria	30
2.2.3: Visible spectra	31
2.2.4: Proton magnetic resonance spectra	31

Page

CHAPTER THREE : SULPHITE ADDITIONS TO 2,4,6-TRINITROTOLUENE AND 2,4,6-TRINITROBENZYL CHLORIDE IN WATER 32

3.1: Introduction 33

3.2: Experimental 34

3.3: Results and Discussion 36

3.3.1: 2,4,6-Trinitrobenzyl chloride 36

3.3.2: 2,4,6-Trinitrotoluene 39

3.3.3: Comparison with other compounds 50

CHAPTER FOUR : THE REACTIONS OF 2,4,6-TRINITROBENZYL CHLORIDE WITH ALKOXIDE IONS 54

4.1: Introduction 55

4.2: Experimental 56

4.3: Results and Discussion 59

4.3.1: General considerations 59

4.3.2: Methoxide ion in methanol 61

4.3.3: Ethoxide ion in ethanol 74

4.3.4: Isopropoxide ion in isopropanol 79

4.3.5: Comparison with other substrates 83

CHAPTER FIVE : THE INTERACTIONS OF 2,4,6-TRINITROTOLUENE WITH SODIUM METHOXIDE, AND THE REACTIONS OF 2,4,6-TRINITROTOLUENE AND 1,3,5-TRINITROBENZENE WITH SODIUM HYPOCHLORITE 87

5.1: Introduction 88

5.2: Experimental 90

5.3: Results and Discussion 91

5.3.1: 2,4,6-Trinitrotoluene and sodium methoxide 91

Page

5.3.2: 1,3,5-Trinitrobenzene and sodium hypochlorite in 50:50 (v/v) methanol:water 103

5.3.3: 2,4,6-Trinitrotoluene and sodium hypochlorite in methanol-water 105

CHAPTER SIX : THE REACTIONS OF 2,4,6-TRINITRO-TOLUENE AND 2,4,6-TRINITROBENZYL CHLORIDE WITH ALIPHATIC AMINES IN DIMEHTYL SULPHOXIDE 107

6.1: Introduction 108

6.2: Experimental 109

6.3: Results 110

6.3.1: Spectroscopic Studies 110

6.3.2: Kinetic and equilibrium data 122

a: General 122

b: Data for TNT 125

c: Data for TNBCl 134

6.4: Discussion 146

6.4.1: Proton Transfer 146

6.4.2: Complex Formation 150

CHAPTER SEVEN : THE REACTIONS OF 1,3,5-TRINITRO-BENZENE WITH SULPHITE, PHENOXIDE, CYANIDE AND DIETHYLMALONATE IONS 155

7.1: Introduction 156

7.2: Experimental 158

7.3: Results 159

7.3.1: Sodium sulphite 159

7.3.2: Sodium phenoxide 163

7.3.3: Potassium cyanide 166

Page

7.3.4: Diethylmalonate 174

APPENDICES 179

1: Derivation of Rate Expressions 180

2: List of Lectures, Seminars Etc. 185

REFERENCES 192

CHAPTER ONE

INTRODUCTION

1.1. The Reactions of Aromatic Nitrocompounds with Nucleophiles.

Aromatic systems are in general unreactive towards nucleophiles. However, there are certain circumstances under which this statement does not hold. One such case is in the reaction of certain aromatic compounds, usually aryl halides, with a strong base such as potassium amide in liquid ammonia. The mechanism of these reactions involves the formation of a benzyne intermediate, in this instance by loss of the halide ion and an adjacent proton from the ring.

More commonly, reaction will occur when the ring system contains suitably placed electron-withdrawing groups which activate the ring towards nucleophiles - the most common such group being the nitro group. For nucleophilic substitution to occur, the ring must also contain a good leaving group. The reaction proceeds by covalent bond formation between the nucleophile and the carbon carrying the leaving group X, to give an intermediate complex, followed by loss of X to give the substitution product. If, however, the aromatic compound does not contain a suitable leaving group, the reaction may stop at the intermediate complex, which is generally known as a σ - or Meisenheimer complex. The existence of stable complexes of the type (1.1) has been taken as evidence for the

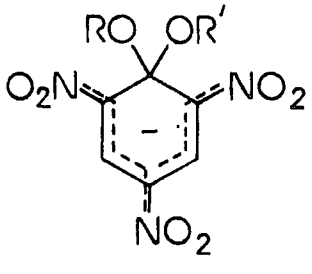

1.1

addition-elimination mechanism in this type of reaction, and such complexes have been used as models for the intermediate. Recent work with flow NMR systems has allowed the identification of such intermediates in nucleophilic substitution reactions.

Other modes of interaction between nucleophiles and activated aromatic compounds are possible. Partial electron transfer from the nucleophile to the ring results in the formation of a charge-transfer complex, whilst complete electron transfer gives a radical ion. Proton abstraction may also occur, possibly from the ring but more probably from a side chain.

1.2. General Aspects of Meisenheimer Complex Chemistry.

The addition of base to solutions containing electron-deficient aromatic compounds produces brightly-coloured solutions, a fact which has been of interest to chemists for some considerable time[1]. Various suggestions were made as to the nature of these coloured species: ionisation of the ring protons[2], addition of base at a carbon carrying a nitro group[3], and addition of base at a carbon carrying a different substituent[4], e.g.(1.2).

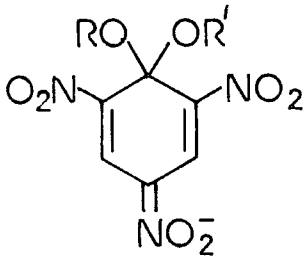

1.2

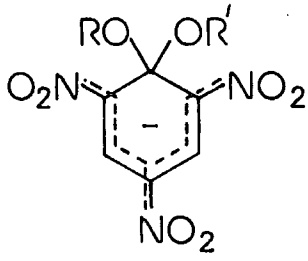

1.3

Meisenheimer[5] produced strong chemical evidence for this quinoidal structure when he showed that reacting methoxide ion with 2,4,6-trinitrophenetole gave the same product as reacting ethoxide ion with 2,4,6-trinitroanisole. Confirmation of this structure came with the application of proton magnetic resonance to the study of this area[6]. Generally, the complexes are represented by the structure (1.3), with the negative charge delocalised around the ring and the electron-withdrawing substituents, although M.O. calculations [7] and ^{13}C NMR studies[8,9] suggest that the para nitro group carries more of the negative charge than the ortho substituents.

Various techniques have been used in the study of Meisenheimer complexes, the most useful in structural determination being proton magnetic resonance spectroscopy

(pmr). First used in the study of Meisenheimer complexes in 1964[6], its applicability has been extended to short-lived species by its incorporation into flow and stopped-flow systems[10].

A number of complexes have been isolated as crystals, and studied by X-ray crystallography. These studies show that in the dialkoxy complexes[11], the ortho nitro groups are coplanar with the ring, while the two alkoxy groups are in a plane perpendicular to it. The carbon-nitrogen bond length for the para nitro group is shorter than for the ortho groups, again indicating the greater negative charge carried by this group.

Meisenheimer complexes show intense absorption bands in the UV/visible region, with extinction coefficients for 1:1 complexes typically in the region of 2×10^4 l mol.$^{-1}$cm^{-1}. The use of these spectra in structural determination is limited by their general similarity. However, their intensity allows kinetic and equilibrium work to be carried out in dilute solutions. Kinetic measurements can be made at a suitable wavelength using conventional spectrophotometry for fairly slow reactions, and stopped-flow or temperature-jump spectrophotometry (or a combination of the two) for faster processes. Equilibrium data can be obtained from measurements of the optical density after reaction using different base concentrations, again at a suitable wavelength. This is usually done using the Benesi-Hildebrand method[12], or a modification of it.

1.2.1. Examples of Structures of σ-Complexes.

a. Complexes with oxygen bases:

The addition of sodium methoxide to a methanolic

solution of 1,3,5-trinitrobenzene (TNB) produces (1.4,R=Me), which has been characterised by NMR[6]. At higher methoxide concentrations, a diadduct (1.5,R=Me) is formed[13]. A similar 1:1 adduct (1.4,R=Et) is formed with ethoxide ion in ethanol[13].

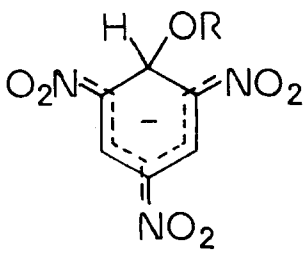

1.4

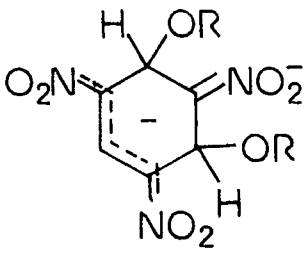

1.5

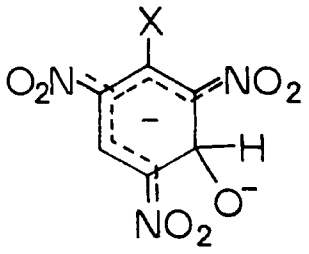

1.6

Hydroxide ion reacts with TNB and other nitroaromatics in a similar way to alkoxide ions, although substitution products form at a somewhat greater rate. The 1:1 adduct from TNB (1.4,R=H) has been isolated[14] from DMSO solutions, and the 1:2 adduct observed[15](1.5,R=H). With some 1-X-2,4,6-trinitrobenzenes, the second interaction with hydroxide ion involves ionisation of the added hydroxyl group[16].(1.6)

With 2,4,6-trinitroanisole (TNA)there are two possible sites for addition. In the case of methoxide ion, the reaction involves initial addition at C-3 to give (1.7), followed by isomerisation to the thermodynamically preffered C-1 adduct[17](1.8). The diadduct (1.9) is formed in concentrated solutions by addition at both positions[18].

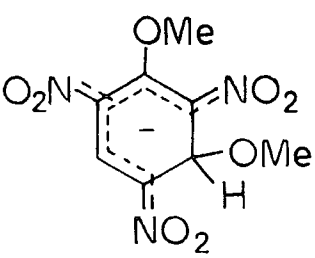

1.7

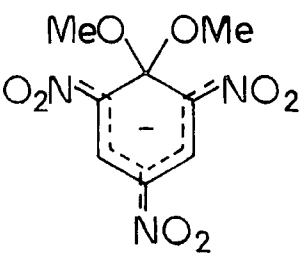

1.8

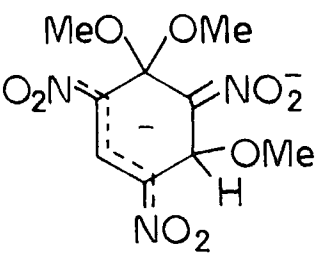

1.9

Ethoxide[19], n-propoxide[20] and isopropoxide[21] show a similar pattern to methoxide in their reactions with the corresponding 1-alkoxy-2,4,6-trinitrobenzene - the adduct at C-3 is formed more rapidly, but that at C-1 is the more stable.

b. Complexes with nitrogen bases:

In solvents such as DMSO, NMR and conductance measurements have shown that TNB forms negatively charged adducts of type (1.10) with ammonia and with primary and secondary amines[22,23]. The mechanism involves addition of the amine to give the zwitterion (1.11), followed by proton loss[23].

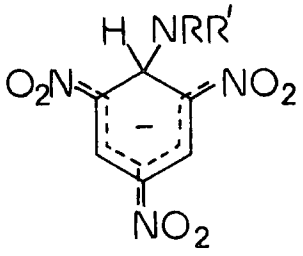

1.10

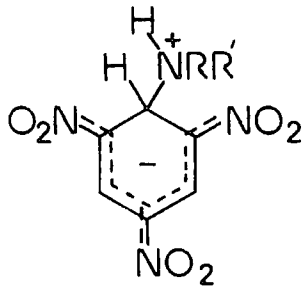

1.11

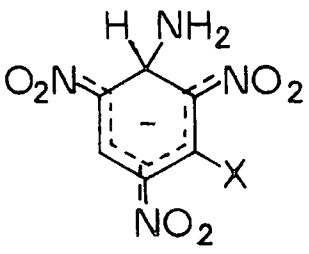

1.12

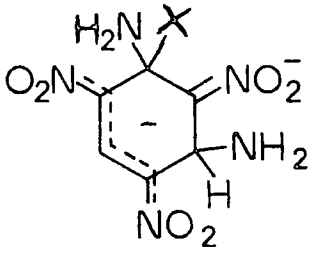

1.13

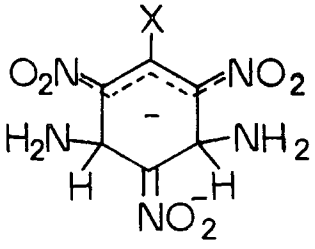

1.14

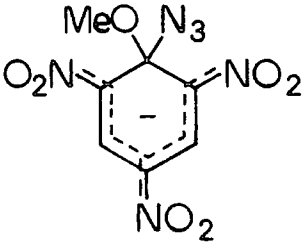

1.15

Kinetic studies[24] with secondary amines have indicated the existence of hydrogen bonding to the ortho nitro group in the zwitterion.

The reactions of a number of 1-X-2,4,6-trinitrobenzenes with potassium amide have been studied in liquid ammonia.[25] The amide ion attacks preferentially at an unsubstituted position to give (1.12). The structure of the diadduct depends on the nature of the X, when X is alkyl, structures of type (1.13) are reported, whilst when X is an amine or

alkoxy group, the structure is (1.14).

Azide ions react with TNA at low temperatures to give[26] (1.15).

c. Complexes with carbon bases:

Ketones with active hydrogens readily form carbanions with bases, and as such can form complexes with nitroaromatics. Thus if the TNB-methoxide adduct is formed in acetone solution, with time the methoxide ion is displaced by the acetonate ion to give [13] (1.16). The reaction of di- and tri-nitro aromatic compounds with acetonate ion is known as the Janovsky reaction[27].

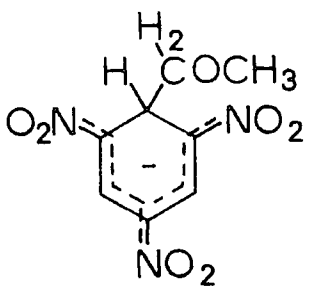

1.16

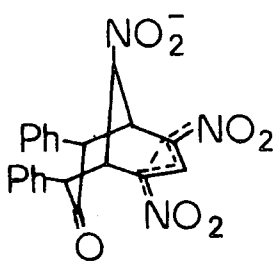

1.17

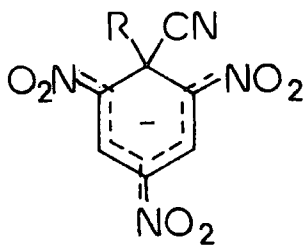

1.18

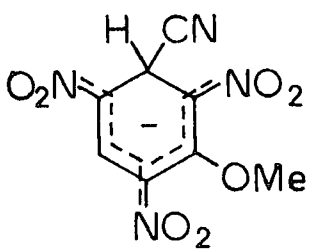

1.19

Where the ketone has two active methylene groups, a 'meta-bridging' reaction can occur, leading to a cyclic product such as [28] (1.17).

Cyanide ions will react with TNB to give a 1:1 adduct[29] (1.18, R=H). Complexes with cyanide ion have also been reported with 2,4,6-trinitrobenzaldehyde (1.18, R=CHO)[29] and TNA (1.18, R=OMe)[29], which also forms an adduct at C-3 (1.19)[30]

Alkyl complexes of TNB have been prepared using

tetra alkyl boron salts[31].

d. Complexes with sulphur bases:

Sulphite ions will readily form 1:1 and 1:2 complexes with TNB and 1-X-2,4,6-trinitrobenzenes[32]. With the exception of those from trinitrobenzaldehyde, where addition occurs at C-1 (1.20,1.21)[33], these adducts are formed by addition at unsubstituted ring positions (1.22,1.23). Kinetic[34] and NMR[35,36] evidence has been found for cis-trans isomerism in the 1:2 adduct with TNB (1.23,X=H).

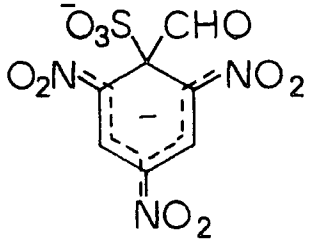

1.20

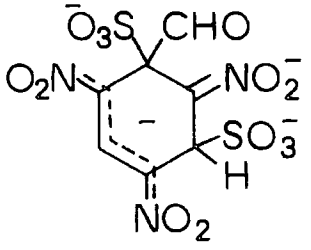

1.21

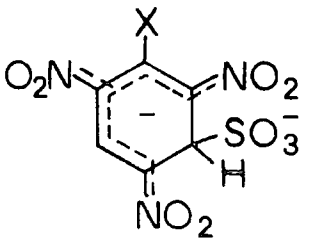

1.22

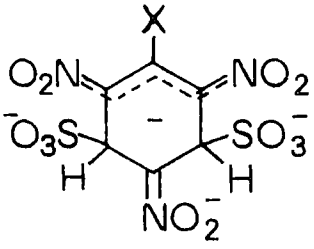

1.23

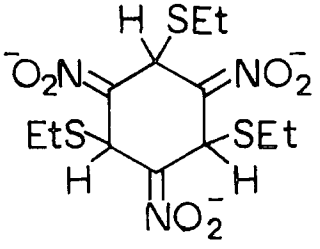

1.24

Thioalkoxide ions react with TNB to give 1:1 and 1:2 complexes analogous in structure to those formed with alkoxide ions[37]. In addition, evidence has been found[38] for the 1:3 adduct (1.24) in mixed solvents with a high water content.

1.2.2. The Stabilities of Meisenheimer Complexes.

The various factors affecting complex stability are closely related, though here for convenience they will be

briefly discussed under two headings - the structure of the reactants, and medium effects.

a. Structural effects:

The major influence on the stabilities of Meisenheimer complexes is the presence of a number of electron-withdrawing groups ortho and/or para to the site of attack, which both activate the ring towards nucleophilic attack and stabilise the adduct thus formed[39]. The most commonly met group is the nitro group, though compounds containing other groups have been studied. The greater the number of groups, the more reactive is the compound towards nucleophiles, though their effects are not additive[39]. The group para to the site of attack is the most important - nucleophiles will generally attack para to a nitro group rather than to less electron-withdrawing substituents.[40,41] This is in accord with the observation that the para substituent carries more charge than those ortho to the site of attack[7,8,9]. This is mainly an electronic effect, as steric effects due to the ortho groups should only be important when the substituent and/or the nucleophile is large[42].

When the substrate is not symmetrically substituted, there are a number of different sites for addition. The para effect mentioned above will be important here - however, other factors may come into play. In the case of methoxide addition to TNA[17,43], addition at an unsubstituted carbon occurs much more rapidly than attack at C-1, but the adduct produced by the latter process is more thermodynamically stable, although both sites are para to nitro groups. The difference is probably best explained by steric effects, which should be negligible in attack at

unsubstituted carbon[43]. Another factor could be ground state stabilisation of the anisole, which is lost on formation of the C-1 adduct, but retained when addition occurs at C-3 [44].

Steric factors may also play a part in the greater stability of the C-1 adduct. Any steric strain between the methoxy group and the adjacent nitro groups in the parent compounds will be released on complex formation, when the substituents are rotated out of the plane of the ring[11]. Another factor will be the stabilisation of the sp^3 hybridised carbon by multiple alkoxy substitution[45].

The stabilities of the complexes of a given substrate will depend on the nature of the attacking nucleophile. In some cases such as that outlined above, special factors are responsible. However, in general, the stability will depend on the carbon basicity of the nucleophile, as distinct from the Bronsted or proton basicity. A scale of the carbon basicities of a range of nucleophiles can be obtained from the equilibrium constants for complex formation with a given substrate in a particular solvent[43]. From such a scale, the order of the carbon basicities of methoxide and thioethoxide is the reverse of their proton basicities[37].

When the ring has more than one type of site, the position of attack may be governed by the nature of the nucleophile. Thus, the stable adducts of TNA with azide ion and diethylamine involve addition at C-1, whilst those with sulphite and acetonate ions are adducts at C-3. This presumably reflects the greater steric requirements of these groups[43].

b. Medium effects:

Most studies on Meisenheimer complexes have been done either in protic solvents, such as water and alcohols, or in dipolar aprotic solvents, such as DMSO. The main difference between these two types of solvent lies in their ability to solvate ions. Small, polar ions such as hydroxide and methoxide are well solvated in protic solvents, but less well so in DMSO. Large, polarisable ions such as σ-complexes are, on the other hand, well solvated by the dipolar solvents and less well so by the polar ones. Thus DMSO would be expected to favour complex formation, and this is in fact what is found for 1:1 adducts.

The greater reactivity of small nucleophiles in aprotic solvents, due to their poor solvation, should lead to the formation of diadducts. However, such species are much more stable in protic solvents: it has been suggested that this is due to their greater resemblance to inorganic salts, which increases their solvation in such solvents[43].

The ionic strength of the solution can affect the stabilities of species by solvation effects similar to those above. In addition, specific ion-pairing effects have been observed between cations and both nucleophiles[21] and complexes[45].

The effects of micelles on the formation of σ-complexes have been investigated[45], anionic micelles reducing stability, neutral micelles having little effect and cationic micelles increasing stability.

1.3. The Reactions of 2,4,6-Trinitrotoluene with Nucleophiles.

A number of possible routes exist for the interaction of 2,4,6-Trinitrotoluene (TNT) with nucleophiles, depending on the nature of the nucleophile, and to some extent on the composition of the solvent. A weak interaction may give rise to charge-transfer complexes, whereas a stronger interaction may lead to the formation of a σ-complex, by addition at C-1 or C-3. Alternatively, the nucleophile may abstract a proton from the methyl group to give the trinitrobenzyl anion. There also exists the possibility of electron transfer to give radical ions.

All of the above interactions have been postulated to explain the colours formed when TNT reacts with alkoxide ions. In 1899, Hantzsch and Kissel[3] reported the preparation of a purple solid from the reaction of TNT with potassium methoxide, which from their analysis they formulated as a monohydrated addition complex. A solid addition product was also reported from the reaction of TNT with sodium n-butoxide[47].

In 1955 Caldin and Long[48] suggested that the purple coloration produced in the reaction of TNT with ethoxide ions was due to the trinitrobenzyl anion (1.25)

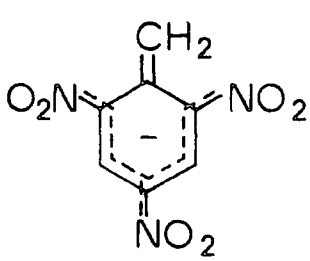

1.25

Further evidence for this assignment came from the observation [49]of a large primary isotope effect when

TNT-d_3 (deuteriated methyl group) was used in place of TNT : with 0·01 M base, the observed rate constant for the reaction with TNT was 1·35 s^{-1}, whilst that with TNT-d_3 was 0·195 s^{-1}. The anion has a three peak UV/visible spectrum, with λ_{max} 371nm (8300), 514nm (13,500), and a shoulder at 620nm (7500).

At higher base concentrations (0·1 M ethoxide) and with 10^{-3} M TNT the rapid formation of a transient brown colour was observed, which was initially attributed to a charge-transfer complex[48]. However, in a later study[50] this initial process was ascribed to the formation of a σ-complex, probably coupled to a radical forming reaction (scheme 1.1).

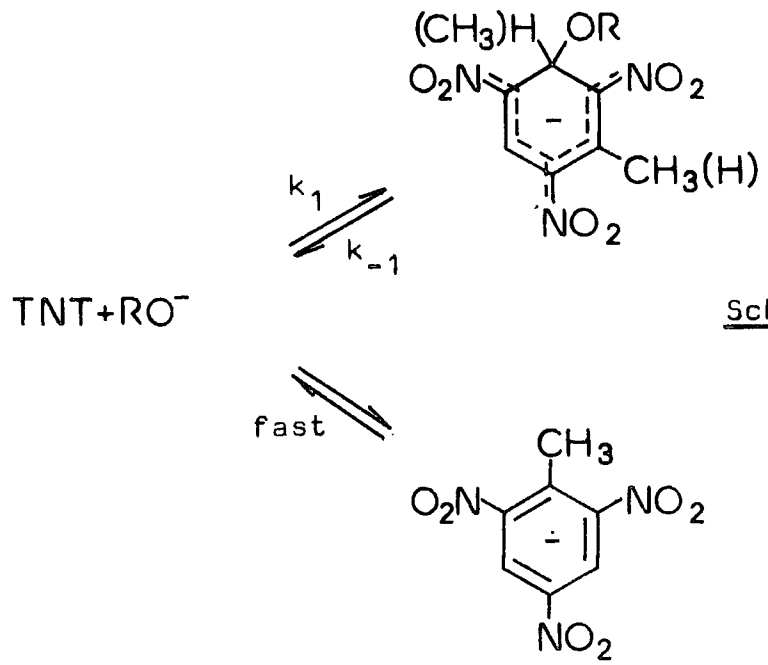

Scheme 1.1

The possibility of a radical-forming process was raised because NMR spectra of this system were wiped out, a problem commonly due to radicals[18]. Bernasconi[50] obtained kinetic and equilibrium data for this reaction, and for the formation of the anion (1.25), both sets being obtained with base in excess over parent. When TNT was in excess

over the base he observed a third process of intermediate rate, which he ascribed to Janovsky complex formation, i.e. addition of the trinitrobenzyl anion to a neutral TNT molecule. This process predominates under these conditions. The rate and equilibrium data for these reactions are in table 1.1.

Table 1.1 Kinetic and equilibrium data for TNT and ethoxide in ethanol (ref. 50)

Process	k_f/l mole^{-1}s^{-1}	k_r/s^{-1}	K/l mole^{-1}
σ-complex	1500-3000	80-200	37·5-7·5
anion	82	$4·5\times10^{-2}$	1820
Janovsky	700	34·5	20·3

The position of addition in each of the two complexes was not determined, due to the failure to obtain NMR spectra of the species.

A similar series of reactions was observed by Bernasconi[50] with methoxide ion in methanol. Here the intensity of the first process was too low to allow measurements to be made, and the reaction was not in fact assigned to σ-complex formation. The relevant data are in table 1.2. NMR spectra were also wiped clear here.

Table 1.2. Kinetic and equilibrium data for TNT and methoxide in methanol (ref. 50)

Process	k_f/l mole^{-1}s^{-1}	k_r/s^{-1}	K/l mole^{-1}
anion	13·3	1·07	12·4
Janovsky	442	24	18·9

In 50% dioxan, 50% water the pattern was again the

same: initial formation of a σ-adduct followed by ionisation of TNT, when the hydroxide concentration was in excess of the parent, and formation of the anion and the Janovsky complex when the parent was in excess.

The problem of the site of addition of the methoxide ion was solved by Fyfe and co-workers[51], who used a flow system to obtain p.m.r. spectra of the species produced. With TNT and methoxide ion in equimolar amounts, in 87·5% DMSO, 12·5% MeOH, two singlets at δ6·18 and δ8·45 were observed. These correspond to the adduct at C-3 (1.26)

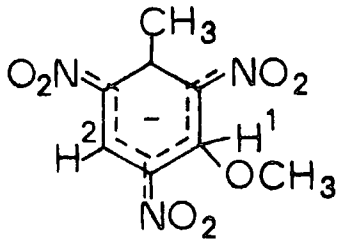

1.26

H^1: 6·18

H^2: 8·45

This species was produced rapidly and decomposed quite slowly - there was little change in the spectrum from 0·3s to 1s after mixing.

If the flow was stopped, a new species began to appear, which after 80s showed two singlets of equal intensity at δ5·53 and δ8·18, corresponding to the trinitrobenzyl anion (1.27).

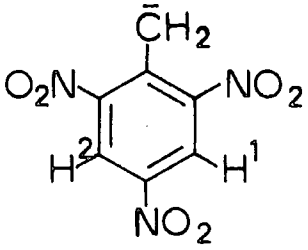

1.27

H^1: 8·18

H^2: 8·18

$-\bar{C}H_2$: 5·53

When the base:parent ratio was 2:1 or greater, a

single species was formed in a rapid reaction, showing four equal peaks at δ8·45, δ6·18, δ6·42, δ6·52. This was assigned as the dianion (1.28).

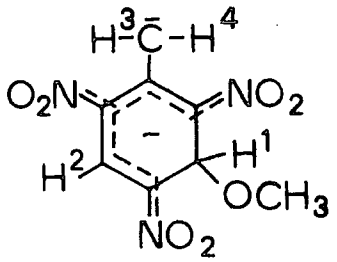

1.28

H^1: 6·18

H^2: 8·45

H^3,H^4: 6·42, 6·52 (unspecified)

When the flow was stopped, after ~3min, the two lines at δ6·42, 6·52 had become an AB multiplet, indicating that rotation around the carbon-ring bond is restricted.

A simultaneous UV/visible study provided support for these assignments. The initially produced species had λ_{max} 433nm, 505nm, typical of a Meisenheimer complex[43], whilst the second species produced had λ_{max} 520nm, ~640nm, similar to those spectra observed by Buncel et al[49]. The dianion showed one absorption at 550nm.

The reaction was also investigated by ESR, and large quantities of radicals were found. The concentration of radicals reached a maximum after ~240s, and then decreased, at a similar rate to the disappearance of the trinitrobenzyl anion. It was suggested that a number of different radicals were formed, one of which may be the radical anion of TNT.

The rapid formation of a brown colour, followed by the slower formation of a purple species was also observed in the reaction of TNT with sodium isopropoxide in isopropanol[52]. Spectra recorded at low temperature allowed the initial product to be identified as a σ-complex, with λ_{max} 435nm, 495nm. A primary isotope effect of 8·4 (at 30°C) was observed using TNT-d_3, showing that in the

formation of the trinitrobenzyl anion the rate-determining step is proton transfer. The rate data in this case do not fit the simple two reaction scheme, and cation pairing

$$TNT + OR^- \rightleftharpoons TNT.OR^-$$

$$TNT + OR^- \rightleftharpoons TNT^- + ROH$$

with both alkoxide ion and products was invoked. The authors deduced that in the formation of the anion the free isopropoxide ion was more reactive than the ion pair, whereas in the formation of the adduct the two species were of similar reactivity. This was rationalised in terms of possible cation stabilisation of the transition state: in the case of the σ-complex a six-membered 'ring' (1.29) can be formed, whereas in proton abstraction the 'ring' would be eight-membered (1.30).

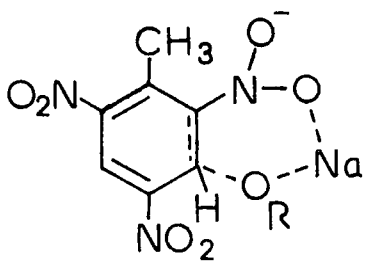

1.29

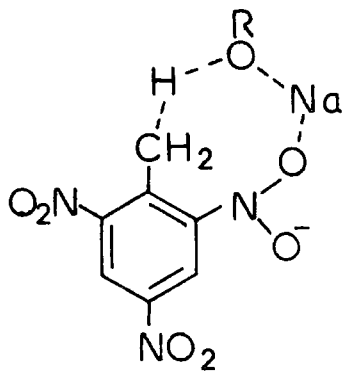

1.30

The addition of salts ($NaClO_4$, $NaBPh_4$) at constant base concentration increased k_{obs} for anion formation by an increase in the rate of the reverse reaction. This was thought to be due either to an increase in the activity of the σ-complex, or perhaps to a specific interaction involving the cation.

The preparation of a solid addition product from the reaction of TNT with sodium n-butoxide was reported in 1919[47]. Subsequent studies[53,54] of the reaction of TNT

with sodium tert-butoxide have shown that the main process is proton abstraction[53]. If crown ether is added to prevent ion pairing[54], the rate of reaction at a given base concentration increases up to a 1:1 ratio of crown ether to tert-butoxide, where the reaction product now consists of a 60:40 mixture of σ-complex and anion. This effect is also seen when tetra-n-butylammonium tert-butoxide is used, the rate coefficient at a given base concentration being the same as that with more than one equivalent of crown ether. Thus the free ion here is more reactive than the ion pair. The rate enhancement is due in part to the fact that in the transition state the charge is less localised than in the reactants, and hence ion pairing in the transition state will be less effective. This effect should be more pronounced in the case of the complex, where extensive delocalisation occurs in the transition state, than in the more localised transition state leading to the anion, and hence the rate of complex formation is affected more than that of ionisation.

In 1924, Muraour[55] reported that TNT would dissolve in aqueous solutions of sodium sulphite, although it did not do so as readily as TNB. A later study of this reaction in more dilute ($\sim 10^{-2}$ M) aqueous sulphite solutions confirmed this observation, and determined the stoichiometry of the reaction as 1:1. The visible spectrum of the product showed λ_{max} at 465nm, and a value for the equilibrium constant for the reaction of 5·6 l mole^{-1} was obtained spectrophotometrically. Kinetic and equilibrium data for this reaction, and that of 2,4,6-trinitrobenzyl chloride with sulphite, will be presented in a later chapter.

A number of studies have been reported on the interactions of TNT with carbon nucleophiles. Two NMR studies obtained the spectrum of a 1:1 cyanide:TNT adduct in $CDCl_3$, at -30^oC[29] and 30^oC[30]. They showed that addition takes place at C-3 (1.30).

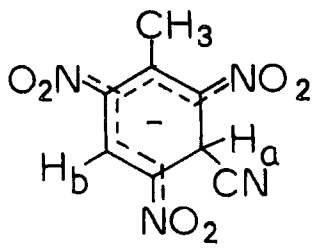

1.31

	CH_3	H_a	H_b	(δvalues)
-30^oC	2·74	5·76	8·65	
30^oC	2·68	5·67	8·52	

A stopped-flow kinetic and equilibrium study[57] of this reaction in isopropanol showed the complex to have λ_{max} at 437nm ($1·69 \times 10^4$) and 535nm ($1·11 \times 10^4$). The equilibrium constant for the formation of this species was $2·01 \times 10^4$ l mole^{-1} and for the forward rate constant 32·6 l mole^{-1}s^{-1}, k_{-1} being too small to measure directly.

Kaminskii et al[58] reported the formation of a 1:1 adduct in the reaction of TNT with acetone in an alkaline medium, by addition of the acetonate ion at C-3 (1.32).

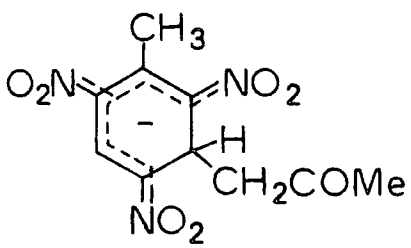

1.32

Strauss and Taylor[59] studied the reactions of a number of 1-substituted-2,4,6-trinitrobenzenes in 1,3-dicarbomethoxyacetone on the addition of excess triethylamine. In the case of TNT, a dark red solution was obtained, turning dark orange on standing. Orange crystals were isolated,

which analysed for a 1:1:1 mixture of the three reactants. The pmr spectrum of these crystals dissolved in deuteriochloroform showed the species to be a cyclic diadduct (1.33).

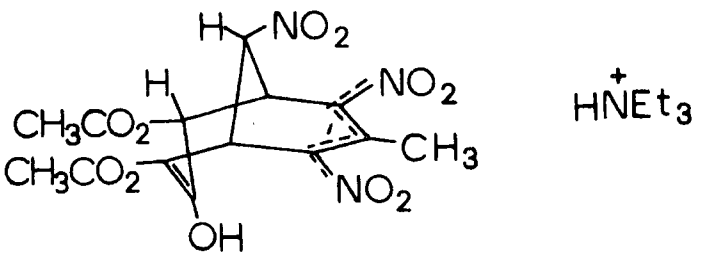

1.33

The structure of this adduct rules out the possibility of formation of the first adduct by addition at C-1, at least on the reaction coordinate.

In 1959, Miller and Wynne-Jones[60] dissolved TNT in pyridine, and observed a strong coloration and an increase in electrical conductivity. Exchange experiments in pyridine-D_2O mixtures showed that proton transfer took place in this system, in contrast to TNB where only electron transfer was observed. However, in carbon tetrachloride solution, 1:1 complexes are reported[61] as being formed between TNT and pyridine and various methyl derivatives. These were identified as $\Pi - \Pi$ charge-transfer complexes, in which the aza aromatic compound is tilted towards the TNT molecule, the nitrogen atom being closest to the acceptor molecule. Similarly, charge-transfer complexes were observed[62] in the reactions of TNT with a selection of N-alkyl p-phenylenediamines.

TNB will react with phenylhydrazine to give a σ-complex[63]. However, there is no evidence for complex formation in the reaction of TNT with this compound; instead,

attack occurs at one of the nitro groups ortho to the methyl group, to give (1.34).

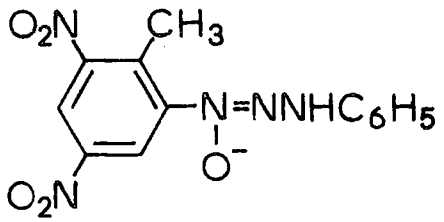

1.34

Okamoto and Wang[64] reported a study of the effect of micelles on the reaction of TNT with amines, in aqueous solution. Comparing the rate of reaction with a surfactant amine (4-dodecyldiethylenetriamine, I) to that with a non-surfactant amine (3,3'-diamino-N-methyldipropylamine, II) they found identical rates up to 5 x 10^{-5}M amine, which is the critical micelle concentration of I. Above this, the rate of reaction with I increased more rapidly, to level off at a rate enhancement by a factor of 55. A cationic micelle increased the rate of reaction of II with TNT by up to a factor of 130, whilst a neutral micelle enhanced the rate by a factor of 8. They assumed that the reaction they were observing was the formation of the trinitrobenzyl anion. However, a later study[65] using a cationic micelle and a similar amine to II (3,3'-diaminodipropylamine) showed the spectrum of the product to be that of a Meisenheimer-type adduct, with λ_{max} 445nm and 530nm. An identical spectrum was obtained with potassium hydroxide as the base, which led to the conclusion that the species produced was the Janovsky complex formed by attack of the TNT^- anion on a neutral TNT molecule.

TNT dissolves in liquid ammonia[25] to give a dark red solution. The NMR spectrum initially shows two doublets

of equal intensity at δ8·31 and δ5·36 (the position and splitting values being similar to those with TNB). This species was assigned the structure (1.35).

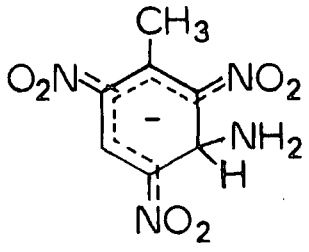

1.35

The methyl protons appear as a singlet at δ2·33, relative intensity 3 - thus there is no evidence for anion formation.

With time the spectrum changes. Two pairs of peaks appear at δ5·20, δ4·90 and δ8·48, δ8·44, with the former in each pair having twice the intensity of the latter. In addition, the methyl resonance is now found at δ1·62, which suggests attack at C-1. Consequently the diadduct structure (1.36) was assigned to this species.

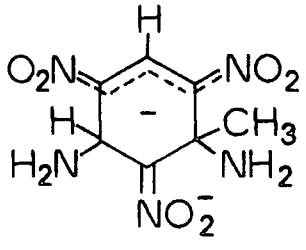

1.36

The two sets of peaks correspond to the two geometrical isomers, with the amide groups cis or trans (similar isomers are observed with TNB and sulphite[34]). The trans isomer was assigned the bands at δ5·20 and δ8·48, and is hence the more stable.

A study[66] of the reaction between TNT and a number of aliphatic amines and diamines suggested the formation of 1:1 charge-transfer complexes. However, a study[67] using

1,5-dimethyl-2,4,8-trinitronaphthalene and diethyl- and triethylamine showed the formation of a benzyl-type anion (scheme 1.2.).

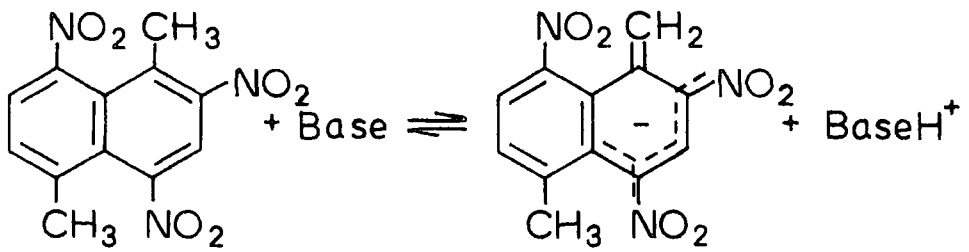

Scheme 1.2.

A study of the reactions of TNT and TNBCl with a number of aliphatic amines, showing both complex formation and proton abstraction, will be reported in a later chapter.

The reaction of TNT with hypochlorite ion is of commercial importance, as its major product is 2,2',4,4',6,6'-hexanitrostilbene (HNS). The addition of a chilled solution of TNT in tetrahydrofuran/methanol to '5%' sodium hypochlorite at 0-15°C leads to a dark red-brown solution, from which a crystalline solid appears - this is HNS[68]. This compound can also be made by the reaction of potassium hydroxide with trinitrobenzyl chloride[69]. TNBCl can itself be isolated in high yield from the TNT - hypochlorite reaction mixture by quenching with dilute acid in the initial stages[68].

The mechanism suggested[68] for the reaction involves the formation of TNBCl from TNT, followed by attack of the TNBCl anion on a neutral TNBCl molecule. (Scheme 1.3)

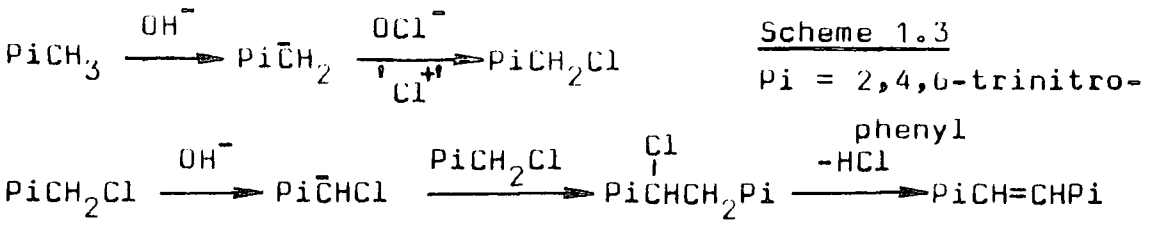

Scheme 1.3

Pi = 2,4,6-trinitrophenyl

The involvement of radicals[70] or carbenes[68] in the reaction mechanism was ruled out on various grounds.

CHAPTER TWO

EXPERIMENTAL

2.1. Materials.

2.1.1. Solvents:

Water: distilled water was boiled for 15 minutes to expel dissolved CO_2, and then protected from the air by a soda-lime guard tube.

Methanol: AnalaR grade, used without further treatment.

Methanol-d_4: Commercial sample, used as supplied.

Ethanol: AnalaR grade, used without further treatment, or boiled and stored as for water.

Isopropanol: AnalaR grade, treated as ethanol.

Dimethyl sulphoxide: Koch-Light puriss. grade, used without further treatment.

DMSO-d_6: commercial sample, used as supplied.

1,4-dioxan: spectroscopic grade, used in making up stock solutions of parent compounds. Reaction solutions contained less than 1% dioxan.

Tetrahydrofuran: AnalaR grade, dried over sodium.

2.1.2.Substrates:

1,3,5-Trinitrobenzene: dried reagent grade, m.p. 123°C (lit.[71] 122·5°C)

2,4,6-Trinitrotoluene: sample supplied by P.E.R.M.E., Waltham Abbey, and dried in air. NMR spectra showed no impurities. M.p. 82°C (lit.[72] 82°C)

2,4,6-Trinitrobenzylchloride: samples supplied wet by P.E.R.M.E., Waltham Abbey, and dried in air. Purity of samples tested by NMR. Those found impure (contaminated with TNT) were recrystallised twice from benzene/pentane - subsequent NMR spectra showed no trace of impurities. M.p. 85°C (lit.[68] 85°C)

2.1.3. Nucleophiles:

Sodium methoxide: prepared by dissolving sodium metal in AnalaR methanol under nitrogen. Samples of the solution thus prepared (usually around 3M) were diluted with methanol and titrated with standard acid. Solutions of sodium methoxide-d_3 in methanol-d_4 were made in the same way.

Sodium ethoxide, sodium isopropoxide: prepared in the same way as sodium methoxide.

Tetraethylammonium isopropoxide: prepared by dilution of 25% aqueous tetraethylammonium hydroxide with isopropanol, and titrated with standard acid. Reaction solutions contained less than 1% water.

Sodium sulphite: AnalaR grade hexahydrate, oven dried.

Benzylamine, n-butylamine, isopropylamine and piperidine: commercial samples, used as supplied.

1,4-diazabicyclo-[2,2,2]-octane (DABCO): reagent grade, used as supplied.

Sodium hypochlorite: commercial solution (10-15% available chlorine) was diluted 1 in 6 to give an approx 0·5M solution. Samples were standardised against sodium thiosulphate after the addition of excess potassium iodide.

Sodium phenoxide: stock solutions were made by the addition of the required amount of 1M sodium hydroxide solution to a solution of AnalaR phenol (weighed out) in water.

Potassium cyanide: AnalaR solid, used as supplied.

Diethylmalonate: commercial specimen, used as supplied. To generate the malonate anion, sodium methoxide was added to the solutions.

2.1.4. Salts:

Sodium sulphate: AnalaR grade, oven dried.

Sodium tetraphenylborate: commercial sample, used as supplied.

Amine perchlorates (all amines except piperidine): stock solutions were prepared by mixing the appropriate weights of the amine and 60% aqueous perchloric acid in a known volume of DMSO.

Piperidine hydrochloride: a commercial 'pure' sample, used as supplied.

2.2. Measurement Techniques.

2.2.1. Rates.

a. Stopped-flow spectrophotometer: The instruments used were 'Canterbury' SF-3A or SF-3L instruments, each with a 2mm pathlength cell, thermostatted at 25°C. First order conditions were maintained by having the base concentration in large excess over that of the parent. Reactions were followed by monitoring the change of absorbance with time at a chosen wavelength. For small changes in absorbance, the measured difference in voltage can be assumed to be directly proportional to the change in optical density (and thus to the change in concentration). Hence, for rate measurements, a plot of $\ln\Delta V$ versus t gives a straight line of slope k_{obs}, where $\Delta V = |V_\infty - V_t|$.

In the cases where a reliable 'infinity' reading could not be obtained, Guggenheim plots were used. In most systems studied, two processes were observed. Where kinetic measurements were desired for the first process, either a suitable wavelength was chosen to avoid interference by the second process, or the processes were separated by visual extrapolation. The rate coefficients quoted are the mean of 4-6 individual runs, and are generally accurate to $\pm 5\%$

b. Slower rates: These were measured either on a Beckmann S-25 recording spectrophotometer, or a Unicam SP-500 instrument. In either case, solutions were thermostatted at 25°C.

2.2.2. Equilibria.

Equilibrium optical density measurements were made at 25°C, using either a Unicam SP500 instrument, with a pathlength of 1cm, or the stopped-flow spectrophotometer. In this case, the optical densities were calculated from

equation 2.1.

$$O.D. = \log \frac{V_o}{(V_o - \Delta V)} \qquad \text{Eq.2.1}$$

where V_o = background voltage (generally 5V)

$\Delta V = V_c - V_s$

V_c = voltage in the absence of the absorbing species

V_s = voltage in the presence of the absorbing species

2.2.3. Visible spectra.

These were either recorded on a Unicam SP8000, Unicam SP8-100 or Beckmann S-25 recording instrument, or measured point by point on the stopped-flow spectrophotometer.

2.2.4. Proton magnetic resonance spectra.

These were measured on:

a. A Varian EM 360L instrument operating at 60 MHz.

b. A Bruker HX 90E instrument operating at 90 MHz, modified for Fourier transform operation and using a deuterium lock. Shift measurements are quoted as 'δ' values relative to internal tetramethylsilane, with the exception of those in water, which were measured relative to internal dioxan, assigned a shift of 3.7 ppm.

CHAPTER THREE

SULPHITE ADDITIONS TO 2,4,6-TRINITROTOLUENE AND 2,4,6-TRINITROBENZYL CHLORIDE IN WATER

3.1. Introduction.

The reactions of sulphite ions with a number of polynitroaromatic compounds have been studied, adducts at both substituted[33] and unsubstituted[32] positions having been observed. Evidence has also been found for cis-trans isomerism in the diadduct of 1,3,5-trinitrobenzene[34-36]. In the case of TNT, the relatively low affinity of the sulphite ion for protons should make proton abstraction a minor process, and simplify the analysis of the kinetic data. A previous study[55] of this reaction reported the formation of a species of unspecified structure, with λ_{max} 465nm, and equilibrium constant 5·6 l mole^{-1}.

3.2. Experimental.

Kinetic measurements were made at suitable wavelengths using the stopped-flow spectrophotometer. Typical runs are shown in table 3.1. Visible spectra were recorded on a Pye-Unicam SP8000 spectrophotometer at 31°C. ^{1}H NMR measurements were made at 90 MHz on a Bruker HX 80E instrument modified for Fourier transform operation and using a deuterium lock. Chemical shifts in media containing DMSO were measured relative to internal tetramethylsilane : those in water were measured relative to internal dioxan, assuming a difference of 3·70 ppm between the two references[73]. Mixed DMSO-water solvents were made by mixing measured volumes of each component.

Table 3.1.

Typical results from kinetic measurements.

(i) Sodium sulphite (0·04 M), TNBCl (5×10^{-5} M)

First process, measured at 460nm.

(ii) Sodium sulphite (0·1 M), TNT (1×10^{-4} M)

Second process, measured at 560nm.

(i)			(ii)		
t (ms)	ΔV^a	k^b (s^{-1})	t (s)	ΔV^a	k^b (s^{-1})
5	5·70		0·1	4·75	
7·5	4·50	95	0·2	3·85	2·10
10	3·50	100	0·3	3·15	2·00
12·5	2·80	89	0·4	2·55	2·11
15	2·15	106	0·5	2·05	2·18
17·5	1·70	94	0·6	1·65	2·17
20	1·30	107	0·7	1·35	2·01
	mean	98·5	0·8	1·10	2·05
			0·9	0·90	2·01
				mean	2·08

a: $\Delta V = V_t - V_\infty$

b: $k = \frac{1}{(t-t')} \ln \frac{\Delta V'}{\Delta V}$

3.3. Results and Discussion.

3.3.1. 2,4,6-Trinitrobenzyl chloride.

In aqueous solution, visible spectra indicate the presence of two equilibria between TNBCl and sulphite. A solution containing 0·01 M sodium sulphite and 2×10^{-5}M TNBCl shows two maxima at 460nm and 540nm. This pink species is attributed to 1:1 interaction. At higher base concentrations a new peak appears in the region of 480nm as the initial peaks decrease, until with 1M sulphite there is one broad peak at 450nm. This is interpreted as formation of a 1:2 adduct, beginning before complete conversion to the 1:1 adduct has occurred. In DMSO-water mixtures, where the 1:1 complex is stabilised relative to the 1:2[7], the spectrum shows a peak at 466nm, with a pronounced shoulder at 530nm.

^{1}H NMR data for these reactions, given in table 3.2, confirm the above assignments.

The spectrum of the parent compound in DMSO-d_6 shows two bands, at δ5·00 (CH_2Cl protons) and δ9·08 (ring protons). On the addition of sodium sulphite in D_2O, these bands disappear and are replaced by two new bands at δ6·13 and δ8·52 and a group of bands around δ5·10. The observation of the two bands due to the ring protons is evidence for the formation of an adduct at C-3 (3.1), one proton(H_b at δ6·13) showing a large upfield shift due to the change in hybridisation of the carbon atom to which it is attached, whilst the other (H_a at δ8·52) remains in a largely aromatic environment. The side chain resonance does not move greatly, but is split into four bands due to non-equivalence of the protons. This is presumably due to restricted rotation of this group in the adduct.

Table 3.2.

^{1}H NMR data for TNT and TNBCl and their adducts with sodium sulphite.

Species	Solvent[a]	δ (ring)	δ(side chain)
TNBCl	DMSO	9·08	5·00
(3.1)	70:30 v/v DMSO-water	8·50 (H_a) 6·13 (H_b)	5·05[b] 5·11[b]
(3.2)	Water	6·0 (H_a,H_b)	4·80[b] 5·1[b]
TNT	DMSO	9·04	2·56
(3.3)	70:30 v/v DMSO-water	8·50[c] (H_a) 6·14[c] (H_b)	2·41
(3.4)	Water	6·0 (H_a,H_b)	2·48

a. All solvents were fully deuterated

b. Doublets, J = 11 Hz

c. Doublets, J = 2 Hz

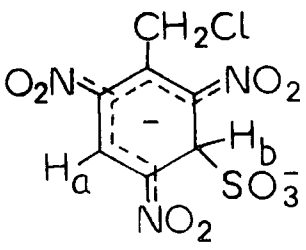

3.1

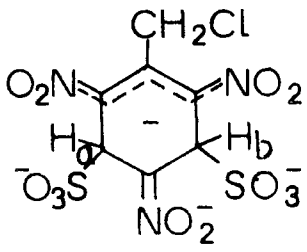

3.2

Dissolving TNBCl in a 1M solution of sodium sulphite in D_2O containing a small amount of dioxan gives rise to a spectrum with a band at δ6·00 and a group of four bands similar to those above, centred around δ5·0. The single band due to ring protons is evidence for structure (3.2), where again the side chain protons are non-equivalent due to hindered rotation.

Stopped-flow spectrophotometry showed the presence of two processes whose rates were well separated. The first was colour forming at all wavelengths studied, whilst the second was colour forming or fading depending on both the wavelength of measurement and the concentration of base used. These two processes were attributed to the formation of 1:1 and 1:2 adducts, the equilibria concerned being equations 3.1 and 3.2 respectively:

$$\text{Parent} + SO_3^{2-} \underset{k_{-1}}{\overset{k_1}{\rightleftharpoons}} (3.1) \qquad \text{Eq. 3.1}$$

$$(3.1) + SO_3^{2-} \underset{k_{-2}}{\overset{k_2}{\rightleftharpoons}} (3.2) \qquad \text{Eq. 3.2}$$

Effects due to the ionic strength of the medium are likely to be important for the second process, but less so for the first. Consequently the first process was studied at low base concentrations, without added salt. Rate and equilibrium data for this reaction were measured at 460nm,

and are presented in table 3.3. As the concentration of base is in large excess over that of the parent, equation 3.3. applies to the observed rate coefficients.

$$k_{obs} = k_{-1} + k_1 [SO_3^{2-}] \qquad \text{Eq. 3.3}$$

A plot of k_{obs} versus sulphite concentration was linear, and yielded values of k_1, 4000 l mole^{-1}s^{-1} and k_{-1}, 77 s^{-1}. Combining these values gave K_1 (= k_1/k_{-1}), 52 l mole^{-1}, in good agreement with the value obtained from the optical density measurements, 56·5 l mole^{-1}.

The second process was also followed at 460nm, the solutions in this case being made up to 0·3 M ionic strength with sodium sulphate. Rate data for this reaction are in table 3.4. First order kinetics will again apply, the observed rate coefficients (k_{obs}) in this case being given by equation 3.4.

$$k_{obs} = k_{-2} + \frac{k_2 K_1 [SO_3^{2-}]^2}{1 + K_1 [SO_3^{2-}]} \qquad \text{Eq. 3.4}$$

Extrapolation of the observed rates to zero sulphite concentration gave a value for k_{-2} of 1·7 ± 0·2 s^{-1}. This value, and the known value of K_1, were used to calculate values of k_2 using equation 3.4. - this procedure gave a value of 55 ± 4 l mole^{-1}s^{-1} for k_2, and hence a value of K_2 (= k_2/k_{-2}) of 32 l mole^{-1}. Values for the rate coefficient calculated from these results were in good agreement with the experimental values.

3.2.2. 2,4,6-Trinitrotoluene.

The visible spectra obtained with TNT and sulphite in water are similar to those with TNBCl. In dilute sulphite solutions (below 0·01 M) a pink species is

Table 3.3.

Kinetic and equilibrium data for the reaction of TNBCl with sodium sulphite in water at 25°C: first process

$[Na_2SO_3]$ (M)	k_{obs} (s^{-1})	O.D.[a] 460nm	K_1[b] (l $mole^{-1}$)
0·002	86	0·013	61
0·004	98	0·021	54
0·006	110	0·030	56
0·008	110	0·037	56
0·010	118	0·043	55
0·015	126	0·054	54

a. After completion of first process. Measurements refer to a 2mm pathlength cell, with 5×10^{-5} M substrate.

b. Calculated using O.D. values and a value of 0·120 for complete conversion, obtained from a Benesi-Hildebrand plot.

Table 3.4.

Kinetic data for the reaction of TN8Cl (5×10^{-5} M) with sodium sulphite in water at 25°C: second process.

$[Na_2SO_3]$ (M)	$[Na_2SO_4]$ (M)	k_{obs} (s^{-1})	k_{calc}[a] (s^{-1})
0·01	0·09	1·94	1·90
0·02	0·08	2·27	2·27
0·04	0·06	3·10	3·20
0·06	0·04	4·05	4·20
0·08	0·02	5·32	5·25
0·10		6·33	6·35

a. Calculated from equation 3.4. with $k_{-2} = 1{\cdot}7\ s^{-1}$, $k_2 = 55\ l\ mole^{-1}s^{-1}$ and $K_1 = 55\ l\ mole^{-1}$.

produced, with λ_{max} at 460nm and 550nm (shoulder), again attributed to 1:1 interaction. Above 0·1 M sulphite, an orange species predominates, whose spectrum has a broad peak at 420nm. This is the product of a 1:2 interaction. DMSO is again found to stabilise the 1:1 adduct relative to the 1:2.

^{1}H NMR spectra confirm the products of the reactions as the adducts (3.3) and (3.4).

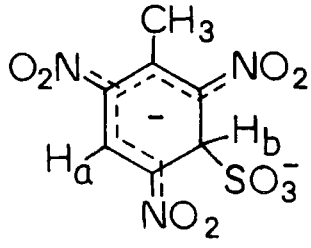

3.3

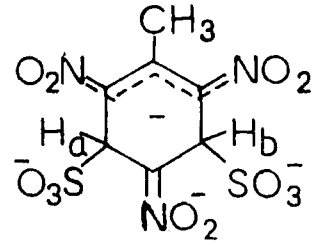

3.4

The spectrum of the parent compound shows two singlets, at δ2.56 (CH_3protons) and δ9·04 (ring protons). A solution of TNT and sulphite (both 0·07 M) in 70:30 v/v DMSO-d_6-D_2O shows two spin-coupled bands (J = 2 Hz) at δ6·14 and δ8·47, with the methyl proton resonance at δ2·41 indicating no addition at C-1. These data are consistent with (3.3), with H_b at δ6·15.

On dissolving TNT in a solution of sodium sulphite in D_2O, again with a small amount of added dioxan, the spectrum obtained showed two peaks: the methyl proton resonance was found at δ2·48, whilst the ring protons occur at δ6·0, showing addition at both C-3 and C-5, (3.4). Unlike the diadduct from 1,3,5-trinitrobenzene[35,36], there was no evidence here for cis-trans isomerism. The data are summarised in Table 3.2.

Stopped-flow investigation of these reactions showed the presence of two processes, again with well-separated

rates. In this case, the first process, a rapid colour-forming reaction associated with the formation of (3.3), had rate coefficients in excess of 250 s^{-1} in the most dilute sulphite solutions which gave measurable absorption, and was hence too rapid for measurement using the stopped-flow method. In view of the stabilisation of the 1:1 adduct by dimethyl sulphoxide, rate measurements were made in mixed DMSO-water media. Rate and equilibrium data for the first process are presented in tables 3.5 (30% DMSO by volume), 3.6 (20%) and 3.7 (10%). As for TNBCl, first order conditions were maintained, and hence equation 3.3 applies to each set. Plots of k_{obs} versus sulphite concentration for each solvent composition were linear, (figure 3.1), allowing values of k_1 and k_{-1} to be obtained. Optical densities at the end of the first process were also measured in each case, and were used to calculate values of K_1. The values obtained for these parameters are in table 3.8. Previous workers have found that properties such as rate constants[74] and acidity functions[75] vary with the DMSO content of mixed media in such a way that plots of the log of the property versus the mole percentage of DMSO are linear. In agreement with this, plots of log K_1 and log k_{-1} against the mole percentage of DMSO were linear, and allowed extrapolation to pure water.

The greater stability of the 1:1 adduct in media containing DMSO probably derives from the lower solvation by DMSO of the polar sulphite ion, and the increased solvation of the polarisable σ-adduct by this component.

The variation in the value of K_1 with the change in solvent composition can be seen to derive from changes in k_1,

Table 3.5.

Kinetic and equilibrium data for the reaction of TNT and sulphite (first process) in 70:30 v/v water:DMSO at 25°C

[sulphite] (M)	k_{obs} (s^{-1})	O.D.[a] 460nm	K_1[b] (l $mole^{-1}$)
0·0025	16·97	0·012	77·4
0·0050	19·29	0·021	79·2
0·0075	21·96	0·028	81·2
0·010	25·01	0·033	80·5
0·020	45·13	0·048	92·3
0·030	47·42	0·050	69·4
0·040	58·03	0·055	72·4

a. Optical densities at end of first process. Measurements refer to a 2mm pathlength cell, with $2·5 \times 10^{-5}$ M substrate.

b. Calculated from O.D. values and a value of 0·074 for complete conversion (Benesi-Hildebrand plot)

Table 3.6.

Kinetic and equilibrium data for the reaction of TNT and sulphite (first process) in 80:20 v/v water:DMSO at 25°C

[sulphite] (M)	k_{obs} (s^{-1})	O.D.[a] 460nm	K_1[b] (l $mole^{-1}$)
0·005	49·5	0·012	21·2
0·010	52·1	0·021	20·2
0·015	58·4	0·031	22·0
0·020	63·9	0·038	21·8
0·040	82·9	0·057	21·0
0·060	99·3	0·068	19·9
0·080	115·2	0·074	18·1

a. Optical densities at end of first process. Measurements refer to a 2mm pathlength cell, with 5×10^{-5} M substrate.

b. Calculated from O.D. values and a value of 0·125 for complete conversion (Benesi-Hildebrand plot)

Table 3.7.

Kinetic and equilibrium data for the reaction of TNT and sulphite (first process) in 90:10 v/v water:DMSO at 25°C

[sulphite] (M)	k_{obs} (s^{-1})	O.D.[a] 460nm	K_1[b] (l $mole^{-1}$)
0·02	157	0·022	6·20
0·04	171	0·040	6·25
0·06	187	0·072	9·37
0·08	218	0·068	6·44
0·10	229	0·082	6·95

a. Optical density at end of first process. Measurements refer to a 2mm pathlength cell, with 1 x 10^{-4} M substrate.

b. Calculated from O.D. values and a value of 0·20 for complete conversion (Benesi-Hildebrand plot)

Table 3.8.

Variation with solvent composition of rate and equilibrium parameters for formation of (3.3) from TNT and sodium sulphite at 25°C.

Vol% DMSO	Mole% DMSO	k_1 (l mole^{-1}s^{-1})	k_{-1} (s^{-1})	K_1[a] (l mole^{-1})	K_1[b] (l mole^{-1})
30	9·6	1100±50	14±0·5	80±5	79±7
20	5·9	920±70	45±2	21±2	21±2
10	2·7	900±100	135±10	7±1	7±1
0[c]	0	800±100	300±30	2·6±0·5	2·6±0·5

a. From kinetic data, $K_1 = k_1/k_{-1}$

b. From optical density data

c. Extrapolated values

Figure 3.1.

Plots of k_{obs} versus sulphite concentration for the reaction of TNT with sodium sulphite in methanol-water mixtures (first process).

A : 10% DMSO

B : 20% DMSO

C : 30% DMSO

Figure 3.1.

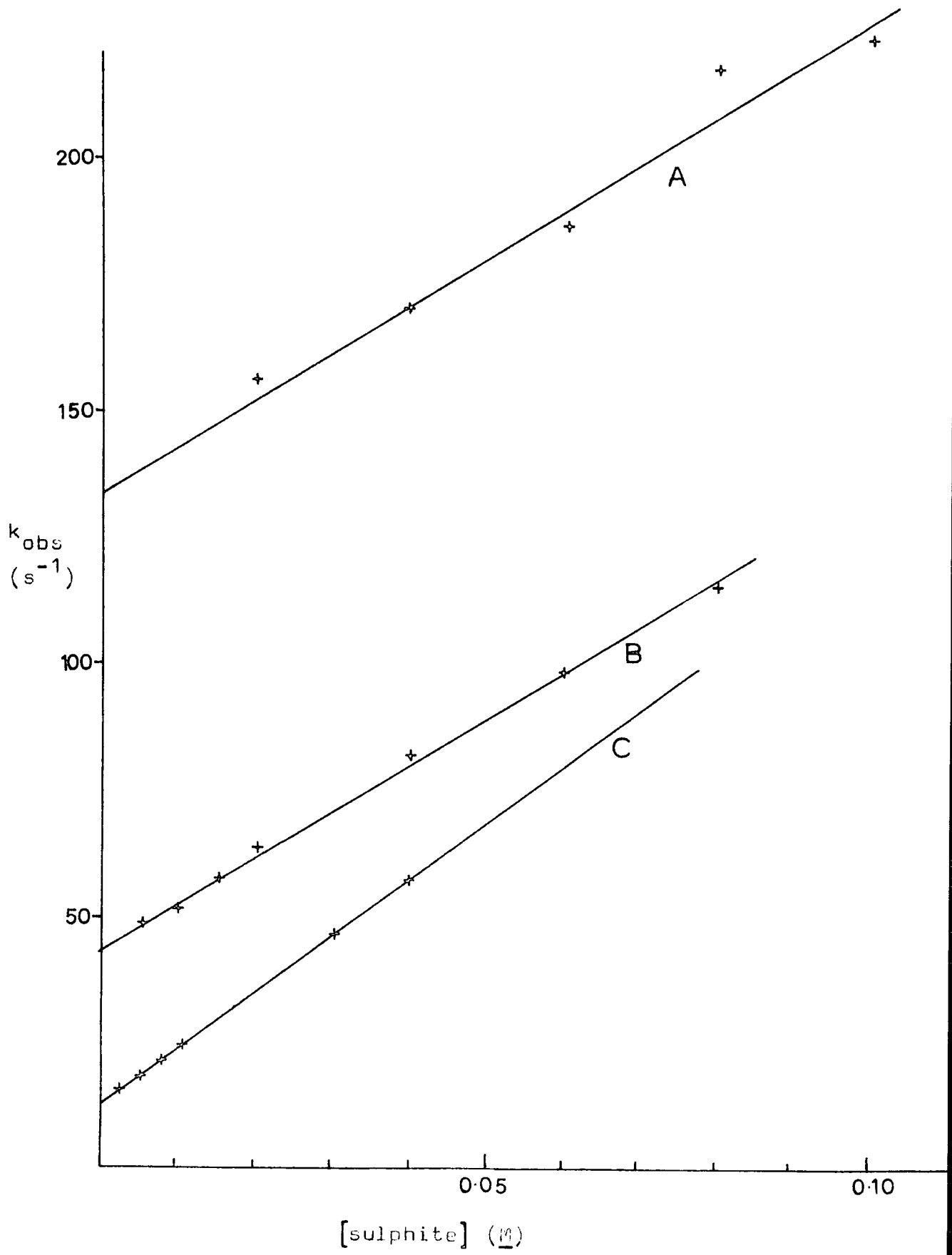

k_{-1} remaining reasonably constant. As found in previous studies[76], this indicates that the transition state for the formation of the 1:1 complex is 'reactant-like'.

The second process, corresponding to the formation of (3.4), was much slower, and rate measurements were conveniently made in water. Measurements were made at two different ionic strengths, with added sodium sulphate, the rate coefficients varying markedly with ionic strength as expected for the formation of a multi-charged species[76]. Rate data are in table 3.9. These were treated in a similar fashion to those of the second process with TNBCl, using K_1= 2·6 and gave the values k_{-2}= 1·16 s^{-1}, k_2= 42 l $mole^{-1}s^{-1}$, $K_2(=k_2/k_{-2})$ = 36 (for ionic strength 0·3 M) and k_{-2}=0·85 s^{-1}, k_2= 160 l $mole^{-1}s^{-1}$, K_2= 188 (for ionic strength 1·5 M).

3.3.3. Comparison with other compounds.

Rate and equilibrium parameters for the two compounds at ionic strength 0·3 M in water are presented in table 3.10, along with the corresponding values for 1,3,5-trinitrobenzene (TNB) and 2,4,6-trinitroanisole (TNA). As with other compounds (with the exception of 2,4,6-trinitrobenzaldehyde)[33] there was no evidence for sulphite addition at a substituted position - this may reflect the adverse steric effects of the two bulky groups attached to the same carbon atom.

The greater stability of the 1:1 adduct of TNBCl over that of TNT is due to the greater electron-withdrawing ability of the chloromethyl group in the former over the methyl group in the latter. The decreased stability of these adducts compared with that from TNB may be due to steric effects. The presence of a bulky group in the 1-position

Table 3.9.

Rate data for the second reaction between TNT and sulphite in water at 25°C.

[sulphite] (M)	k_{obs}[a] (s^{-1})	k_{calc}[b] (s^{-1})	k_{obs}[c] (s^{-1})	k_{calc}[d] (s^{-1})
0·01	1·19	1·17		
0·02	1·20	1·20	1·01	1·01
0·04	1·27	1·32		
0·05			1·79	1·77
0·06	1·49	1·50		
0·08	1·74	1·74		
0·10	2·10	2·03	4·00	4·13
0·20			11·3	11·7
0·30			22·3	21·9
0·40			34·3	33·6

a. Ionic strength 0·3 M with sodium sulphate.

b. Calculated from equation 3.4 with k_{-2}= 1·16 s^{-1}, k_2= 42 l $mole^{-1}s^{-1}$ and K_1= 2·6 l $mole^{-1}$.

c. Ionic strength 1·5 M with sodium sulphate.

d. Calculated from equation 3.4 with k_{-2}= 0·85 s^{-1}, k_2= 160 l $mole^{-1}s^{-1}$ and K_1= 2·6 l $mole^{-1}$.

Table 3.10

Kinetic and equilibrium data for some sulphite additions in water at 25°C with ionic strength 0·3 M.

	k_1 (l mole^{-1}s^{-1})	k_{-1} (s^{-1})	K_1 (l mole^{-1})	k_2 (l mole^{-1}s^{-1})	k_{-2} (s^{-1})	K_2 (l mole^{-1})
TNB[b]	3.5×10^4	125	290	1·2[a]	0·13	9·2
				195	21	9·3
TNA[c]	$4·8 \times 10^3$	35	140	170	0·12	$1·4 \times 10^3$
TNT	800	300	2·6	42	1·16	36
TNBCl	4×10^3	77	55	55	1·7	32

a. Data refer to formation of cis- and trans-isomers.

b. Ref. 34.

c. Ref. 76.

will hinder planarity of the adjacent nitro groups, which is an important factor in charge-stabilisation in the adducts.

It has been suggested [77] that the extent of solvation of adducts may play an important part in determining their relative stabilities. In this case, the presence of the hydrophobic methyl group in the TNT adducts may hinder the solvation of the adjacent nitro groups to some extent, this being important particularly in the adducts.

No kinetic or NMR evidence was found for cis-trans isomerism in the diadducts - as with other compounds it seems likely that one isomer (probably the trans) is favoured.

CHAPTER FOUR

THE REACTIONS OF 2,4,6-TRINITROBENZYL CHLORIDE WITH ALKOXIDE IONS

4.1. Introduction.

If the reaction of 2,4,6-trinitrotoluene and sodium hypochlorite is quenched with dilute acid shortly after its initiation, a high yield of 2,4,6-trinitrobenzyl chloride (TNBCl) is obtained[68]. This compound is likely to be an intermediate in the formation of 2,2',4,4',6,6',-hexanitrostilbene (HNS) by the above reaction and HNS can in fact be made by the reaction of TNBCl with potassium hydroxide[69]. The conversion of TNT into HNS is accompanied by the production of intensely coloured species in solution, which may result from processes, such as complex formation, not on the reaction pathway. In order to obtain information on species possibly responsible for these colours, the reactions of TNBCl with a number of alkoxide ions were studied.

4.2. Experimental.

Visible spectra were measured on Unicam SP500 or SP8000 instruments, or measured point by point on the stopped-flow.

^{1}H NMR measurements were made using a Bruker HX 90E instrument, modified for F.T. operation and using a deuterium lock. All shifts are relative to internal tetramethylsilane.

Kinetic measurements for the slowest process in the TNBCl-ethoxide system were made using a Unicam SP500 instrument. Other rates were measured by the stopped-flow technique. In most cases, the various processes had well-separated rates, so that reasonable 'infinity' values could be obtained. However, the second process in the reaction of TNBCl with ethoxide interfered with measurements on the first. In this case, it was assumed[50] that in the early stages the optical density change due to the second reaction was approximately linear with time. Consequently, the first process could be seen as an exponential superimposed on a straight line (the second process extrapolated back to zero time) and hence its rate could be evaluated. Typical results are shown in table 4.1, where the rate constants are calculated from the integrated form of the rate expression.

Table 4.1.

Typical results from rate measurements.

(All measured at 430nm.)

i. TNBCl = 1×10^{-5} M
NaOMe = 0·01 M
Data refer to k_{med}

t (ms)	ΔV^a	k^b (s^{-1})
20	3·60	
40	2·90	10·0
60	2·40	10·1
80	1·95	10·2
100	1·55	10·1
120	1·30	10·2
140	1·05	10·3
160	0·90	9·9
	Mean	10·1

ii. TNBCl = 1×10^{-5} M
NaOEt = 2×10^{-3} M
Data refer to k_{med}

t (ms)	ΔV^a	k^b (s^{-1})
100	5·75	
125	5·00	5·6
150	4·30	6·0
175	3·75	5·5
200	3·25	5·7
225	2·85	5·3
250	2·45	6·0
300	1·90	5·1
350	1·45	5·4
	Mean	5.6

(continued)

a. $\Delta V = V_t - V$

b. $k = \frac{1}{(t-t')} \ln \frac{\Delta V'}{\Delta V}$

Table 4.1. (cont.)

iii. TNBCl = 1×10^{-5} M

$NMe_4O^iPr = 3 \times 10^{-4}$ M

t (ms)	ΔV^a	k^b (s^{-1})
10	4·60	
20	3·65	23
30	2·95	21
40	2·35	23
50	1·95	19
60	1·60	20
70	1·35	17
80	1·10	20
	Mean	20

a. $\Delta V = V_t - V$

b. $k = \frac{1}{(t-t')} \ln \frac{\Delta V'}{\Delta V}$

4.3. Results and Discussion.

4.3.1. General Considerations.

The kinetic and spectroscopic results presented below provide evidence for three types of 1:1 interaction between TNBCl and alkoxide ions, though not all are observed with every alkoxide. These are assigned, in order of decreasing rate, to addition at C-3 to give (4.1), addition at C-1 to give (4.2) and removal of a proton from the side chain to give (4.3). The observed rate coefficients for these three processes are designated as k_{fast}, k_{med} and k_{slow} respectively. The rate data is interpreted in terms of three competing equilibria, as shown in scheme 4.1.

As the base concentration was kept in large excess over that of the parent, first-order conditions apply. The variations of the observed rate coefficients with base concentration are thus given by equations 4.1-4.3.

$$k_{fast} = k_3 [OR^-] + k_{-3} \qquad \text{Eq. 4.1.}$$

$$k_{med} = \frac{k_1 [OR^-]}{1 + K_3 [OR^-]} + k_{-1} \qquad \text{Eq. 4.2.}$$

$$k_{slow} = \frac{k_p [OR^-]}{1 + K_1 [OR^-]} + k_{-p} \qquad \text{Eq. 4.3.}$$

The derivation of 4.3. assumes that the value of K_1 is much larger than that of K_3, which was found to be the case for all the alkoxides studied. When $K_1 [OR^-] \gg 1$, equation 4.3. reduces to equation 4.4.

$$k_{slow} = \frac{k_p}{k_1} + k_{-p} \qquad \text{Eq. 4.4.}$$

Scheme 4.1.

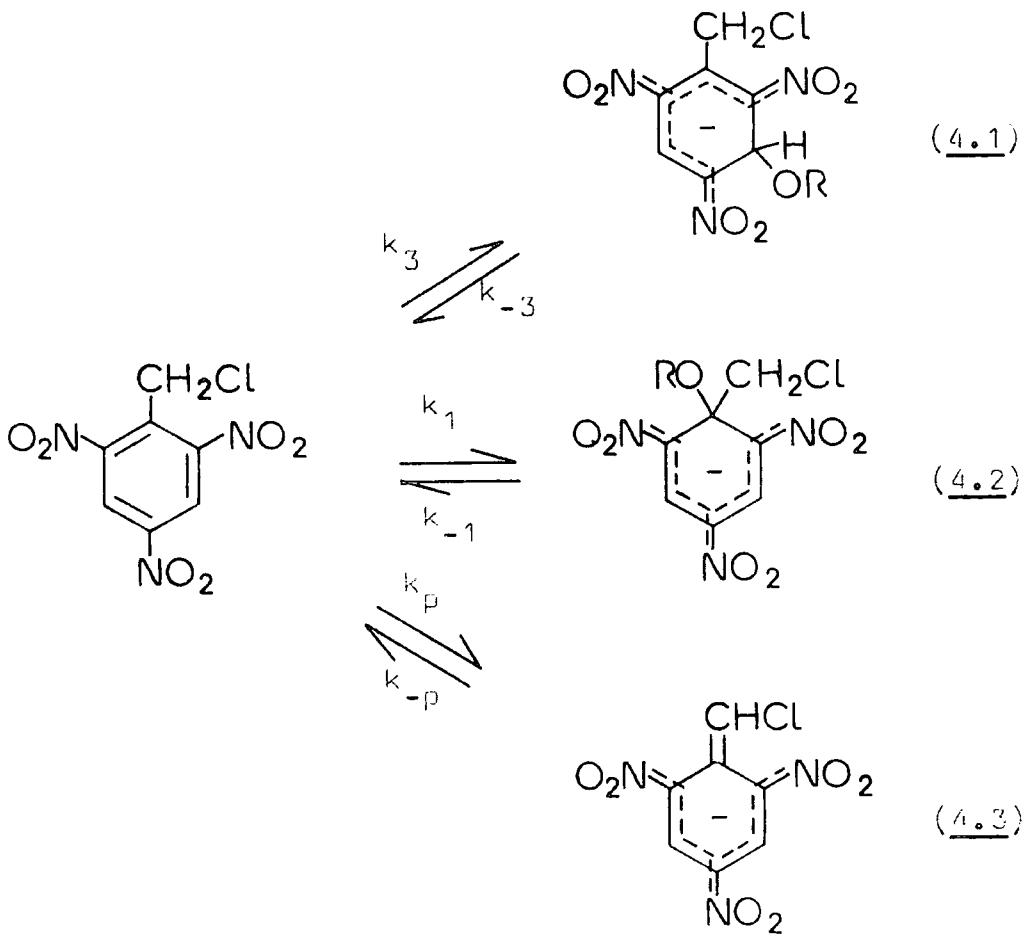
CH2Cl
O2N
NO2
H
OR
NO2
(4.1)
k3
k-3
CH2Cl
O2N
NO2
NO2
k1
k-1
RO
CH2Cl
O2N
NO2
NO2
(4.2)
kp
k-p
CHCl
O2N
NO2
NO2
(4.3)

4.3.2. Methoxide ion in methanol.

Visible spectra of solutions containing TNBCl (5×10^{-5} M) and sodium methoxide (10^{-3} M-10^{-2} M) showed two peaks at λ430nm and 500nm, initially of roughly similar intensities, with two shoulders, the more pronounced at λ 370nm and the other around 650nm. The relative intensities of the two main peaks varied with both time and base concentration, indicating the presence of more than one species. Spectra recorded point by point on the stopped-flow confirmed this: with 10^{-5} M TNBCl and 10^{-2} M base, the species produced initially has λ_{max} 430nm and 510nm, typical of a σ-adduct. The spectrum of this solution changes with time, eventually having maxima similar to those above (figure 4.1.). This spectrum is due to a mixture, in approximately equal proportions, of the initially produced σ-adduct and the conjugate base (4.3), whose spectrum in this instance was generated by adding 0·01 M DABCO to a solution of TNBCl in DMSO.

The 1:1 adduct appears to be stabilised relative to the conjugate base by DMSO, the spectrum of a solution of TNBCl ($2{\cdot}5 \times 10^{-5}$ M) and sodium methoxide (10^{-3} M) in 80:20 v/v DMSO:MeOH showing only the wavelength maxima (at 430nm and 520nm) characteristic of the adduct.

Proton magnetic resonance measurements allowed the identification of the site of addition in the σ-adduct (i.e. at C-3 (4.1) or at C-1 (4.2)). Measurements were made in methanol, DMSO and two mixed solvents, all solvents being fully deuterated.

The spectrum of the parent compound in methanol showed two peaks, at δ9·05 (ring protons) and δ5·08 (CH_2Cl protons). With one half equivalent of sodium methoxide-d_3

Figure 4.1.

Visible spectra of TNBCl (4×10^{-5} M) in the presence of base

A : spectrum, measured by stopped-flow, of the σ-adduct (4.2, R=Me) initially produced in the presence of 10^{-2} M sodium methoxide in methanol.

B : spectrum of the same solution at equilibrium.

C : spectrum of the conjugate base (4.3) produced by the addition of 10^{-2} M DABCO in DMSO solution.

Figure 4.1.

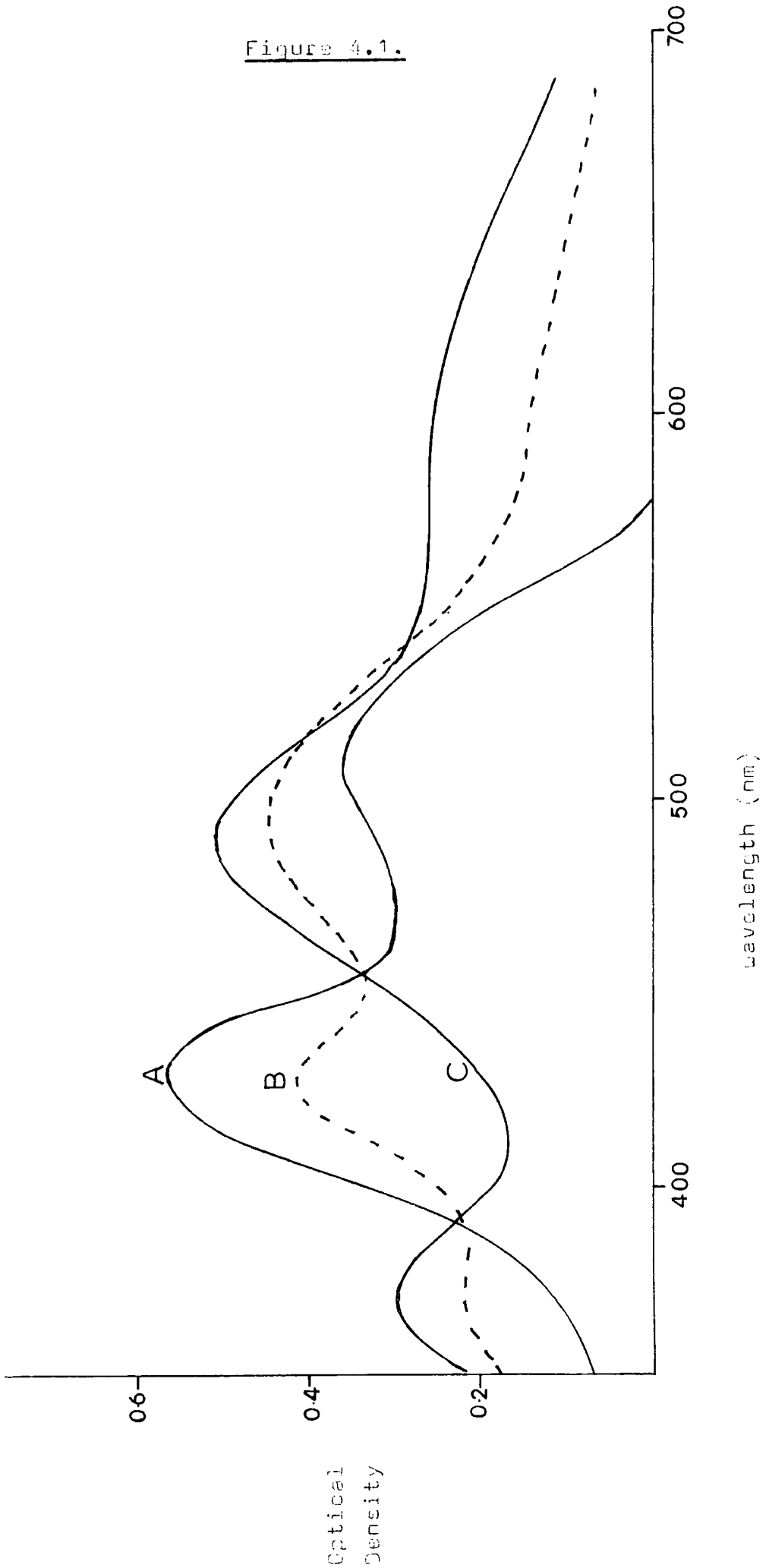

these peaks were reduced in intensity, and three new peaks of roughly equal intensity appeared. These were a singlet at δ6·94, and two doublets at δ8·17 and δ8·56: these data are consistent with the formation of the conjugate base (4.3) in which rotation about the C-CHCl bond is restricted due to its partial double bond character. Similar spectra were obtained with up to one equivalent of base, and no signals which could be assigned to a σ-adduct were observed.

The reverse situation was found in DMSO, where conjugate base formation was not observed (figure 4.2). In this solvent, the peaks due to the parent are found at δ9·09 and δ5·00. The addition of one half equivalent of base resulted in the appearance of two new bands, at δ4·70 and δ8·68. The absence of a band in the area around δ6·0 argues against addition at an unsubstituted carbon, and the adduct is thus assigned the structure (4.2, R=Me). These two peaks increase in intensity, at the expense of those of the parent, with increasing base concentration, conversion appearing complete with 1·5 equivalents of base. Using undeuteriated methoxide, a band was observed at δ3·0, which was attributed to the methoxy protons in the adduct.

In 50:50 DMSO:Methanol, only formation of the complex (4.2, R=Me) was observed, with peaks at δ4·73 (CH_2Cl) and δ8·75 (ring protons).

Both species were observed in 25:75 v/v DMSO:methanol solvent mixture,up to a base:parent ratio of 1:1. The conjugate base peaks were found at δ6·90, (CHCl protons) and δ8·20, δ8·50 (ring protons), these last two being spin-coupled with J 2·3 Hz. The peaks due to the σ-complex· were found at δ8·75 (ring protons) and δ4·70 (CH_2Cl protons).

Figure 4.2.

NMR spectra of TNBCl (0·2 M) and sodium methoxide-d_3 in DMSO-d_6.

A : with 0·5 equivalents of methoxide.

B : with 1·0 equivalents of methoxide.

Figure 4.2.

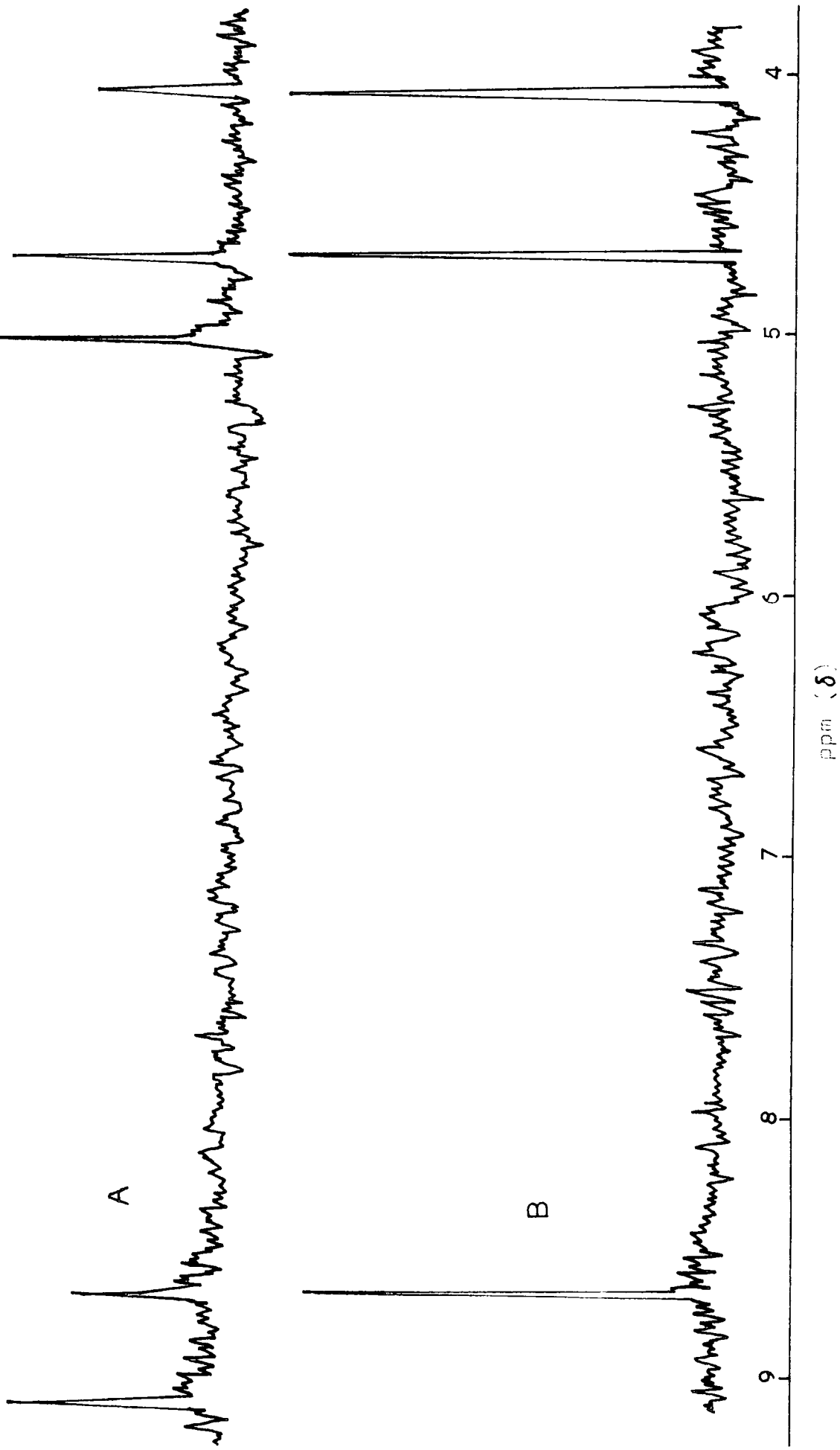

In the presence of more than one equivalent of base, two new doublets, with J 3 Hz, are observed at δ6·2[illegible] and 8·68, together with a singlet at 7·55. These indicate the formation of the dianion (4.4, R=Me) analagous to that formed from TNT[51]. (figure 4.3)

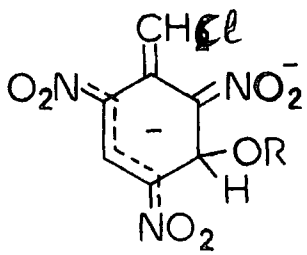

4.4

The NMR data are summarised in table 4.2.

In agreement with the spectral data, stopped-flow spectrophotometry revealed the presence of two processes in methanol, which were assigned to the formation of (4.2, R=Me) (rate coefficient k_{med}) and (4.3) (k_{slow}). The relevant rate and equilibrium data are in table 4.3. The rate coefficients of the faster process are independent of the parent concentration, but increase with the base concentration. A plot of k_{med} versus sodium methoxide concentration is linear which indicates that equation 4.2 reduces in this case to equation 4.5, and thus that $K_3\ [OMe^-] \ll 1$.

$$k_{med} = k_1\ [OMe^-] + k_{-1} \qquad \text{Eq. 4.5}$$

The values obtained from this plot were k_1= 770 ± 30 l mole^{-1}s^{-1}, and k_{-1}= 2·2 ± 0·2 s^{-1}, which combine to give $K_1 (=k_1/k_{-1})$= 350 ± 50 l mole^{-1}. This is in good agreement with the values obtained from optical density measurements at 430nm (330 ± 35 l mole^{-1}) and 500nm (370 ± 35 l mole^{-1}).

Optical density measurements at 500nm at the end of

Figure 4.3.

NMR spectrum of TNBCl (0·2 M) with 1·5 equivalents of sodium methoxide-d_3 in 75/25 CD_3OD/DMSO-d_6.

Figure 4.3.

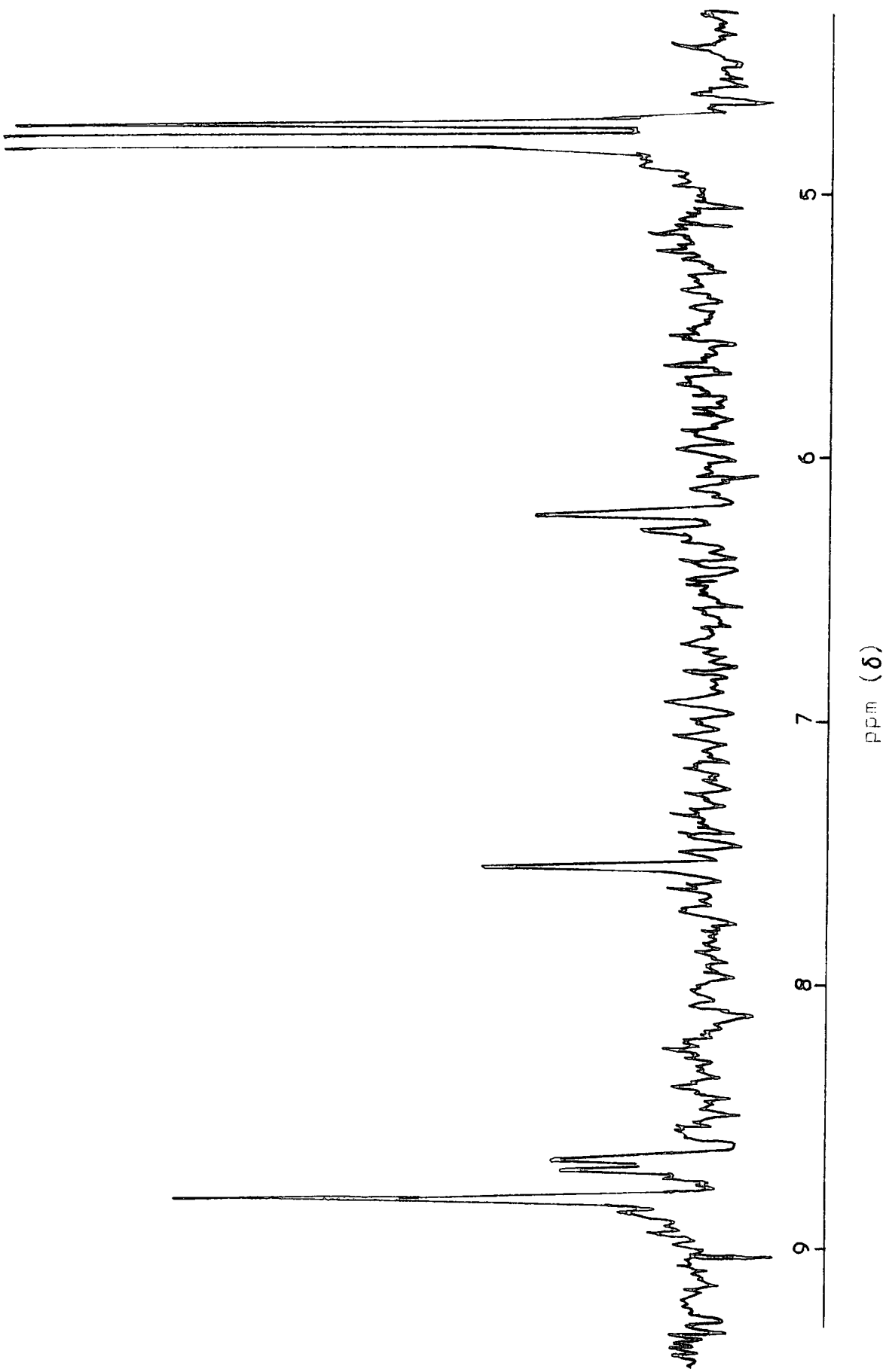

Table 4.2.

Chemical shifts[a] for products of reactions of TNBCl with methoxide.

Solvent[b]	Species	Ring	Side chain	Methoxy
Methanol	TNBCl	9·05	5·08	
"	(4.3)	8·17[c] 8·56[c]	6·94	
DMSO	TNBCl	9·09	5·00	
"	(4.2, R=CD_3)	8·68	4·70	
75:25 MeOH:DMSO	TNBCl	9·06	5·07	
	(4.2, R=CD_3)	8·75	4·70	
	(4.2, R=CH_3)	8·70	4·68	3·00
	(4.3)	8·20[d] 8·50[d]	6·90	
	(4.4, R=Me)	6·22[e] 8.68[e]	7·55	

a. δ values, relative to internal TMS.

b. Fully deuteriated.

c. Doublets.

d. Doublets, J = 2·3 Hz.

e. Doublets, J = 3 Hz.

Table 4.3.

Kinetic and equilibrium data for the reaction of 2,4,6-trinitrobenzyl chloride with sodium methoxide in methanol at 25°C.

[NaOMe] (M)	10^5 [TNBCl] (M)	k_{med} (s^{-1})	O.D.[a] 430nm	K_1 (1 $mole^{-1}$)	O.D.[a] 500nm	K_1 (1 $mole^{-1}$)	O.D.[b] 500nm	K_T (1 $mole^{-1}$)
0·001	1·0	3·0	0·0077	360	0·0047	380	0·0079	590
0·002	1·0	3·9	0·0133	320	0·0075	390	0·012	640
0·002	5·0	3·9	0·051	270	0·033	320	0·055	540
0·002	10·0	4·0	0·0112	320	0·072	370	0·115	590
0·004	1·0	5·4	0·0164	330	0·0107	420	0·015	600
0·007	1·0	7·3	0·0205	340	0·0120	340	0·0168	540
0·010	1·0	10·1	0·0231	380	0·0132	350	0·0185	660

a. After completion of σ-complex formation. Benesi-Hildebrand plots give 0·029 (430nm) and 0·017 (500nm) for the O.D. for complete conversion; with 1 x 10^{-5} M substrate, and 2mm pathlength cells.

b. After completion of both processes. Benesi-Hildebrand plot gave 0·0213 for O.D. for complete conversion; 10^{-5} M parent, 2mm cells.

the second process allowed calculation of an overall equilibrium constant, K_T. Combining the value for K_1, 350 l mole^{-1}, with that obtained for K_T, 600 ± 50 l mole^{-1}, gives a value for K_p, 250 l mole^{-1}, from equation 4.6.

$$K_T = K_1 + K_p \qquad \text{Eq. 4.6}$$

Rate measurements (see table 4.3) on the slow process showed that in the range of methoxide concentration 0·01 M-0·1 M the rate coefficient is independent of base concentration: hence equation 4.4 applies. Using the limiting rate, 0·11 s^{-1}, together with the values for K_1 and K_p, gave values of k_p= 16 l mole^{-1}s^{-1}, and k_{-p}= 0·065 s^{-1}.

No evidence was found for the formation of (4.1, R=Me) in the solutions used in this work. This can be attributed to the low stability expected for this adduct. The values of the equilibrium constants for methoxide addition at an unsubstituted carbon are, for 1,3,5-trinitrobenzene[44] 20 l mole^{-1}, for 2,4,6-trinitroanisole[17] 2·7 l mole^{-1} and for 2,4,6-trinitrotoluene[78] 0·07 l mole^{-1}. Also, by analogy to the sulphite additions described in the previous chapter, the ratio of the equilibrium constants for TNBCl and TNT should be of the order of 25. Thus the concentrations of the C-3 adduct in equilibrium with TNBCl and base in the solutions used are likely to be small.

The value obtained for the rate constant for methoxide departure, k_{-1}, provides further evidence for addition at C-1. Typically, values for methoxide expulsion from a ring-carbon carrying hydrogen are of the order of 300 s^{-1}, significantly higher than the value of 2·2 s^{-1} found here.

Table 4.4.

Rate coefficients for equilibration of (4.2) and (4.3) in methanol at 25°C.

[NaOMe] (M)	k_{slow} (s^{-1})
0·01	0·116
0·02	0·118
0·04	0·113
0·07	0·107
0·10	0·108

4.3.3. Ethoxide Ion in Ethanol.

Visible spectra (see figure 4.4) of solutions containing sodium ethoxide (10^{-3}M-10^{-2}M) and TNBCl (4×10^{-5}M) showed the rapid formation of an orange species, with λ_{max} 430nm and 510nm, followed by the appearance of a second species having λ_{max} 370nm, 500nm and 650nm, both species being present st equilibrium. These data are interpreted in terms of the formation of a σ-adduct, with subsequent equilibration with the conjugate base (4.3).

With 0·1 M base, the initial orange coloration was replaced fairly rapidly by a crimson-pink colour, with λ_{max} at 516nm. This is likely to be due to a 1:2 interaction, forming either a dianion similar to that with methoxide, or a diadduct by addition of two ethoxide ions.

^{1}H NMR spectra were in agreement with these results. On the addition of one half equivalent of base to a solution of TNBCl in DMSO-d_6, the peaks due to the parent decreased in intensity, whilst two new bands appeared at δ4·68 and δ8·68. This is in accord with the formation of a σ-adduct by addition at C-1 (4.2, R=Et). The methylene protons in the adduct were also observed, as a peak at δ3·09 separate from the bulk resonance at δ3·37.

A similar pattern was observed with one and two equivalents of base. Also, a peak developed with time at δ7·25 in these solutions, possibly due to formation of the conjugate base. However, no corresponding ring proton peaks were observed.

Stopped-flow spectrophotometry revealed the presence in dilute base solutions of three processes in this system, which were interpreted in terms of scheme 4.1. At ethoxide concentrations greater than 0·002 M, a rapid colour-forming

Figure 4.4.

Visible spectra of TNBCl (5×10^{-5} M) and sodium ethoxide (1×10^{-3} M) in ethanol, taken at 2 minute intervals (A - D), showing the equilibration between (4.2, R=Et) and (4.3)

Figure 4.4.

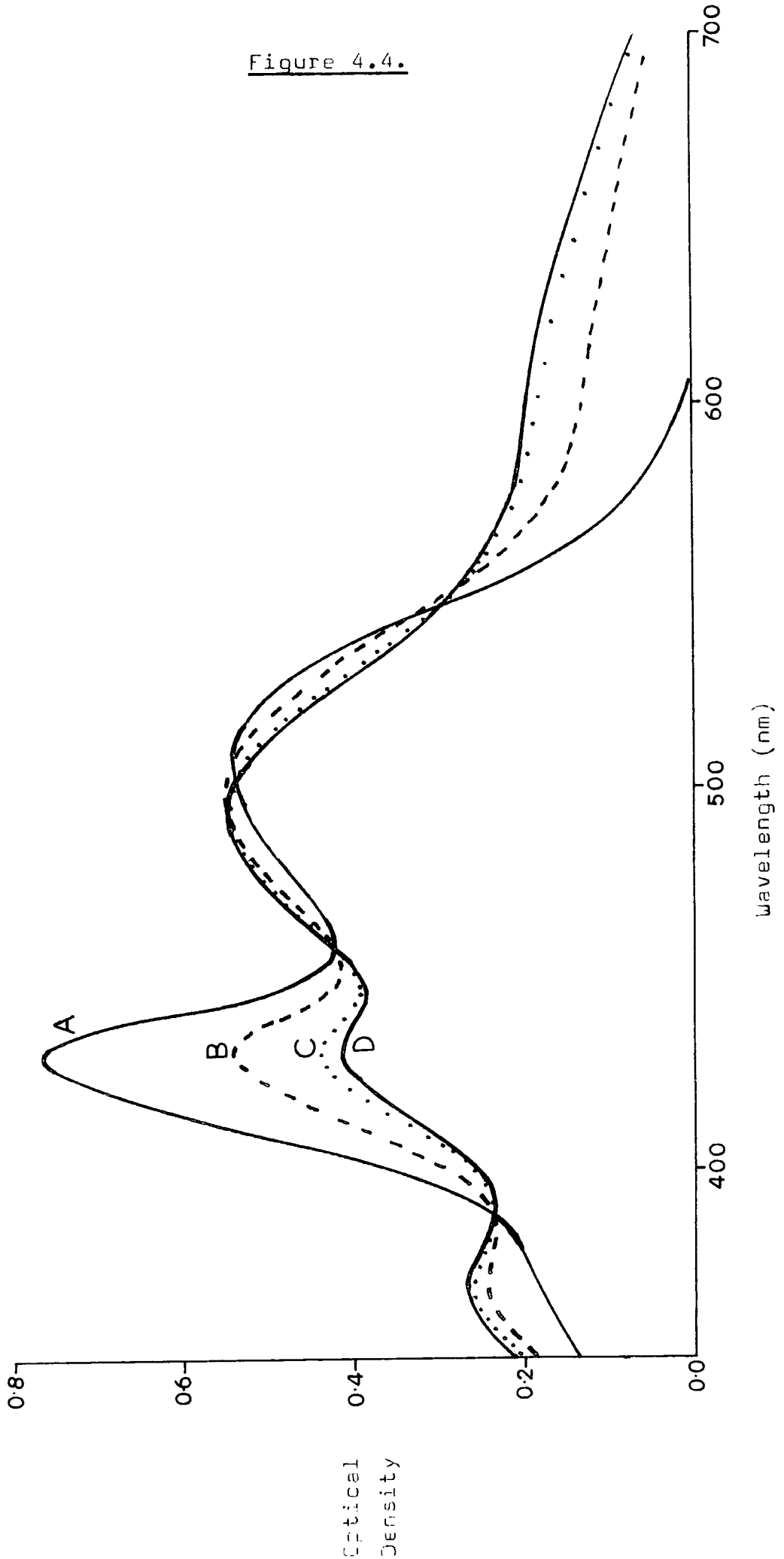
A
B
C
D
0·8
0·6
0·4
0·2
0·0
Optical Density
400
500
600
700
Wavelength (nm)

reaction was observed, whose spectrum, as obtained from measurements on the stopped-flow had λ_{max} 430nm and 510nm. In view of the subsequent equilibration of this species, which was also quite fast, and the stability of the C-1 adduct as deduced from the NMR measurements, this species was assigned the structure (4.1, R=Et). The equilibration reaction means that the values of the rate coefficient for this first process, k_{fast} (see table 4.5) are subject to quite large errors - consequently, a plot of k_{fast} versus ethoxide concentration gave a straight line, as expected from equation 4.1, with a slope (k_3) of 10^4 l mole^{-1}s^{-1}, but with an uncertain intercept (k_{-3}).

The second process is also colour-forming, and corresponds to the formation of (4.2, R=Et). This is the species responsible for the orange colour observed in the visible spectra, and has an almost identical visible spectrum to that of (4.1, R=Et). The similarity of the spectra of such isomeric adducts is not unexpected, having been observed in the case of the methoxide adducts of 2,4,6-trinitroanisole[17]. Rate data for this process were measured at 430nm, and are also in table 4.5. The variation of the rate coefficients, k_{med}, is described by equation 4.2, and an iterative procedure was used to calculate values for the rate and equilibrium parameters. The equation is well fitted with K_3 700 l mole^{-1}, k_1 7000 l mole^{-1}s^{-1} and k_{-1} negligibly small. Using this value for K_3, and the known value of k_3, a value for k_{-3}, ($=k_3/K_3$) of 14 s^{-1} was obtained. The optical density values measured at the end of this second process are independent of the base concentration down to the lowest concentrations used (10^{-3} M). This indicates a very high

Table 4.5.

Kinetic data for the reaction of 2,4,6-trinitrobenzyl chloride with sodium ethoxide in ethanol at 25°C.

[NaOEt] (M)	k_{fast} (s^{-1})	k_{med} (s^{-1})	k_{med}[a] calc(s^{-1})	O.D.[b] 430nm	k_{slow} (s^{-1})
0·001		3·8	4·1	0·029	
0·0013		4·4	4·8	0·032	
0·0015		5·0	5·1	0·029	0·0071
0·0017		5·3	5·4	0·031	
0·002		5·7	5·8	0·030	
0·0026		6·4	6·5	0·031	
0·003	35±10	6·8	6·8	0·029	0·0067
0·005	60	7·4	7·7	0·029	0·0074
0·0075	85	8·7	8·8	0·030	0·0079
0·010	117				

a. Calculated from equation 4.2 with K_3 700 l $mole^{-1}$, k_1 7000 l $mole^{-1}s^{-1}$ and k_{-1} 0.

b. After completion of the second rate process, k_{med}.

value for K_1 : 90% conversion to complex at 10^{-3} M base would require a value for K_1 of 9000 l $mole^{-1}$, so the actual value is likely to be greater than 10^4 l $mole^{-1}$.

The third process observed was slow enough to follow by conventional spectrophotometry. The rate coefficients for this reaction, equilibration between (4.2, R=Et) and (4.3) are independent of base concentration, as expected for the case where K_1 $[OR^-]$ is very much greater than unity.

4.3.4. Isopropoxide ion in isopropanol.

Visible spectra indicate the rapid formation of a σ-adduct, with λ_{max} 430nm and 505nm, when solutions of TNBCl and sodium isopropoxide are mixed. Over a period of time, a small peak develops at 380nm, and the lower wavelength peak due to the complex decreases in intensity indicative of the formation of the conjugate base. However, as this reaction was so slow, and was accompanied by irreversible decomposition reactions, it was not quantitatively studied. NMR measurements on this system did not allow the unambiguous identification of any of the species produced.

Rate measurements were made at 430nm, and are in table 4.6. The effects of the high degree of ion association in sodium isopropoxide ($K_{Na^+PrO^-}$ = 1·9 x 10^4 l $mole^{-1}$)[79] can be seen in the plot of rate coefficient against sodium isopropoxide concentration (figure 4.5) which shows obvious curvature. The use of tetramethylammonium isopropoxide greatly reduces the extent of ion-pairing in dilute solutions. For these solutions, a plot of the observed rate coefficients versus isopropoxide concentration was linear, giving a slope of 10^5 l $mole^{-1}s^{-1}$, and passing through the origin. To obtain data for the

Table 4.6.

Rate coefficients for the addition of isopropoxide ion to TNBCl (1×10^{-5} M) in isopropanol at 25^{o}C.

10^4 [NaO^iPr] (M)	10^4 [NMe_4O^iPr] (M)	[$NaBPh_4$] (M)	k_{fast} (s^{-1})
4·0			11
7·0			20
10			32
20			46
40			73
70			118
100			162
5		0·01	5
20		0·01	20
35		0·01	33
50		0·01	54
	3		20
	3·8		35
	4·5		40
	6·0		54
	7·5		76
	10		93

Figure 4.5.

Plot of k_{obs} versus base concentration for the complex-forming reaction between isopropoxide and TNBCl in isopropanol.

Figure 4.5.

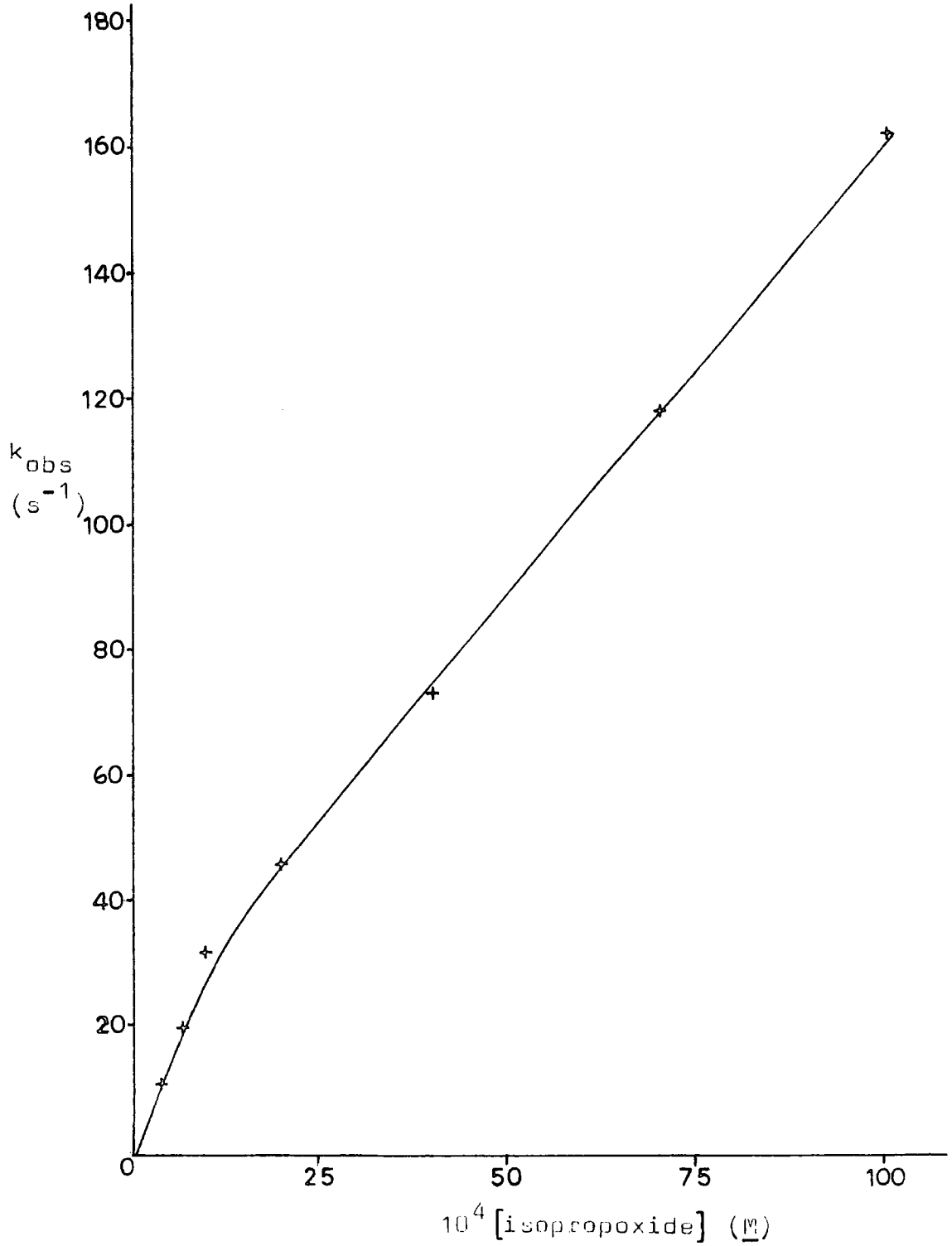
180
160
140
120
100
80
60
40
20
0
k_{obs} (s^{-1})
25
50
75
100
10^4 [isopropoxide] (M)

opposite limit, sodium tetraphenylborate was added to ensure complete ion-pairing - here again a straight line was obtained, in this case with a slope of 10^4 l $mole^{-1}s^{-1}$ and again with a negligible intercept. These values indicate a much greater reactivity for the free isopropoxide ion than for the ion pair, a situation which has been observed[21] in the addition of isopropoxide ion to 1,3,5-trinitrobenzene.

Optical density measurements at the end of the reaction indicate that conversion to the complex is virtually complete in all solutions used. This is to be expected from the very high carbon basicity [21] of the isopropoxide ion, which leads to large values for the equilibrium constants with, as found, a high value for the forward rate constants and very low values for the reverse rate constants. Thus the equilibration of this species, which is kinetically favoured, with the thermodynamically preferred species will be very slow. The nature of the complex formed in these reactions cannot be unequivocally determined, but is more likely to be the C-3 adduct. The forward rate constant for (unpaired) isopropoxide addition to 1,3,5-trinitrobenzene is $2{\cdot}6 \times 10^5$ l $mole^{-1}s^{-1}$ [21], of the same order of magnitude as that obtained in this case.

4.3.5. Comparison with other substrates.

The data for the reactions discussed above are collected in table 4.7, together with corresponding data for 2,4,6-trinitrotoluene and 1,3,5-trinitrobenzene. The TNT data for methoxide addition are taken from the next chapter, and are included here for the sake of completion. The most obvious difference between TNT and TNBCl is

Table 4.7.

Comparison of the reaction of 2,4,6-trinitrobenzyl chloride, 2,4,6-trinitrotoluene and 1,3,5-trinitrobenzene with sodium methoxide in methanol and sodium ethoxide in ethanol at 25°C.

	k_3 ($l\ mole^{-1}s^{-1}$)	k_{-3} (s^{-1})	K_3 ($l\ mole^{-1}$)	k_1 ($l\ mole^{-1}s^{-1}$)	k_{-1} (s^{-1})	K_1 ($l\ mole^{-1}$)	k_p ($l\ mole^{-1}s^{-1}$)	k_{-p} (s^{-1})	K_p ($l\ mole^{-1}$)
TNBCl-OMe			20	770	2·2	350	16	0·065	250
TNT-OMe	280	3000	0·07				13·3[a]	1·1[a]	12·4[a]
TNB-OMe[b]	7300	330	20						
TNBCl-OEt	10000	14	700	7000	1	10000			
TNT-OEt[a]							82	0·045	1800
TNB-OEt[b]	40000	20	2000						

a. Ref 50

b. Ref 44 (refers to addition at an unsubstituted position)

that the thermodynamically-preferred alkoxide adduct from TNBCl is formed by addition at C-1, rather than C-3 as in the case of TNT[51]. In a similar pattern to methoxide attack on 2,4,6-trinitroanisole[17], the adduct at C-3 is formed more rapidly, but is not as stable as the C-1 adduct. However, in this case the reasons for this behaviour will be different to those in the anisole case. The greater inductive withdrawal of the chloromethyl group in TNBCl compared with the methyl group of TNT is one factor which will favour alkoxide attack at the 1-position. However, the major influence is likely to be steric. Relief of steric strain between the ortho nitro groups and the 1-substituent will be greater in the case of the bulky CH_2Cl group than for the less-strained TNT molecule.

The value of the equilibrium constant for addition at C-1 is greater than that for C-3 addition as a result of the considerably lower rate of expulsion of alkoxide ion from the former adduct, the forward rate constant for C-1 addition being smaller than that for C-3.

The ethoxide adduct of 1,3,5-trinitrobenzene is slightly more stable than the C-3 adduct of TNBCl, both adducts involving addition at an unsubstituted carbon. Here the inductive effect of the CH_2Cl group is presumably offset by its steric effect, which will hinder the ability of the adjacent nitro groups to accept negative charge.

A comparison of the values of K_p, the equilibrium constant for transfer of a side-chain proton, for TNT and TNBCl shows that the electronegative chlorine atom enhances the acidity of the adjacent proton. However, the enhancement here is by a factor of approximately twenty, whereas the reported[80] enhancement for 4-nitrobenzyl chloride

over 4-nitrotoluene is approximately 700. As the NMR data show, the CHCl-ring carbon bond in the conjugate base (4.3) has some double bond character, and hence the chlorine atom will be held to some extent in the plane of the ring. In this position it will interact unfavourably with the adjacent nitro group, and hence its acid-enhancing properties will be reduced, no such interactions occurring in the trinitrobenzyl anion.

CHAPTER FIVE

THE INTERACTIONS OF 2,4,6-TRINITROTOLUENE WITH SODIUM METHOXIDE, AND THE REACTIONS OF 2,4,6-TRINITROTOLUENE AND 1,3,5-TRINITROBENZENE WITH SODIUM HYPOCHLORITE

5.1. Introduction.

The reactions of 2,4,6-trinitrotoluene with sodium methoxide have been the subject of a number of investigations. Bernasconi[50] observed two processes in methanol under conditions of excess base, the slower of which was assigned to proton transfer to give the conjugate base (5.2) (scheme 5.1). Measurements on the fast process were not made, however, because the equilibrium concentration of the species produced was too small.

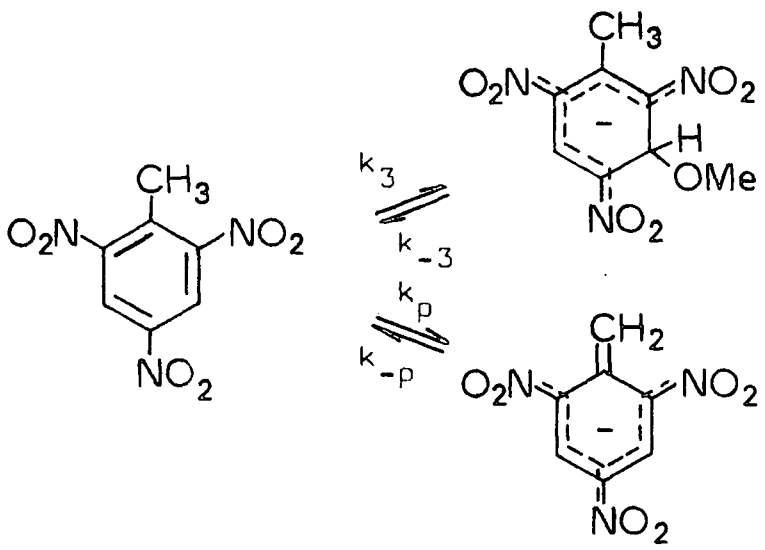

Scheme 5.1

A flow-NMR study[51] in DMSO-rich media identified the product of the fast reaction as the C-3 adduct (5.1).

In the work reported in this chapter use was made of the stabilisation of the adduct by DMSO to obtain kinetic and equilibrium data for its formation in DMSO/MeOH mixtures. These data were then extrapolated to obtain values in pure methanol.

The intense colours produced in the reaction of TNT with sodium hypochlorite to give hexanitrostilbene could be due to species such as (5.1) and (5.2). In order to assess this possibility, and the nucleophilicity of the

hypochlorite ion, the reaction of sodium hypochlorite with 1,3,5-trinitrobenzene in methanol/water was studied, and compared with results obtained with TNT under the same conditions.

5.2. Experimental.

Visible spectra were recorded on a Unicam SP8000 instrument, or measured point by point on the stopped-flow spectrophotometer.

Kinetic measurements were made at suitable wavelengths using the stopped-flow spectrophotometer.

Methanol/dimethylsulphoxide solvent mixtures were made up by mixing measured volumes of each component.

Hypochlorite solutions were buffered at pH 10 using borax/sodium hydroxide buffer solutions.

5.3. Results and Discussion.

5.3.1. 2,4,6-Trinitrotoluene and Sodium Methoxide.

Stopped-flow spectrophotometry revealed the presence in dilute methoxide solutions of two processes attributable to 1:1 interaction, in methanol:dimethylsulphoxide mixtures containing 40,50 and 60% DMSO by volume. The faster of these gave a species whose spectrum, obtained from stopped-flow measurements, showed λ_{max} 430nm and 495nm, whilst the second gave rise to a species with λ_{max} 370nm, 525nm and 650nm (Figure 5.1). These are attributed to the formation of the σ-adduct (5.1) and the conjugate base (5.2) respectively.

Kinetic measurements were made under first order conditions with the concentration of sodium methoxide in large excess over that of the parent. As the rates of the two processes were well separated, equations 5.1 and 5.2 apply.

$$k_{fast} = k_3 \left[MeO^-\right] + k_{-3} \qquad \text{Eq. 5.1.}$$

$$k_{slow} = k_{-p} + \frac{k_p \left[MeO^-\right]}{1 + K_3 \left[MeO^-\right]} \qquad \text{Eq. 5.2.}$$

Measurements on the first process were made at 430nm, and the rate and equilibrium data are in tables 5.1-5.3. For each solvent composition plots of k_{fast} versus methoxide concentration were linear, as expected from equation 5.1, and yielded values of k_3, k_{-3} and K_3(from k_3/k_{-3}). Optical densities measured at the end of this process were used to calculate values for K_3, which in each

Figure 5.1.

Visible spectra, obtained by stopped-flow spectrophotometry, of A, the σ-adduct (5.1) and B, the conjugate base (5.2) in 60/40 (v/v) DMSO/methanol.

Figure 5.1.

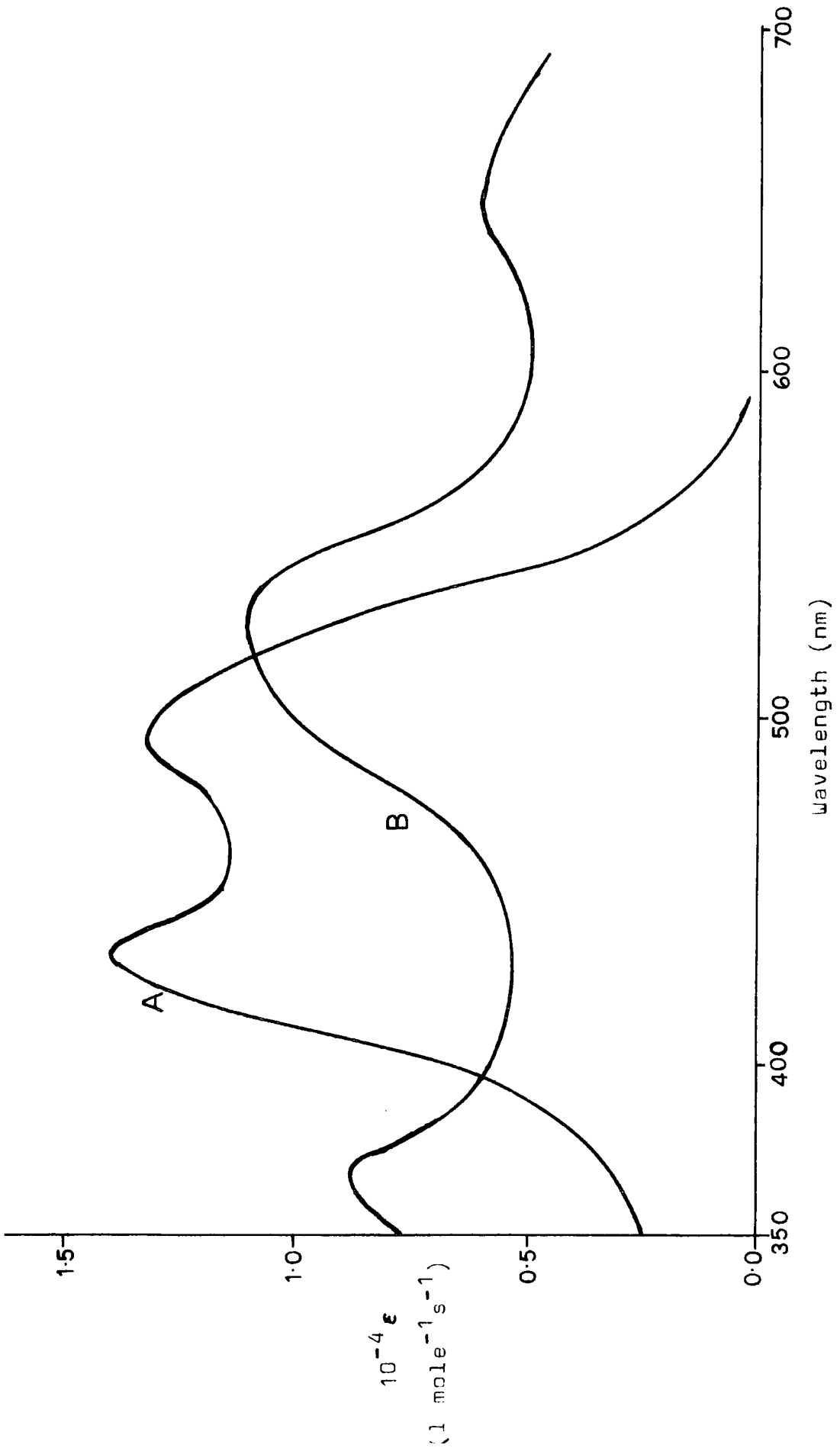
A
B
1·5
1·0
0·5
0·0
350
400
500
600
700
Wavelength (nm)
$10^{-4}\,\varepsilon$
(l mole^{-1}s^{-1})

Table 5.1.

Kinetic and equilibrium data for the 1:1 interaction of 2,4,6-trinitrotoluene and sodium methoxide in 40:60 (v/v) DMSO-methanol at 25°C.

[NaOMe] (M)	k_{fast} (s^{-1})	O.D.[a] 430nm	K_3[b] (l $mole^{-1}$)	k_{slow} (s^{-1})	k_{calc}[c] (s^{-1})	O.D.[d] 600nm
0·005	122	0·0126	23	1·00	1·00	0·045
0·010	124	0·0241	25	1·61	1·79	0·045
0·015	138	0·0355	28	2·68	2·43	0·045
0·020	142	0·0407	26	3·39	2·96	0·045
0·025	171	0·0464	25	3·37	3·41	0·044
0·030	180					
0·040	207					
0·050	244					

a. After completion of first process; 4×10^{-5} M parent; 2mm pathlength cell.

b. Calculated from O.D. values and a value of 0·120 for complete conversion (Benesi-Hildebrand plot)

c. Calculated from equation 5.3 with k_p 225 l $mole^{-1}s^{-1}$ and K_3 26 l $mole^{-1}$.

d. After completion of second process.

Table 5.2.

Kinetic and equilibrium data for the 1:1 interaction of 2,4,6-trinitrotoluene and sodium methoxide in 50:50 (v/v) DMSO-methanol at 25°C.

[NaOMe] (M)	k_{fast} (s^{-1})	O.D.[a] 430nm	K_3[b] (l $mole^{-1}$)	k_{slow} (s^{-1})	k_{calc}[c] (s^{-1})	O.D.[d] 600nm
0·0024	46	0·0174	170	0·90	0·92	0·022
0·0048	63	0·0258	157	1·44	1·44	0·021
0·0071	73	0·0331	173	1·75	1·76	0·021
0·0095	86	0·0363	161	2·02	2·02	0·021
0·0119	99	0·0415	189	2·27	2·17	0·022

a. After completion of first process; 2×10^{-5} M parent; 2mm pathlength cell.

b. Calculated from O.D. values and a value of 0·060 for complete conversion (Benesi-Hildebrand plot)

c. Calculated from equation 5.3, with k_p 530 l $mole^{-1}s^{-1}$ and K_3 160 l $mole^{-1}$.

d. After completion of second process.

Table 5.3.

Kinetic and equilibrium data for the 1:1 interaction of 2,4,6-trinitrotoluene and sodium methoxide in 60:40 (v/v) DMSO-methanol at 25°C.

[NaOMe] (M)	k_{fast} (s^{-1})	O.D.[a] 430nm	K_3[b] (l $mole^{-1}$)	k_{slow} (s^{-1})	k_{calc}[c] (s^{-1})	O.D.[d] 600nm
0·002	35	0·0199	990	0·51	0·60	0·010
0·006	34	0·0243	1070	0·78	0·75	0·010
0·008	84	0·0254	920	0·79	0·78	0·010
0·010	138	0·0273	1010	0·86	0·84	0·010

a. After completion of first process; 1 x 10^{-5} M parent; 2mm pathlength cells.

b. Calculated from O.D. values and a value of 0·030 for complete conversion (Benesi-Hildebrand plot)

c. Calculated from equation 5.3, with k_p 1000 l $mole^{-1}s^{-1}$ and K_3 1100 l $mole^{-1}$.

d. After completion of second process.

case were in good agreement with those obtained from kinetic measurements. Measurements in media of other composition were not made due to the unavoidably high uncertainties in the values of k_3 (in media containing less than 40% DMSO) and k_{-3}(media containing more than 60% DMSO).

Measurements on the second process were made at 600nm, where there was no optical density change due to the first process: these data are also in tables 5.1-5.3. The optical density at completion of this process was independent of the concentration of methoxide for each solvent system, indicating a very high value for K_p in each system used. Consequently, in the analysis of the kinetic data, k_{-p} was assumed to be negligible, and hence equation 5.2 reduced to 5.3. Reciprocal plots according

$$k_{slow} = \frac{k_p [MeO^-]}{1 + K_3 [MeO^-]} \qquad \text{Eq. 5.3.}$$

$$1/k_{slow} = 1/k_p [MeO^-] + K_3/k_p \qquad \text{Eq. 5.4.}$$

to equation 5.4 were used to obtain values for k_p. Values for the rate coefficients for this process were calculated from the derived parameters, and are presented in tables 5.1-5.3.

A third process, which was very slow on the stopped-flow timescale, was also observed, consistent with the formation[51] of the dianion (5.3). Quantitative measurements

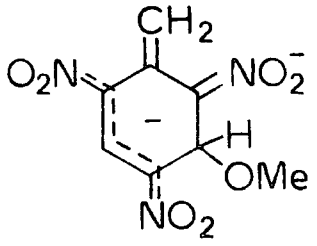

5.3

were not made on this reaction.

Rate and equilibrium parameters for the first two processes are collected in table 5.4. As before (chapter three), plots of k_3 and k_{-3} versus the mole fraction of DMSO allowed extrapolation to pure methanol (see figure 5.2), and the derived values are also in table 5.4.

An acidity function approach was also used, as an alternative route to the determination of K_3. A J_m acidity function, defined by equation 5.5, had previously been determined in methanol-dimethylsulphoxide mixtures containing 0·098 M sodium methoxide, using σ-complex formation from 1-X-3,5-dinitrobenzenes[75].

$$J_m = p(K_3K_{MeOH}) + \log_{10} [\text{complex}] / [\text{parent}] \quad \text{Eq. 5.5.}$$

This function was appropriate for this case, since, as with TNT, base addition occurs at an unsubstituted ring position in these compounds. Stopped-flow spectrophotometry was used to measure values of optical density at the completion of the first process, and these were used to calculate indicator ratios. The data are in table 5.5. Using the known values of J_m, values of $p(K_3K_{MeOH})$ were calculated. Subtraction of the value of pK_{MeOH} (16·92) gave a value for pK_3 of 1·26 ± 0·1, leading to a value for K_3 of $(5·5 \pm 1·5) \times 10^{-2}$ l mole^{-1}.

These results give an overall value for K_3 of 0·07 ± 0·03 l mole^{-1}, which can be compared with a value of 20 l mole^{-1} for methoxide addition to 1,3,5-trinitrobenzene at an unsubstituted position. The polar effect of the methyl group in TNT will be a factor in reducing complex stability, as will its steric effect. The presence of the methyl group will introduce steric strain around

Rate and equilibrium parameters for the reactions of 2,4,6-trinitrotoluene with sodium methoxide.

Solvent	k_3 ($l\ mole^{-1}s^{-1}$)	k_{-3} (s^{-1})	K_3^a ($l\ mole^{-1}$)	K_3^b ($l\ mole^{-1}$)	k_p ($l\ mole^{-1}s^{-1}$)
60% DMSO (v/v)	12000 ± 100	10 ± 3	1200 ± 300	1000 ± 200	1000 ± 200
50% DMSO (v/v)	5400 ± 200	35 ± 2	155 ± 15	165 ± 10	530 ± 30
40% DMSO (v/v)	2800 ± 200	100 ± 5	28 ± 3	25 ± 2	225 ± 25
Methanol[c]	280 ± 50	3000 ± 500	0·09 ± 0·03	0·10 ± 0·03	20 ± 5

Table 5.4.

a. From kinetic data

b. From equilibrium data

c. Extrapolated values

Figure 5.2.

Variation with solvent composition of kinetic parameters for the formation of(5.1).

A : k_3

B : k_{-3}

Figure 5.2.

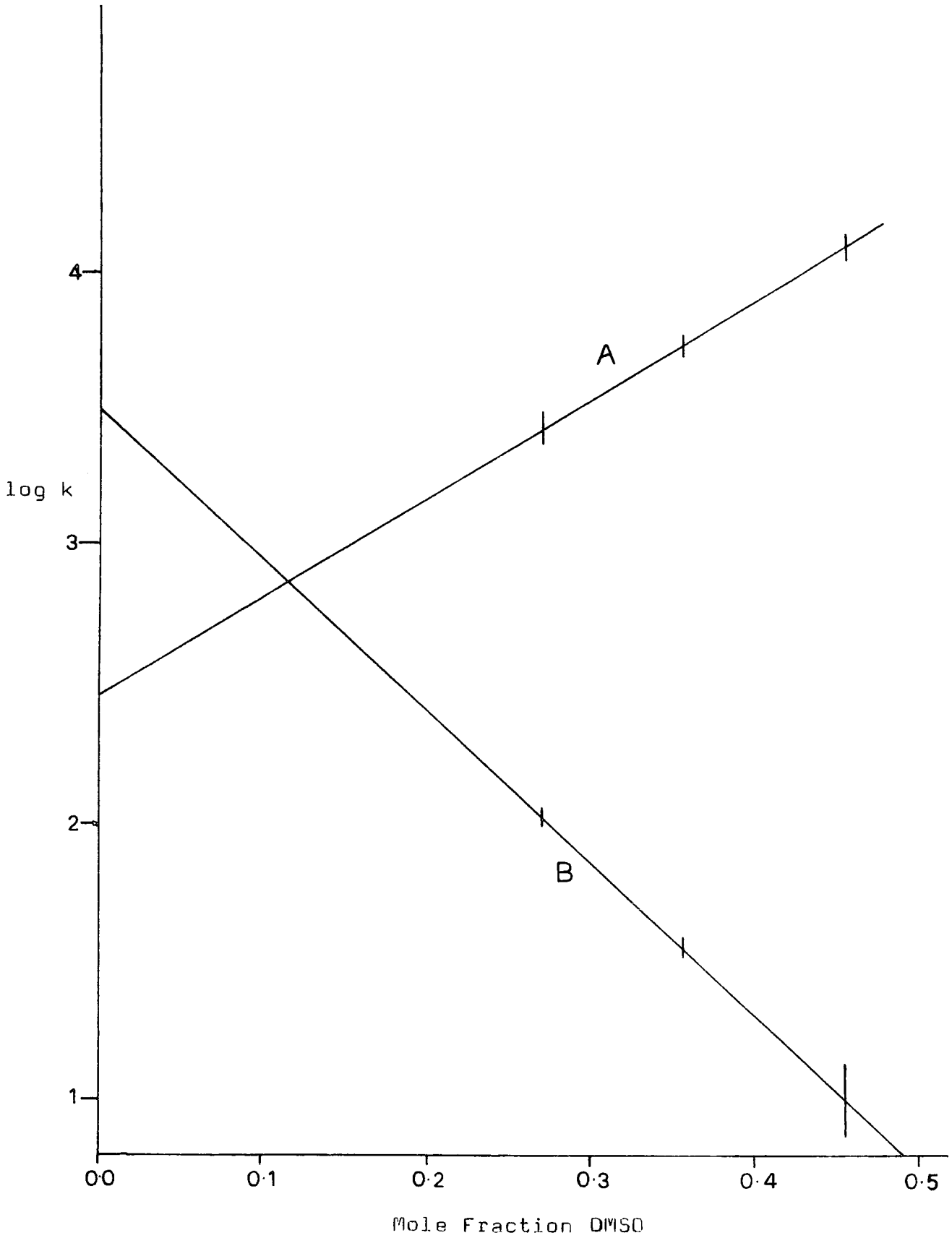

Table 5.5.

Calculation of the value of K_3 using J_m acidity function.

Volume % DMSO	O.D.[a] 430nm	$\log_{10}$ [complex]/[parent]	J_m[b]	$p(K_3K_{MeOH})$
25	0·0048	-0·73	17·46	18·19
30	0·0083	-0·43	17·82	18·25
35	0·0150	-0·01	18·15	18·16
40	0·0232	+0·50	18·53	18·03
50	0·0281	+1·07	19·35	18·28
60	0·0302			
70	0·0307			

a. For 1×10^{-5} M parent, with a 2mm pathlength cell

b. From reference 75

the 1-position, hindering the planarity of the adjacent nitro groups and hence reducing their ability to accept negative charge. The reduced stability of the TNT adduct compared with that from TNB derives from both a smaller value for the forward rate constant (280 l $mole^{-1}s^{-1}$ against 7300 l $mole^{-1}s^{-1}$) and a higher value for the rate constant for the reverse reaction (3000 s^{-1} against 330 s^{-1}).

In contrast to 2,4,6-trinitrobenzyl chloride, where at equilibrium both the σ-adduct and the conjugate base are present, the thermodynamically stable product of the reaction of TNT with methoxide is the conjugate base (5.2). The value for k_p of 20 ± 5 l $mole^{-1}s^{-1}$ obtained here can be compared with a previous value[50] in methanol of 13·3 l $mole^{-1}s^{-1}$, where the value of K_p was 12·4 l $mole^{-1}$.

5.3.2. 1,3,5-Trinitrobenzene and Sodium Hypochlorite in 50:50 (v/v) methanol:water.

The visible spectrum, measured on a conventional spectrophotometer, of a solution containing 1,3,5-trinitrobenzene (2×10^{-4} M) and sodium hypochlorite (0·05 M) showed two peaks, at λ430nm and 480nm, similar to those of alkoxide complexes. Examination by stopped-flow spectrophotometry revealed the presence of two well-separated colour forming reactions at 480nm.

The faster of these two was too rapid for measurement on the stopped-flow timescale, whilst the second had a half-life of $\sim 0{\cdot}1 s^{-1}$. These were followed by a much slower irreversible fading process. The relevant data is in table 5.6.

The possible nucleophiles in this system are hydroxide, methoxide and hypochlorite ions, the data being in accord

Table 5.6.

Reaction of 1,3,5-Trinitrobenzene with Sodium Hypochlorite in 50:50 (v/v) methanol:water at 25°C.

[TNB] (M)	[NaOCl] [a] (M)	O.D.[b] 490nm	O.D.[c] 490nm	k_{obs} [d] (s^{-1})
$5x10^{-4}$	0·025	0·00524	0·00745	8·1±0·5
$5x10^{-4}$	0·063	0·00877	0·0132	7·3±1
$5x10^{-4}$	0·125	0·0182	0·0292	7·5±1

a. Buffered at pH 10

b. After completion of first process - 2mm pathlength cell

c. After completion of both colour-forming processes - 2mm pathlength cell

d. Refers to the slower of the two colour-forming processes

with addition by the first two only. Data published by Bernasconi and Bergstrom[81] on methoxide and hydroxide additions indicate that, under these conditions, the rate constant associated with methoxide addition to TNB has a value of $\sim 300\ s^{-1}$, while the corresponding value for hydroxide addition is $\sim 10\ s^{-1}$. Consequently, the faster process, too rapid to measure by stopped-flow, was attributed to methoxide addition, and the second, measured, process to hydroxide addition. Further evidence for these assignments comes from the fact that the optical densities at the end of the two processes are in a constant ratio. This is in accord with addition by nucleophiles present in solution in a constant ratio, whereas if one of the processes were due to hypochlorite addition, the relative magnitude of the change due to that process would be expected to increase with increasing hypochlorite concentration. Thus it appears that the hypochlorite ion, the anion of hypochlorous acid (pK_a 7·53), is too weak a nucleophile to form σ-adducts with TNB in this solvent.

5.3.3. 2,4,6-Trinitrotoluene and Sodium Hypochlorite in methanol-water.

Visible spectra of solutions of TNT (10^{-4} - 10^{-3} M) and sodium hypochlorite (0·1 M) in 50:50 (v/v) methanol:water showed two peaks at 430nm and 510-520nm, the orange-red colour fading quite rapidly.

In contrast to this, solutions containing TNT and sodium methoxide in 70:30 (v/v) methanol:water had the purple coloration typical of the conjugate base (5.2), with λ_{max} 365, 510 and 650nm, in agreement with previous work[50,51].

These spectra indicate that the conjugate base (5.2) is not the major coloured species produced from TNT in the presence of hypochlorite, although it is probably an intermediate in the formation of TNBCl from TNT. In view of the evidence in this chapter which shows TNT to be less susceptible to addition than TNB, it seems unlikely that the process occuring is direct addition of hypochlorite ion to the TNT ring, as this does not occur with TNB. Another possibility as the source of the colour is the Janovsky complex formed by attack of the trinitrobenzyl anion on a neutral TNT molecule, but this too is unlikely as this complex is reported to absorb at 450nm and 550nm in alcohol[50]. In view of this evidence, it seems probable that the orange-red colour referred to above derives from σ-adducts formed by methoxide and/or hydroxide addition to TNBCl (formed from TNT by the action of hypochlorite), perhaps together with the conjugate base of TNBCl.

CHAPTER SIX

THE REACTIONS OF 2,4,6-TRINITROTOLUENE AND 2,4,6-TRINITROBENZYL CHLORIDE WITH ALIPHATIC AMINES IN DIMETHYLSULPHOXIDE

6.1. Introduction.

The reaction of 1,3,5-trinitrobenzene with aliphatic amines has been studied by a number of methods[22,23,82], and kinetic studies of the reactions of amines with other substrates have provided important evidence in support of the intermediate complex mechanism in aromatic nucleophilic substitution reactions[39,42]. There has been little work on the reactions of the title compounds with amines, although ^{1}H NMR evidence[25] indicates that, in liquid ammonia, TNT forms a 1:1 adduct with amide ion by addition at the 3-position, and a 1:2 adduct by addition at C-1 and C-3. A study[67] has also been reported of proton abstraction by diethyl- and triethyl-amines from a closely-related compound, 1,5-dimethyl-2,4,8-trinitronaphthalene, in dimethylsulphoxide. In this chapter, kinetic and equilibrium data are reported for the reactions of TNT and TNBCl with n-butylamine, isopropylamine, benzylamine, piperidine and diazabicyclo-[2,2,2]-octane (DABCO).

6.2. Experimental.

Visible spectra were recorded using a Unicam SP8000 or Beckman S25 spectrophotometer, or measured point by point using the stopped-flow spectrophotometer.

^{1}H NMR measurements were made using Bruker HX90E and Varian EM360L instruments. Shifts are quoted relative to internal tetramethylsilane, and the solvent used was dimethylsulphoxide-d_6. Anionic species were generated by the addition of amine to 0·1 M substrate solution, or by the addition of amine to solutions containing the substrate and sodium methoxide in a 1:1 mole ratio[83].

Rate measurements were made using the stopped-flow spectrophotometer or the Beckman S25 instrument. Optical density values were obtained from stopped-flow measurements, or directly using the Unicam SP500 spectrophotometer.

6.3. Results.

6.3.1. Spectroscopic Studies.

The addition of 2,4,6-trinitrotoluene to solutions of various amines (1×10^{-3} M) in DMSO resulted in the formation of a purple species, whose spectrum (λ_{max} 377nm, 530nm and 640nm) was that of the conjugate base (6.1, X=H)

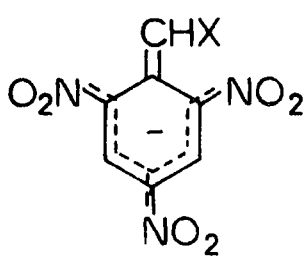

6.1.

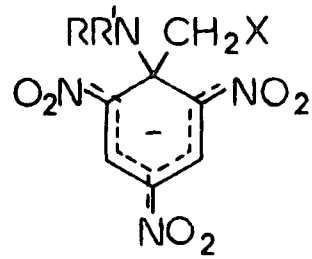

6.2.

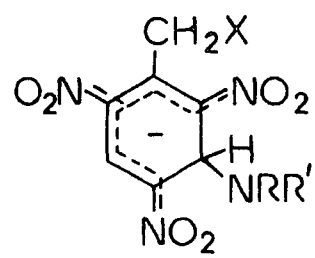

6.3.

When higher concentrations (up to 0·1 M) of the primary and secondary amines were used, a transient red colouring was observed, preceding formation of the conjugate base. Under these conditions, the visible spectra measured after the attainment of equilibrium showed only the presence of the conjugate base. Optical density measurements using the stopped-flow spectrophotometer showed the red species to have a spectrum with maxima at 450nm and 510nm, typical of a σ-adduct (Figure 6.1). The two peaks had an intensity ratio of 1·1, the former being the more intense.

^{1}H NMR spectra of TNT in DMSO-d_6 containing amines were not particularly clear, even when sodium methoxide-d_3 was added to generate the amide ion. However, spectra with excess n-butylamine and benzylamine showed bands at δ5·54 and δ8·2, attributable to the side-chain and ring protons respectively in the conjugate base. No peaks were observed due to σ-adducts.

Figure 6.1.

Visible spectrum, measured by stopped-flow spectrophotometry, of the σ-adduct rapidly produced from TNT (1×10^{-5} M) in the presence of piperidine (0·5 M) and piperidine hydrochloride (0·1 M).

Figure 6.1.

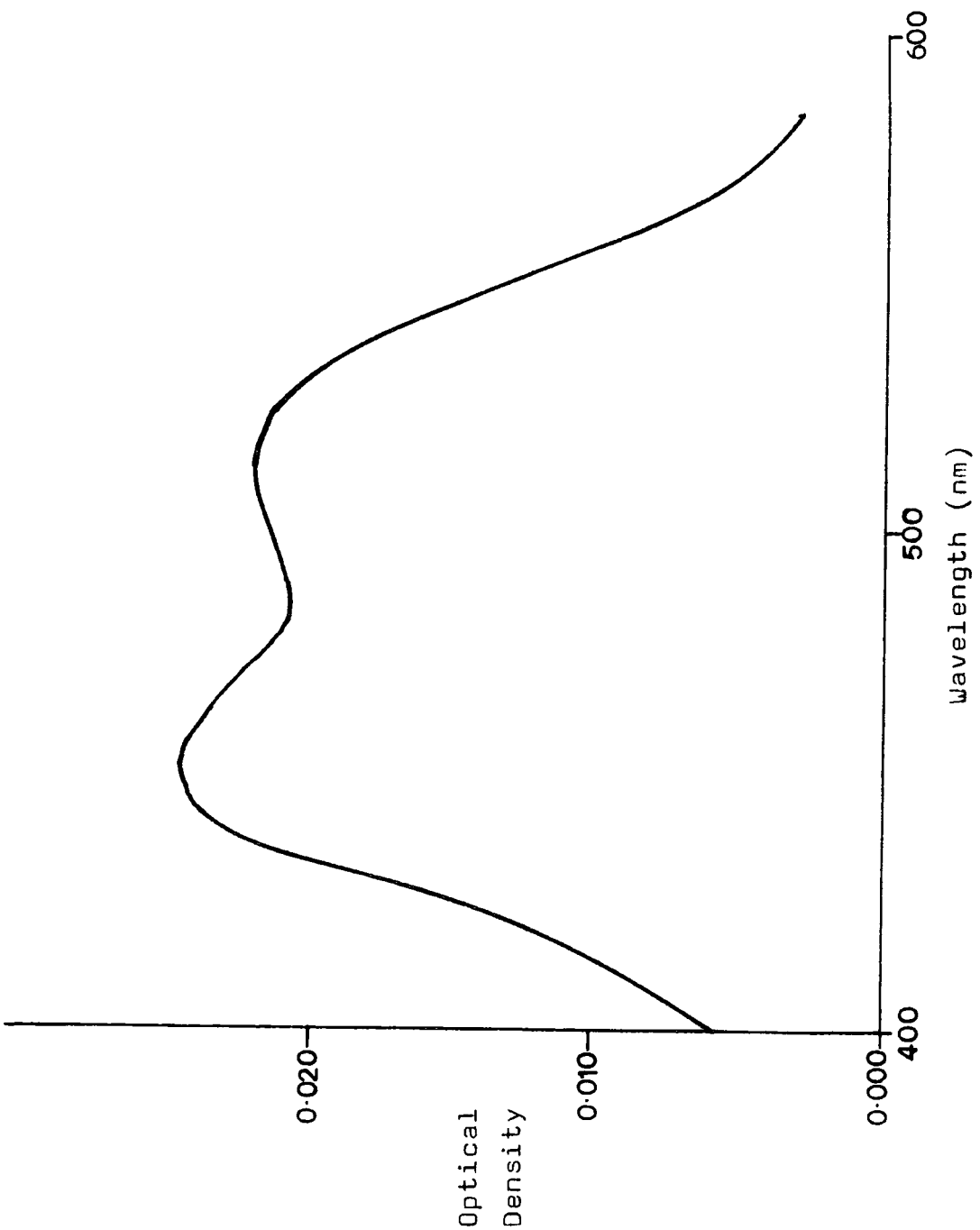

A more complicated situation was found when TNBCl was used in place of TNT. With the tertiary amine DABCO, as expected, the spectrum produced was that of the conjugate base (6.1, X=Cl), with λ_{max} 373nm, 490nm and 600nm. The three primary amines (n-butylamine, isopropylamine and benzylamine) rapidly gave strong red colours with TNBCl, the visible spectra showing peaks at 452nm and 540-550nm characteristic of addition complexes. The values of the extinction coefficients for these species at these two wavelengths were in the ratio 1·7 1·8:1, the lower wavelength peak again the stronger. As with TNT, these bands decreased with time, and the intensity in the region of 370nm and 650nm increased, indicative of the formation of the conjugate base. However, in these cases both species were present at equilibrium - figure 6.2 illustrates this for isopropylamine. The secondary amine piperidine also gave an immediate red colour with TNBCl. However, the spectrum of this adduct showed maxima at 450nm and 510nm (the intensity ratio at these wavelengths being 1·1) and spectra recorded at equilibrium showed only a small amount of this species present.

^{1}H NMR spectra of solutions containing TNBCl and amine were somewhat clearer than those with TNT. The spectrum of the parent compound in DMSO-d_6 showed two singlets at δ9·1 and δ5·0. With one mole equivalent of n-butylamine, the spectra showed, in addition to the parent bands, a singlet at δ7·10 attributable to the conjugate base (the side chain proton in the conjugate base was found at δ6·9 in work with methoxide ion reported in chapter four). However, the ring protons of this species were not observed. With ten equivalents of the

Figure 6.2.

Visible spectra of TNBCl (4×10^{-5} M) with isopropylamine (0·2 M) and isopropylammonium perchlorate (0·1 M) in DMSO recorded at 2 minute intervals, A - D, showing the initial formation of σ-adduct followed by equilibration with the conjugate base.

Figure 6.2.

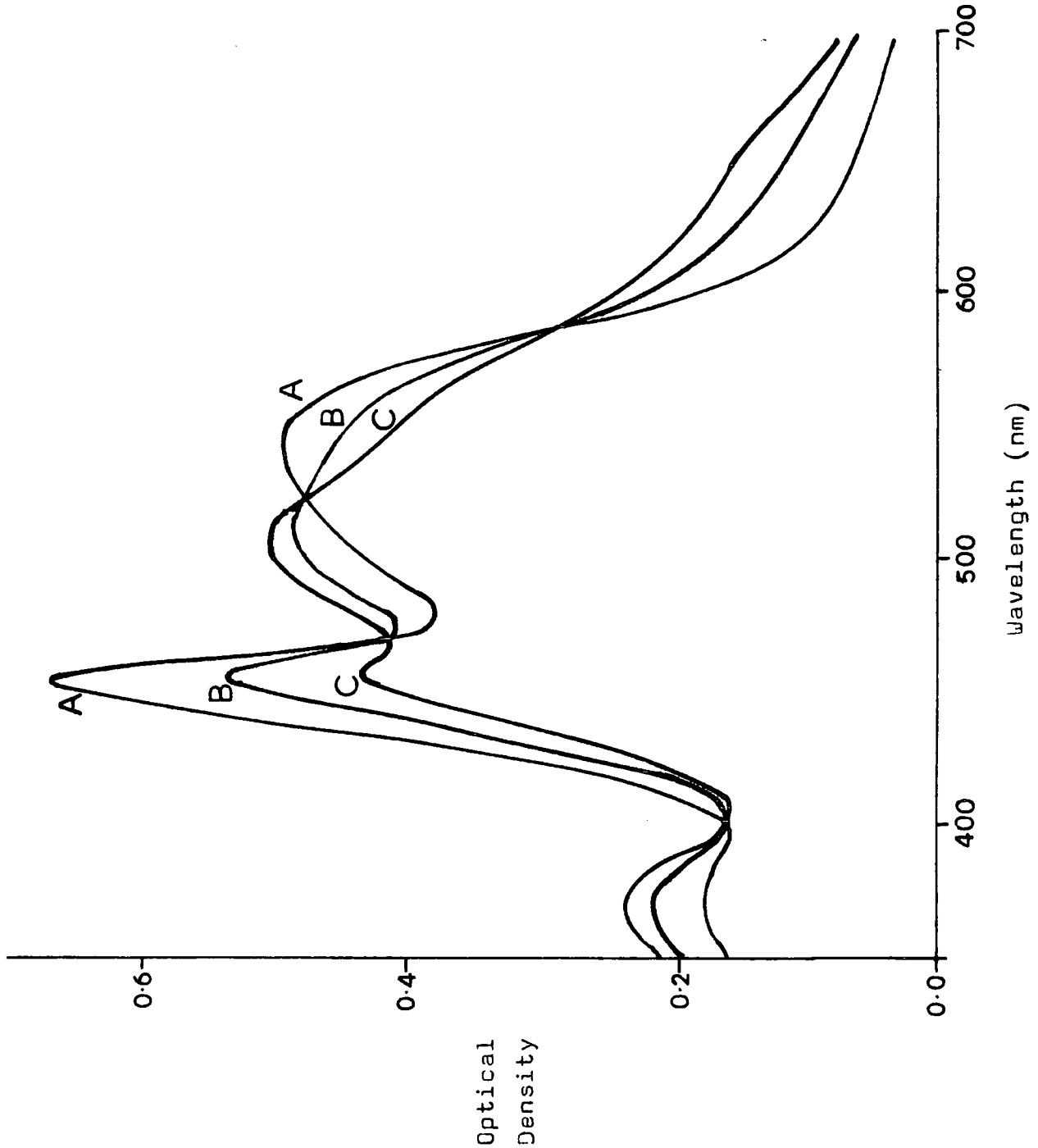
0·0
0·2
0·4
0·6
Optical Density
400
500
600
700
Wavelength (nm)
A
B
C
A
B
C

same amine, the spectrum (Figure 6.3) showed bands at δ8·48 and δ4·57, corresponding respectively to the ring protons and side chain protons in the adduct (6.2, X=Cl, R=n-Bu, R'=H). In view of the evidence[83] that clear NMR spectra of amide adducts can be obtained by the generation of amide ions from amines using sodium methoxide in DMSO, this technique was used here. The $NaOCD_3$ solution was added to that of the parent immediately before the addition of the amine. As the amount of n-butylamine added to a 1:1 mole ratio of TNBCl:$NaOCD_3$ was increased the bands at δ8·70 and δ4·70 due to the methoxide adduct at C-1 were replaced by bands at δ8·48 and δ4·57 due to the amide adduct (Figure 6.4). The appearance of the bands due to the amide adduct slightly to high field of those due to the methoxide adduct is in accord with previous observations[23,83] on related adducts with 1,3,5-trinitrobenzene.

Spectra recorded with isopropylamine as the base showed similar features. With up to one mole equivalent of amine, a peak was observed at δ7·12, due to the side chain proton of (6.1, X=Cl). Again the ring protons were not observed, though here the broad amino proton resonance occurred in the area where they would be expected to appear. With a tenfold excess of amine, the spectrum showed bands at δ8·48 and δ4·54, consistent with (6.2, X=Cl, R=isopropyl, R'=H). Other bands appeared fairly rapidly in these solutions, at δ8·32, δ8·03, δ7·5, δ5·32 - these are probably due to decomposition products.

Spectra of TNBCl in the presence of piperidine or benzylamine gave less clear results. At low amine concentrations, bands indicating the presence of the

Figure 6.3.

NMR spectrum of TNBCl (0·2 M) with 10 equivalents of n-butylamine in DMSO-d_6.

Figure 6.3.

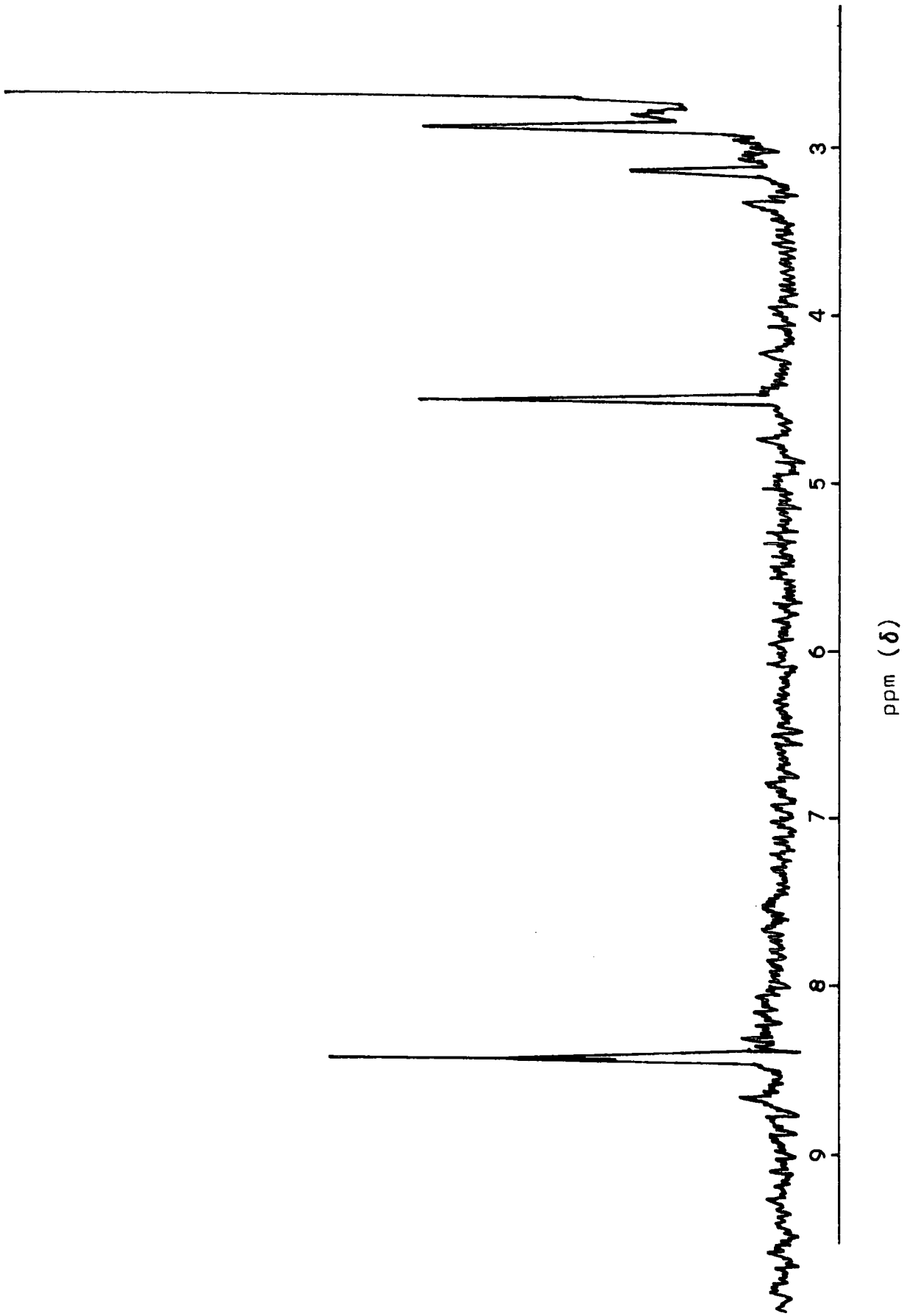

Figure 6.4.

NMR spectrum of TNBCl (0·2 M) with 1 equivalent of sodium methoxide-d_3 and 2 equivalents of n-butylamine in DMSO-d_6.

Figure 6.4.

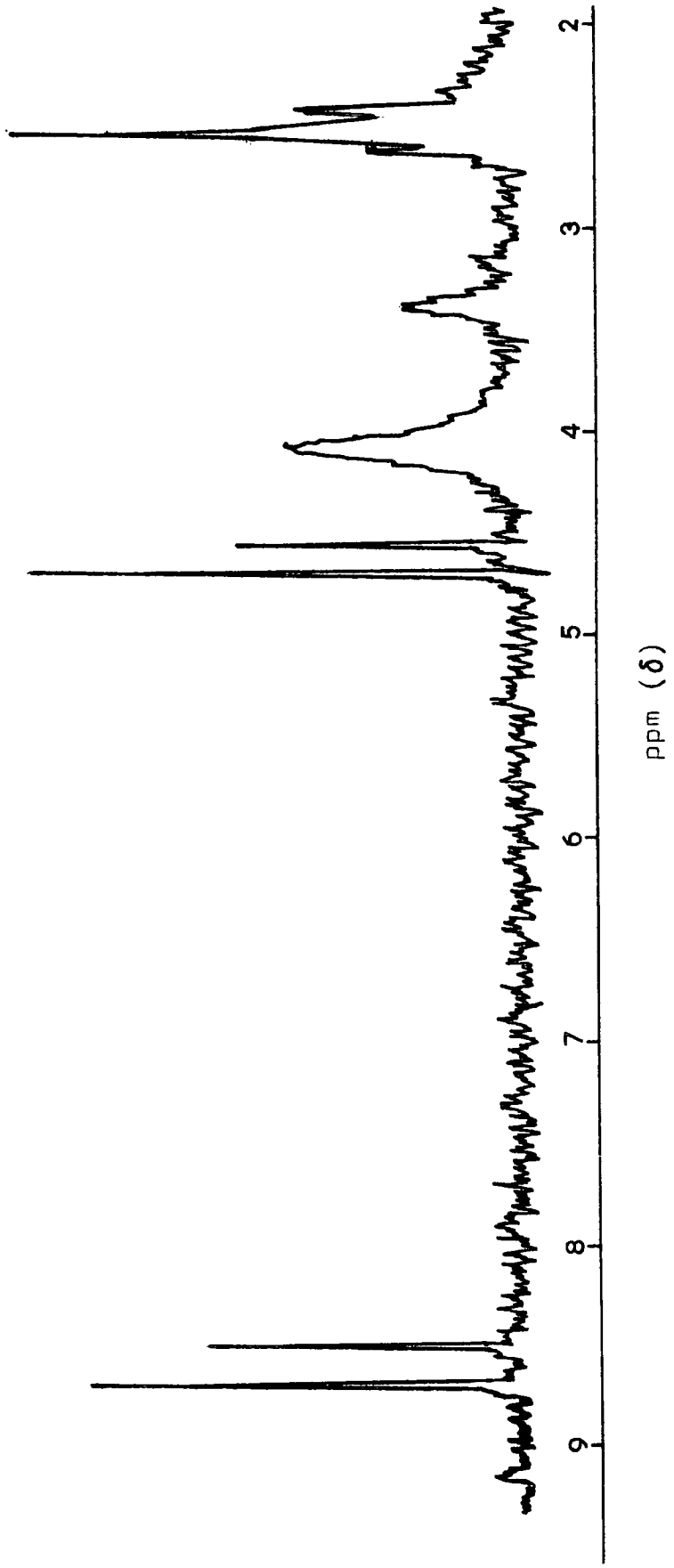

conjugate base were observed, but there was no direct evidence for adduct formation at higher concentrations. However, in some solutions a band was observed in the position reported[83] for the ring protons of the benzylamide group in adducts with various polynitro aromatic compounds. Solutions containing methoxide and amine showed only bands due to the methoxide adduct. This probably reflects the lower thermodynamic stabilities of the adducts formed from these amines.

6.3.2. Kinetic and Equilibrium Data.

a. General.

Measurements were made with amine concentrations in large excess of that of the parent, and with a constant concentration (usually 0·1 M) of the corresponding ammonium salt. This had three effects: it buffered the solutions so that the adverse effects of traces of acid or base were avoided, it allowed data to be collected at constant ionic strength, and lastly it simplified the kinetic analysis.

The two equilibria present in these systems involve the conversion of the parent compound (P) into either the σ-adduct (P.NRR') or the conjugate base (6.1) and are described by equations 6.1 and 6.2. The corresponding equilibrium constants, K_c and K_p respectively, are defined by equations 6.3 and 6.4. The ratio of the concentrations of the two products at equilibrium is given by equation 6.5, and in agreement with this expression it was found experimentally that the fraction of the parent compound present as the σ-adduct at equilibrium increased with the amine concentration.

In all cases, the formation of the σ-adduct was a much faster process than the removal of the side-chain proton. In this work, kinetic measurements were not made on the formation of the σ-adduct, but it is likely that the reaction involves a two step process via a zwitterionic intermediate, as in the reaction of 1,3,5-trinitrobenzene with amines[82]. With the formation of a σ-adduct preceding proton abstraction, the first order rate coefficient, k_{obs}, for the latter process is

$$P + 2R'RNH \underset{}{\overset{K_c}{\rightleftharpoons}} P.NRR'^{-} + R'RNH_2^+ \qquad \text{Eq. 6.1}$$

$$P + R'RNH \overset{K_p}{\rightleftharpoons} (6.1) + R'RNH_2^+ \qquad \text{Eq. 6.2}$$

$$K_c = \frac{[P.NR'R^-]\,[RR'NH_2^+]}{[P]\,[RR'NH]^2} \qquad \text{Eq. 6.3}$$

$$K_p = \frac{[(6.1)]\,[RR'NH_2^+]}{[P]\,[RR'NH]} \qquad \text{Eq. 6.4}$$

$$\frac{[P.NR'R^-]}{[(6.1)]} = \frac{K_c}{K_p}\,[R'RNH] \qquad \text{Eq. 6.5}$$

$$k_{obs} = \frac{k_p\,[RR'NH]}{1 + \dfrac{K_c[RR'NH]^2}{[RR'NH_2^+]}} + k_{-p}\,[RR'NH^+] \qquad \text{Eq. 6.6}$$

$$k_{obs} = k_p\,[RR'NH] + k_{-p}\,[RR'NH_2^+] \qquad \text{Eq. 6.7}$$

given by equation 6.6. In cases where little σ-adduct is formed initially, or with the tertiary amine DABCO, this reduces to equation 6.7. Differentiation of equation 6.6 reveals a turning point, which is a maximum: the predicted maximum value of k_{obs} was in fact observed for a number of amines. Equation 6.6 also predicts that the rate of formation of the conjugate base should decrease with decreasing concentration of the ammonium salt. This too was observed, visible spectra of TNBCl (4×10^{-5} M) in DMSO containing a primary or secondary amine but without added salt indicated that equilibration between the σ-adduct and the conjugate base is a very slow process.

b. Data for TNT.

The simplest system is that with the tertiary amine DABCO, where only one process (proton abstraction) was observed. Rate and equilibrium data, measured by stopped-flow spectrophotometry, are in table 6.1. A plot of k_{obs} versus amine concentration was linear, and yielded values of k_p, 20·6 l $mole^{-1}s^{-1}$, and k_{-p}, 230 l $mole^{-1}s^{-1}$. Combination of these values gave a value for K_p of $(8·8 \pm 0·4) \times 10^{-2}$, in agreement with values calculated from equilibrium optical densities.

Formation of the conjugate base was the only process observed with piperidine at amine concentrations less than 0·1 M (with 0·1 M piperidinium chloride). Above this concentration, a faster colour-forming process was observed, giving a species with a spectrum typical of a σ-adduct (figure 6.1). Rate coefficients for the slower process, and optical densities at the end of each process, were measured and the data are in table 6.2. The observed rate coefficients pass through a maximum value, as predicted by equation 6.6, and give a good fit to this equation with k_p 20 l $mole^{-1}s^{-1}$, k_{-p} 2·0 l $mole^{-1}s^{-1}$, and K_c 3·5 l $mole^{-1}$.

Similar behaviour to that of piperidine was observed with benzylamine in the presence of 0·1 M benzylammonium perchlorate. Above 0·05 M amine, the formation of the conjugate base was preceded by σ-complex formation, whilst below this value only the former process was observed. Optical density measurements at 450nm at the end of the more rapid process allowed the calculation of a value for K_c of 0·19 l $mole^{-1}$. Using this value, the observed rate data were fitted to equation 6.6, giving

values of k_p, 1·5 l mole^{-1}s^{-1}, and k_{-p}, 1·2 l mole^{-1}s^{-1}. The data are in table 6.3.

With n-butylamine, in the presence of 0·1 M salt, two processes were observed at amine concentration greater than 0·01 M (table 6.4). Optical density values measured at the end of the fast colour-forming process gave a value for K_c of 20 l mole^{-1}. With K_c in this range, the K_c term in equation 6.6 is small for amine concentrations up to 0·02 M. Hence a plot of k_{obs} versus amine concentration was linear, yielding values of k_p, 8·9 ± 0·4 l mole^{-1}s^{-1}, and k_{-p}, 0·33 ± 0·05 l mole^{-1}s^{-1}. Combination of these values gave a value for K_p of 27 ± 5, in agreement with that obtained from optical density measurements.

At isopropylamine concentrations below 0·1 M, with 0·1 M salt, there was little initial formation of the σ-adduct, and consequently a plot of k_{obs} versus amine concentration was linear, as expected from equation 6.7. This plot gave values of k_p, 3·2 l mole^{-1}s^{-1} and k_{-p}, 0·23 l mole^{-1}s^{-1}, and hence by combination K_p, 14, which was in agreement with the value obtained from equilibrium optical density measurements at 650nm. With higher amine concentrations, a faster colour-forming process was observed, and optical density measurements at the end of this process led to a value of 0·11 l mole^{-1} for K_c. The data are in table 6.5.

Table 6.1.

Rate and equilibrium data for the reaction of 2,4,6-trinitrotoluene with DABCO in dimethyl sulphoxide containing 0·05 M $DABCOH^+ClO_4^-$ at 25°C.

[DABCO] (M)	k_{obs} (s^{-1})	O.D.[a] 500nm	K_p[b]
0·005	11·6 ± 0·2		
0·010	11·7		
0·020	12·0		
0·040	12·9	0·0143	0·11
0·200	15·9	0·0417	0·08
0·300	18·0	0·0557	0·08
0·400	19·8	0·0722	0·09

a. At equilibrium: 1 x 10^{-4} M TNT; 2mm pathlength cell
A Benesi-Hildebrand plot gives a value for complete conversion of 0·174.

b. Calculated using:
O.D. (500nm)[DABCO H^+]/(0·174 - O.D. (500nm)) [DABCO]

Table 6.2.

Rate and equilibrium data for the reactions of 2,4,6-trinitrotoluene with piperidine in dimethylsulphoxide containing 0·1 M piperidinium chloride at 25°C.

[Piperidine] (M)	k_{obs} (s^{-1})	k_{calc}[a] (s^{-1})	O.D.[b] 525nm	K_c[c] (1 $mole^{-1}$)	O.D.[d] 525nm
0·01	0·40	0·40			0·0114
0·02	0·58	0·59			0·0151
0·05	0·97	1·10			0·0178
0·10	1·75	1·70	0·0083	3·7	0·0202
0·20	2·0	1·9	0·0178	3·5	0·0241
0·30	1·8	1·7	0·0240	4·1	0·0250
0·40	1·5	1·4	0·0258	3·4	0·0243
0·50	1·3	1·2	0·0283		0·0255

a. Calculated from equation 6.6 with k_p 20 l $mole^{-1}s^{-1}$, k_{-p} 2·0 l $mole^{-1}s^{-1}$, and K_c 3·5 l $mole^{-1}$.

b. After completion of first process: 2mm cells; 1×10^{-5} M TNT. A Benesi-Hildebrand type plot gives a value for complete conversion of 0·0305 ($\epsilon 1{\cdot}52 \times 10^4$ l $mole^{-1}cm^{-1}$)

c. Calculated using:

$$\text{O.D.(525nm)}\,[\text{pip H}^+]\,/(0{\cdot}0305-\text{O.D.(525nm)})\,[\text{pip}]^2$$

d. After completion of second process.

Table 6.3.

Rate and equilibrium data for the reactions of 2,4,6-trinitrotoluene with benzylamine in dimethylsulphoxide containing 0·1 M benzylammonium perchlorate at 25°C.

[Benzylamine] (M)	k_{obs} (s^{-1})	k_{calc}[a] (s^{-1})	O.D.[b] 450nm	K_c[c] (l $mole^{-1}$)	O.D.[d] 640nm
0·005	0·11	0·13			
0·010	0·13	0·14			
0·030	0·18	0·17			
0·050	0·20	0·20			0·043
0·070	0·23	0·23	0·0017	0·22	0·053
0·090	0·26	0·26	0·0026	0·20	0·061
0·15	0·35	0·34	0·0070	0·20	0·080
0·20	0·40	0·40	0·011	0·20	0·09
0·30	0·51	0·51	0·022	0·19	0·10
0·40	0·60	0·59	0·036	0·19	0·11
0·50	0·61	0·64	0·048	0·19	0·11
0·70	0·69	0·68	0·069	0·18	0·12

a. Calculated from equation 6.6 with k_p 1·5 l $mole^{-1}s^{-1}$, k_{-p} 1·2 l $mole^{-1}s^{-1}$ and K_c 0·19 l $mole^{-1}$.

b. After completion of first process; 2mm cells; 4×10^{-5} M TNT. A Benesi-Hildebrand plot gives a value for complete conversion of 0·15 ($\varepsilon 1{\cdot}9 \times 10^4$ l $mole^{-1}cm^{-1}$)

c. Calculated using:

$$O.D.(450nm)\ [Amine\ H^+]/(0{\cdot}15 - O.D.(450nm))\ [Amine]^2$$

d. After completion of both processes with 1×10^{-4} M TNT.

Table 6.4.

Rate and equilibrium data for the reaction of 2,4,6-trinitrotoluene with n-butylamine in dimethyl sulphoxide in the presence of 0·1 M n-butylammonium perchlorate at 25°C.

[n-Butylamine] (M)	k_{obs} (s^{-1})	k_{calc}[a] (s^{-1})	O.D.[b] 450nm	K_c[c] (l $mole^{-1}$)	O.D.[d] 650nm	K_p[e]
0·005	0·082	0·077			0·036	28
0·007	0·092	0·095			0·042	30
0·010	0·120	0·120	0·0026	18	0·045	26
0·020	0·210	0·200	0·013	24	0·050	23
0·050	0·360	0·340	0·050	20	0·058	

a. Calculated from equation 6.6 with k_p 9 l $mole^{-1}s^{-1}$, k_{-p} 0·33 l $mole^{-1}s^{-1}$ and K_c 20 l $mole^{-1}$.

b. After completion of first process; 4×10^{-5} M TNT; 2mm pathlength cell.

c. Calculated assuming an extinction coefficient of $1{\cdot}9 \times 10^4$ l $mole^{-1}cm^{-1}$ for the σ-adduct at 450nm.

continued.

Table 6.4.(continued)

d. After completion of both colour forming reactions. At the base concentrations used little σ-adduct is present at equilibrium. A Benesi-Hildebrand plot gives a value of 0·061 for complete conversion to conjugate base.

e. Calculated from O.D. values in previous column.

Table 6.5.

Rate and equilibrium data for the reaction of 2,4,6-trinitrotoluene with isopropylamine in dimethyl sulphoxide with 0·1 M isopropylamine perchlorate at 25°C.

[Isopropylamine] (M)	$10^2 k_{obs}$ (s^{-1})	O.D.[a] 450nm	K_c[b] (l $mole^{-1}$)	O.D.[c] 650nm	K_p[d]
0·005	4 ± 0·2			0·014	17
0·0075	4·5			0·015	13
0·010	5·5			0·018	15
0·020	8·7			0·023	16
0·050	18·4			0·026	13
0·10	34·3			0·028	14
1·0		0·044	0·13		
1·5		0·055	0·11		
2·0		0·059	0·09		
2·5		0·067	0·12		

continued.

Table 6.5.(continued)

a. After completion of first process; 2×10^{-5} M TNT; 2mm cells.

b. Calculated from O.D.(450nm) data assuming an extinction coefficient of 19000 l $mole^{-1}cm^{-1}$.

c. At completion of reaction. A Benesi-Hildebrand plot gives a value for complete conversion to conjugate base of 0·030.

d. Calculated from O.D.(650nm) data.

c. Data for TNBCl.

As with TNT, the most straightforward reaction was that involving DABCO, where only proton abstraction occurred. A linear plot of k_{obs} versus amine concentration, according to equation 6.7, gave values of k_p, 16·4 l mole^{-1}s^{-1}, and k_{-p}, 4·1 l mole^{-1}s^{-1}, which, combined, gave a value for K_p of 4·0 in agreement with that obtained from optical density measurements. The data are in table 6.6.

Data for the reaction of piperidine with TNBCl in solutions containing 0·1 M piperidinium chloride are in table 6.7. With piperidine concentrations greater than 0·005 M two processes were observed using stopped-flow spectrophotometry, the faster of the two corresponding to formation of an adduct, and the slower to formation of the conjugate base. Optical density measurements at 600nm indicated that at equilibrium conversion to the conjugate base was complete with amine concentrations from 0·005 M to 0·2 M. Measurements of the optical density at the end of the first process at 450nm and 490nm led to values for K_c of 225 l mole^{-1} and 170 l mole^{-1} respectively. A plot of the values of k_{obs}, which passed through a maximum as the base concentration was increased, versus the parameter $[Am]/1 + K_c\frac{[Am]^2}{[AmH^+]}$, using a value of 200 l mole^{-1} for K_c, was linear and gave a value for k_p of 42 l mole^{-1}s^{-1}. However, k_{-p} could not be determined accurately from this plot as the intercept was too small. A series of optical density measurements (table 6.8) were made on solutions containing low piperidine concentrations, where the amount of complex present at equilibrium was assumed to be negligible.

These gave a value for K_p of 420 ± 40, and hence a value for k_{-p} ($=k_p/K_p$) of 0·1 l $mole^{-1}s^{-1}$ was obtained.

Optical density measurements at the end of the complex-forming reaction with n-butylamine gave a value for K_c of $(2{\cdot}0 \pm 0{\cdot}2) \times 10^4$ l $mole^{-1}$, showing the σ-complex to have high stability. The subsequent equilibration reaction was slow enough to be followed using a conventional spectrophotometer. The observed rate constants decreased with increasing amine concentration, approaching the limiting value of $k_{-p}[n\text{-}BuNH_3^+]$. Equation 6.6 was well fitted with the above value of K_c, k_p 17 l $mole^{-1}s^{-1}$ and k_{-p} 0·02 l $mole^{-1}s^{-1}$. Data are in table 6.9.

Two processes were observed at all isopropylamine concentrations used (table 6.10).
Optical density measurements at the end of the rapid colour-forming process gave a value for K_c of 1230 ± 100 l $mole^{-1}$. Analysis of the rate data according to equation 6.6 gave a value for k_p of 9·5 ± 0·5 l $mole^{-1}s^{-1}$, with the contribution to the rate due to k_{-p} too small to allow the calculation of this parameter.

Equilibrium optical densities were measured at 450nm and 640nm for a number of solutions (table 6.11). The extinction coefficients of the σ-complex at these wavelengths were determined from solutions containing no added salt, whilst those for the conjugate base were determined in the presence of DABCO. These extinction coefficients were used to calculate the relative concentrations of the anionic species present at equilibrium, and thus a value for the ratio K_c/K_p of

1·3 ± 0·1 was calculated from equation 6.5. Using the value for K_c above, K_p was found to have a value of 950, and hence k_{-p} ($=k_p/K_p$) had the value 0·01 l $mole^{-1}s^{-1}$.

A similar approach was adopted with benzylamine, both products being present at equilibrium. Here, the amount of parent present was also calculated, allowing values for K_p, 22 ± 2, and K_c, 300 ± 100 l $mole^{-1}$, to be obtained (table 6.12). Values for K_c in reasonable agreement with this were obtained from optical density measurements, from stopped-flow spectrophotometry , at the completion of the rapid reaction. The measured rate coefficients for formation of the conjugate base (table 6.13) were fitted to equation 6.6, using a value of 300 l $mole^{-1}$ for K_c, and yielded values for k_p, 1·25 l $mole^{-1}s^{-1}$, and k_{-p}, 0·055 l $mole^{-1}s^{-1}$.

Table 6.6.

Rate and equilibrium data for the reaction of TNBCl with DABCO in dimethyl sulphoxide in the presence of 0·05 M DABCO perchlorate at 25°C.

[DABCO] (M)	k_{obs} (s^{-1})	O.D.[a] 500nm	K_p
0·005	0·30	0·08	3·6
0·010	0·36	0·12	3·6
0·020		0·18	3·8
0·025	0·61		
0·040		0·22	3·5
0·050	1·03		

a. Measured with [TNBCl] 1 x 10^{-4} M using a 2mm cell. For complete conversion to conjugate base, a Benesi-Hildebrand plot gives a value of 0·295.

Table 6.7.

Rate and equilibrium data for the reaction of TNBCl with piperidine in dimethyl sulphoxide containing 0·1 M piperidinium chloride at 25°C.

[Piperidine] (M)	k_{obs} (s^{-1})	k_{calc}[a] (s^{-1})	O.D.[b] 450nm	K_c[c] (l $mole^{-1}$)	O.D.[d] 600nm
0·005	0·21	0·21			0·0089
0·010	0·38	0·36			0·0085
0·015	0·43	0·44			0·0098
0·020	0·50	0·48			0·0091
0·025	0·50	0·48	0·0160	230	0·0102
0·035	0·46	0·44	0·0197	220	0·0108
0·050	0·38	0·36	0·0232	245	0·0106
0·075	0·30	0·27	0·0249	210	0·0097
0·10	0·25	0·21	0·0253		0·0107
0·15	0·19	0·15			0·0100
0·20	0·12	0·12			0·0093

continued.

Table 6.7.(continued)

a. Calculated from equation 6.6 with k_p 42 l $mole^{-1}s^{-1}$, k_{-p} 0·1 l $mole^{-1}s^{-1}$, and K_c 200 l $mole^{-1}$.

b. After completion of first process; [TNBCl] 1 x 10^{-5} M; 2mm cells. A Benesi-Hildebrand plot gives a value of 0·027 for complete conversion.

c. The data at 450nm leads to a value for K_c of 225 ± 30 l $mole^{-1}$. A second set of data was obtained at 490nm and yields a value for K_c of 170 ± 30 l $mole^{-1}$.

d. After completion of reaction forming conjugate base.

Table 6.8.

Equilibrium data for proton transfer from TNBCl to piperidine in DMSO containing 0·1 M piperidinium chloride at 25°C.

[Piperidine] (M)	O.D.[a] 500nm	K_p[b]
0·0005	0·350	460
0·00075	0·382	430
0·0010	0·405	430
0·0020	0·442	380

a. For [TNBCl] 4 x 10^{-5} M with 1cm cell.

b. Calculated assuming no σ-adduct formation with O.D. 0·50 for complete conversion.

Table 6.9.

Equilibrium and rate data for the reaction of TNBCl with n-butylamine in dimethyl sulphoxide containing 0·1 M n-butylammonium perchlorate at 25°C.

$[n\text{-}BuNH_2]$ (M)	O.D.[a] 450nm	$10^{-4}K_c$ (l mole^{-1})	k_{obs} (s^{-1})	k_{calc}[b] (s^{-1})
0·002	0·031	2·0		
0·005	0·058	1·9	0·017	0·016
0·0075	0·065	2·1		
0·010			0·0096	0·010
0·020			0·0065	0·0063
0·030			0·0051	0·0050
0·039			0·0041	0·0042
0·049			0·0038	0·0037

a. After completion of first process, with 2×10^{-5} M TNBCl ; 2 mm cell. A Benesi-Hildebrand plot gives a value of 0·071 for complete conversion.

b. Calculated from equation 6.6 with k_p 17 l mole$^{-1}s^{-1}$, k_{-p} 0·02 l mole$^{-1}s^{-1}$ and K_c 2×10^4 l mole^{-1}.

Table 6.10.

Rate and equilibrium data for the reaction of TNBCl with isopropylamine in dimethyl sulphoxide with 0·1 M isopropylamine perchlorate at 25°C.

[Isopropylamine] (M)	O.D.[a] 450nm	K_c (l mole^{-1})	k_{obs} (s^{-1})	k_{calc}[b] (s^{-1})
0·005	0·019	1100	0·037	0·037
0·0075	0·038	1300	0·040	0·043
0·010	0·050	1300	0·044	0·044
0·015	0·067	1300	0·035	0·039
0·020	0·074	1200	0·032	0·033
0·050	0·084		0·014	0·016

a. After completion of rapid colour forming reaction. TNBCL, 2 x 10^{-5} M. Measured with 2mm cell. Benesi-Hildebrand plot gives value of 0·0893 for complete conversion.

b. Calculated from equation 6.6 with K_c 1230 l mole^{-1}, k_p 9·5 l mole$^{-1}s^{-1}$ and k_{-p} negligibly small.

Table 6.11.

Equilibrium constants for the reaction of TNBCl with isopropylamine[a] in dimethyl sulphoxide with 0·1 M isopropylamine perchlorate at 25°C.

[Isopropylamine] (M)	O.D. 640nm	O.D. 450nm	Relative Concentrations Conjugate base	σ-adduct	K_c/K_p (l mole^{-1})
0·05	·180	·316	0·89	0·065	1·4
0·10	·167	·335	0·82	0·11	1·3
0·20	·161	·400	0·79	0·19	1·2
0·30	·156	·470	0·76	0·27	1·2

a. [TNBCl], 4×10^{-5} M. The values of the extinction coefficients of the conjugate base were determined in the presence of DABCO and were: 640nm, 5100 l mole^{-1}cm^{-1}; 450nm 7400 l mole^{-1}cm^{-1}. Values of the extinction coefficients of the σ-adduct were determined in solutions containing no added salt, where isomerisation was slow, and were : 640nm, 0 ; 450nm, 22,300 l mole^{-1}cm^{-1}.

Table 6.12.

Equilibrium constants for the reactions of TNBCl[a] with benzylamine in dimethyl sulphoxide at 25°C.

[Benzylamine] (M)	[Benzylammonium Perchlorate][b] (M)	O.D. 450nm	O.D. 620nm	Relative concentrations[c] Conjugate base	σ-adduct	Parent	K_p	K_c (l mole^{-1})
0·010	0·10	0·267	0·146	0·62	0·09	0·29	22	310
0·020	0·10	0·361	0·156	0·66	0·18	0·16	21	280
0·005	0·05	0·254	0·155	0·66	0·06	0·28	23	450
0·010	0·05	0·306	0·176	0·75	0·09	0·16	23	280
0·20	0·05	0·379	0·174	0·74	0·17	0·09	21	240

a. TNBCl 4 x 10^{-5} M. Measurements made with SP 500 spectrophotometer.

b. Solutions made up to constant ionic strength, I = 0·1 M, with tetraethylammonium perchlorate.

c. Measurements made with DABCO gave values for the extinction coefficients of the conjugate as 7400 (450nm) and 5900 l mole^{-1}cm^{-1} (620nm). Values of the extinction coefficients of the σ-adduct, determined in solutions without added salt where isomerisation was slow, were 23200 l mole^{-1}cm^{-1} (450nm) and 0 (620nm).

Table 6.13.

Rate and equilibrium data for the reaction of TNBCl with benzylamine in dimethyl sulphoxide in the presence of 0·1 M benzylammonium perchlorate at 25°C.

[Benzylamine] (M)	O.D.[a] 450nm	K_c (l mole^{-1})	k_{obs} (s^{-1})	k_{calc}[b] (s^{-1})
0·01	0·0083	340	0·015	0·015
0·02	0·0224	530	0·020	0·017
0·04	0·0284	380	0·012	0·014
0·06	0·0297	250	0·012	0·012
0·10	0·0317	240		

a. After completion of first process; 1 x 10^{-5} M TNBCl; 2mm cell. O.D. for complete conversion is 0·033.

b. Calculated from equation 6.6 with k_p 1·25 l mole$^{-1}s^{-1}$, k_{-p} 0·055 l mole$^{-1}s^{-1}$ and K_c 300 l mole^{-1}.

6.4. Discussion.

6.4.1. Proton Transfer.

The rate and equilibrium parameters for this process are summarised in table 6.14. In view of the high dielectric constant of DMSO, and the fact that it shows good solvating properties for polarisable ions, extensive ion association of the charged species present in these systems would not be expected. Hence the values of K_p for a given substrate should give a measure of the basicities of the amines used in this solvent. These values increase in the order DABCO < benzylamine < piperidine < isopropylamine , n-butylamine. This order is similar to that in water, as defined by the pKa values of the amines, although piperidine is the most basic of these amines in aqueous solution. However, a recent study[85] has shown that in transfer from water to DMSO, the basicity of secondary and tertiary amines is decreased, whilst that of primary amines is enhanced. These effects probably account for the different order of basicity found here.

A comparison of the values of K_p, k_p and k_{-p} for TNT and TNBCl with each amine is presented in table 6.15. As expected, the chlorine atom in the side-chain of TNBCl has an acid-strengthening effect. Again, the enhancement is by a smaller factor than that found with 4-nitrobenzyl-chloride and 4-nitrotoluene, which is 700[80]. The steric effect of the two adjacent nitro groups, which will interact unfavourably with the chlorine atom in the conjugate base, is the probable cause of this reduction in the acid-strengthening effect.

It can be seen from this table that the greater acidity

Table 6.14.

Summary of kinetic and equilibrium parameters[a] for reactions of TNT and TNBCl with amines in dimethyl sulphoxide in DMSO at 25°C.

TNT	k_p (l mole^{-1}s^{-1})	k_{-p} (l mole^{-1}s^{-1})	K_p	K_c (l mole^{-1})	K_c/K_p (l mole^{-1})	pKa (water)[b]
DABCO	20·6	230	0·09			8·8
Piperidine	20	2·0	10	3·5	0·35	11·2
Benzylamine	1·5	1·2	1·25	0·2	0·16	9·4
n-Butylamine	9	0·33	27	20	0·75	10·6
Isopropylamine	3·2	0·23	14	0·1	0·007	10·6

a. Measurements at ionic strength 0·1 M, except data with DABCO which are at I = 0·05 M.

b. ref. 84

continued.

Table 6.14.(continued)

TNBCl	k_p ($l\ mole^{-1}s^{-1}$)	k_{-p} ($l\ mole^{-1}s^{-1}$)	K_p	K_c ($l\ mole^{-1}$)	K_c/K_p ($l\ mole^{-1}$)	pKa (water)[b]
DABCO	16·4	4·1	4·0			8·8
Piperidine	42	0·1	420	200	0·48	11·2
Benzylamine	1·25	0·055	22	300	13·5	9·4
n-Butylamine	17	0·02	850	20000	23	10·6
Isopropylamine	9·5	0·01	950	1230	1·3	10·6

b. ref. 84

Table 6.15.

Comparison of equilibrium and rate constants for reactions of TNBCl and TNT with amines in DMSO

	$\frac{K_p\ (TNBCl)}{K_p\ (TNT)}$	$\frac{k_p\ (TNBCl)}{k_p\ (TNT)}$	$\frac{k_{-p}\ (TNBCl)}{k_{-p}\ (TNT)}$
DABCO	45	0·8	0·02
Piperidine	42	2·1	0·05
Benzylamine	18	0·9	0·05
n-Butylamine	31	1·9	0·06
Isopropylamine	66	3·0	0·04

of TNBCl is due largely to the slower rate of protonation of the conjugate base (as indicated by k_{-p}), the rate constants for protonation of the two substrates being similar in value for a given amine. This may be indicative of a transition state which is reactant-like, in which proton transfer from the parent compound to the amine has not progressed very far, (reactant-like transition states have been postulated for complex formation reactions involving nitro-aromatic compounds[76]). Further support for this idea comes from the values of k_p and k_{-p} (table 6.14); for a given substrate, the values of k_p vary much less with the nature of the amine than do the corresponding k_{-p} values. This point is also illustrated by Bronsted-type plots (figure 6.5); plots of log k_p versus log K_p have small slopes, whilst those of log k_{-p} versus log K_p have slopes close to unity. The values for benzylamine, however, did not fit such plots, the values of k_p and k_{-p} both being well below the line defined by the other points. This may indicate the presence of some unfavourable interaction in the transition state for proton removal from the parent compounds with this particular amine. Another possibility is that there is charge-transfer interaction between the aromatic rings of the substrate and the amine, which stabilises the initial and final states, but not the transition state.

6.4.2. Complex Formation.

Formation of a σ-complex, which involves the formation of a covalent bond between the amine and a ring-carbon atom, is more likely to be susceptible to steric effects than the proton transfer reaction.

Figure 6.5.

Bronsted-type plots for proton abstraction from TN8Cl by amines.

+: log k_p versus log K_p

⊙: log k_{-p} versus log K_p

The numbers refer to the different amines as follows:

1 : DABCO

2 : Piperidine

3 : Benzylamine

4 : n-Butylamine

5 : Isopropylamine

Figure 6.5.

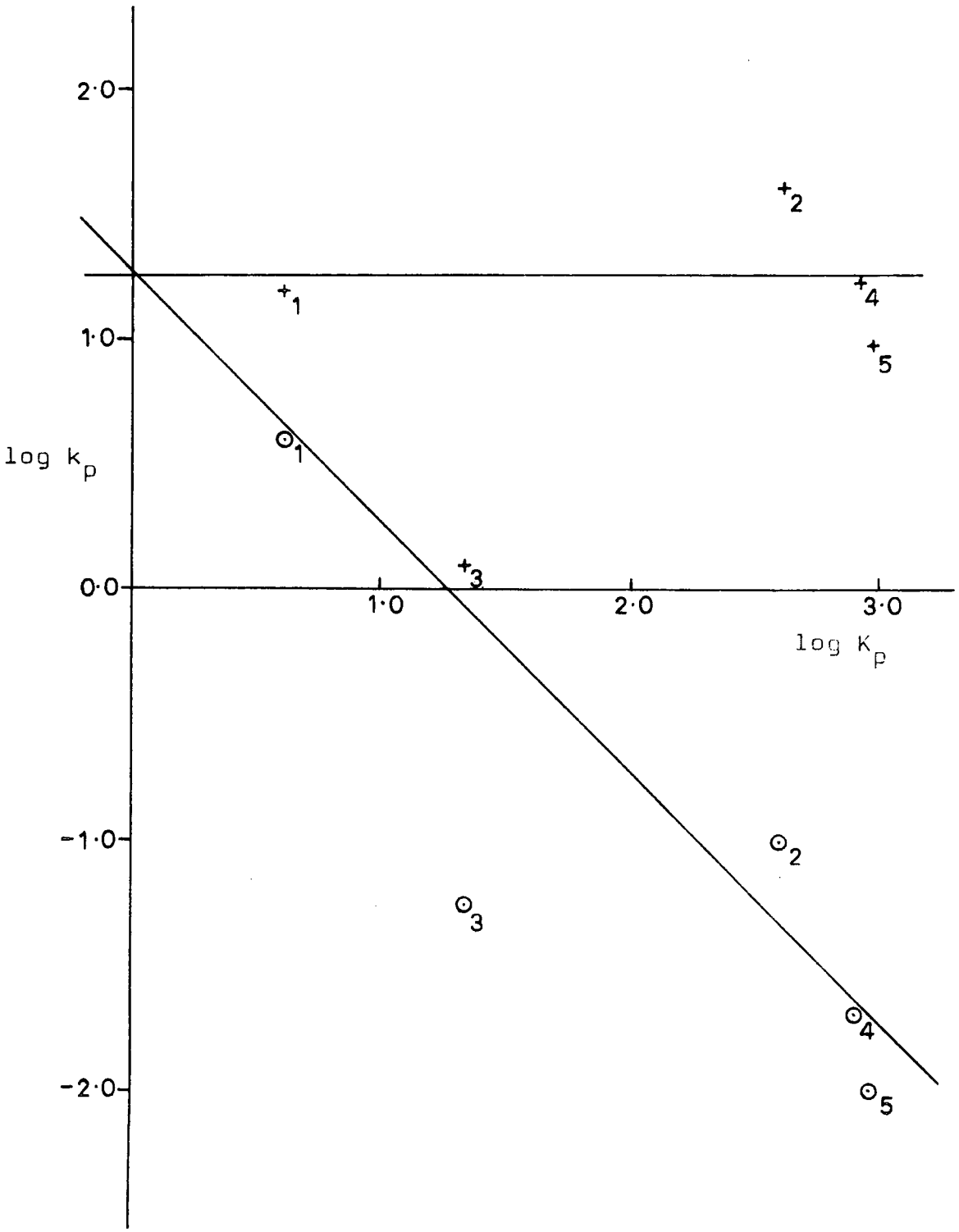

Addition may occur at the 1-position, to give (6.2), or at the 3-position to give (6.3). NMR spectra with TNT as the substrate do not allow the site of addition to be determined. The 1:1 adducts of TNT which have been observed up to now (with alkoxides[51], sulphite* and amide ion in liquid ammonia[25]) have all resulted from attack at the 3-position, and so it seems likely that amine addition occurs at the same position. There is also a close similarity between the spectrum, obtained from stopped-flow measurements, of the piperidine adduct (figure 6.1) and that of the 3-methoxy adduct (chapter five, figure 5.1) obtained in a similar manner, although this is not conclusive evidence as isomeric complexes are known to have very similar spectra[32,43]. The shift of the peaks in the spectrum to longer wavelengths on changing from an oxygen to a nitrogen base is expected on the basis of past results[32,43]. It thus seems probable that the amine adducts of TNT have the structure (6.3, X=H)

The values of K_c (in table 6.14) exhibit a similar order to the values of K_p, with the exception of isopropylamine which has a much lower value of K_c than that expected from the K_p value. This depressed value may be due to unfavourable steric interactions in the σ-adduct (6.3, X=H, R=isopropyl, R'=H). A similar effect has been observed[82] in the adduct formed from 1,3,5-trinitrobenzene and isopropylamine, although here the reduction in stability was not as great as that found with TNT.

*See chapter three

In the case of TNBCl, definite NMR evidence was obtained for the addition of n-butylamine and isopropylamine at C-1 to give adducts of structure (6.2, X=Cl). The visible spectra of these adducts, and that formed with benzylamine, have similar features,with maxima at 452nm and 540-550nm, the former having much the higher intensity in each case. This suggests that the benzylamine adduct has the structure (6.2, X=Cl, R=Bz, R'=H). In contrast to this, the spectrum of the adduct formed between TNBCl and piperidine has maxima at 450nm and 510nm, the peaks in this case being of similar intensity. The spectrum is in fact very similar to that of the piperidine-TNT adduct. This perhaps indicates a different mode of interaction in this case, with piperidine addition occurring at the 3-position to give an adduct of type (6.3, X=Cl).

The two factors most likely to encourage attack at the 1-position in TNBCl relative to TNT are the inductive effect of the chloromethyl group relative to the methyl group, and the steric strain at the 1-position caused by the bulky chloromethyl group which will be relieved on complex formation as this group is bent out of the ring plane. The higher ratio of K_c to K_p for n-butylamine and benzylamine can be rationalised in this way. However, the presence of two bulky groups at the 1-position in the adduct will also cause steric strain at this position. It has already been shown in chapter three that addition of the bulky sulphite ion occurs at the 3-position of TNBCl, and not at the 1-position. Thus this effect may reduce the K_c/K_p ratio for isopropylamine , and inhibit attack of piperidine at the 1-position.

CHAPTER SEVEN

THE REACTIONS OF 1,3,5-TRINITROBENZENE WITH SULPHITE, PHENOXIDE, CYANIDE AND DIETHYLMALONATE IONS

7.1. Introduction.

The reactions of 1,3,5-trinitrobenzene with a number of nucleophiles to form 1:1 addition complexes follow a simple, one-step equilibrium as in equation 7.1.

$$TNB + Nu^- \underset{k_r}{\overset{k_f}{\rightleftharpoons}} TNB.Nu^- \qquad \text{Eq. 7.1}$$

$$k_{obs} = k_r + k_f [Nu^-] \qquad \text{Eq. 7.2}$$

The observed rate coefficient, k_{obs}, is given by equation 7.2 under first order conditions.

The value of the forward rate constant, k_f, is a measure of the nucleophilicity of the particular base in question, and the value of k_r, the reverse rate constant, is a measure of its leaving group ability. In an attempt to establish a scale of these two properties for a number of nucleophiles, the kinetics of their reactions with TNB in a number of mixed solvents were observed.

The nucleophiles used (sulphite, phenoxide, cyanide and diethylmalonate ions) are all known to form complexes with TNB. Sodium sulphite forms 1:1[86] and 1:2[73] complexes with TNB, the 1:2 complex existing as both cis and trans isomers[34-36].

The phenoxide ion has been shown to form complexes with TNB in which bonding occurs via the carbon atom para[87] or ortho[88] to the hydroxy group. Bond formation via the oxygen atom has been observed[89] as the kinetically-favoured process, on the temperature-jump timescale.

Cyanide ion has been known to react with TNB to form brightly coloured species for some time[3,5], and a

σ-complex structure for the product has been confirmed by NMR[90].

The reaction of diethylmalonate with TNB has not previously been studied but the analagous compound dimethylmalonate forms a σ-complex with TNB in the presence of a base to generate the carbanion[91].

7.2. Experimental.

Visible spectra were recorded using a Unicam SP8000 instrument.

Optical density measurements were made using the stopped-flow spectrophotometer or a Unicam SP500 instrument.

Reaction rates were measured using the stopped-flow spectrophotometer.

7.3. Results.

7.3.1. Sodium Sulphite.

The reaction between sodium sulphite and TNB was studied in methanol containing 50% and 25% water by volume. In both solvents only one colour-forming process was observed, consistent with the formation of (7.1)

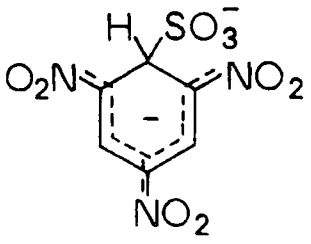

(7.1)

Rate and optical density data for this reaction are in table 7.1. In all cases, the sulphite concentration was in large excess over that of the parent compound, and so first-order kinetics were observed. The variation of k_{obs} with sulphite concentration is given by equation 7.2, with $Nu^- = SO_3^{2-}$, and the appropriate plots were linear.

The values obtained from these plots were : in 50/50 (v/v) methanol/water, k_f $2{\cdot}83 \times 10^4$ l $mole^{-1}s^{-1}$, and k_r $12{\cdot}25$ s^{-1}, and in 75/25 (v/v) methanol/water, k_f $4{\cdot}34 \times 10^4$ l $mole^{-1}s^{-1}$ and k_r $2{\cdot}15$ s^{-1}. This last figure is subject to quite a large error, as the intercept of the plot was small. The values,and the derived values of the equilibrium constant K, are in table 7.2, where they are compared with values obtained[34] in pure water. The value of k_f does not vary a great deal with solvent composition, the increase in the stability of the complex (as measured by K) with increasing methanol content being

due to the decreasing value of k_r. This is again indicative of a reactant-like transition state[76], in which changes in solvation and charge-distribution have not proceeded very far. The results also show that the polarisable complex is better solvated by methanol than by water and/or that the sulphite ion is poorly solvated by methanol.

Table 7.1.

Kinetic and equilibrium data for sulphite addition to 1,3,5-trinitrobenzene in methanol-water mixtures.

% MeOH (volume)	[sulphite] (M)	k_{obs} (s^{-1})	O.D.[a] 460nm
75	0·0005	20·1	0·025
75	0·0010	46·8	0·030
75	0·0015	65·1	0·029
75	0·0020	90·1	0·030
75	0·0030	89·6	0·028
50	0·0005	25·5	0·017
50	0·0010	40·2	
50	0·0015	53·8	0·026
50	0·0020	67·6	0·028
50	0·0030	104·4	0·028

a. Optical density at end of reaction, for a 2mm pathlength cell.

Table 7.2.

Kinetic and equilibrium parameters for sulphite addition to 1,3,5-trinitrobenzene.

% MeOH (volume)	k_1 ($l\ mole^{-1}s^{-1}$)	k_{-1} (s^{-1})	K^a ($l\ mole^{-1}$)
0	$3{\cdot}50 \times 10^4$	125	290
50	$2{\cdot}83 \times 10^4$	12·25	2310
75	$4{\cdot}34 \times 10^4$	2·15	20200

a. $K = k_1/k_{-1}$

7.3.2. Sodium Phenoxide.

The addition of aqueous sodium phenoxide (0·125 M, with 0·125 M phenol) to a methanolic solution of 1,3,5-trinitrobenzene (4×10^{-4} M), to give a 50/50 (v/v) methanol/water mixture, resulted in the production of an orange colouration with λ_{max} at 425nm and 490nm. This is in contrast with the results reported[87] for this reaction in 80/20 DMSO/water, where the spectrum of the complex formed (bonding occurring via C-4 in the phenoxide ring) having peaks at 468nm and 570nm. A series of visible spectra recorded on a conventional spectrophotometer showed a decrease in the intensities of the peaks as the amount of free phenol was increased, with the phenoxide concentration kept constant. This evidence suggests that the phenoxide ion is not likely to be acting as a nucleophile in this system, the more likely source of the colour being attack by methoxide and/or hydroxide ion.

Stopped-flow spectrophotometry revealed the presence of three processes in this system. The first was a rapid colour-forming process, with a half-life too small to allow measurement by this technique. The second was also colour-forming, having a half-life of around 25ms, and was accompanied by a smaller change in optical density than the first. The final process was a slow colour-fading reaction, and was not studied. Kinetic and optical density values are in table 7.3. The ratio of the optical density values at the end of the two colour-forming processes is reasonably constant for all phenol concentrations, a similar situation to that found with sodium hypochlorite and TNB (chapter five). Consequently, it appears that in this solvent system the attacking

species are methoxide and hydroxide ions, giving rise to the two colour-forming processes.

The spectrum of a solution containing sodium phenoxide (5×10^{-3} M), phenol ($2{\cdot}5 \times 10^{-3}$ M) and TNB (2×10^{-5} M) in 90/10 (v/v) DMSO/water showed two peaks, at 435nm and 510nm. Again, the intensities of these absorptions decreased as the concentration of the phenol was increased. The positions of the peaks agree with those observed for a solution of sodium hydroxide (1×10^{-3} M) and TNB ($1{\cdot}8 \times 10^{-5}$ M) in the same solvent.

Two processes were observed at 480nm when this system was studied by stopped-flow spectrophotometry, the more rapid being colour-forming and the second colour-fading. Data are in table 7.4. The phenol-phenoxide equilibrium is described by equation 7.3.

$$PhOH + OH^- \overset{K}{\rightleftharpoons} PhO^- + H_2O \qquad \text{Eq. 7.3}$$

From this,

$$[OH^-] = K \frac{[PhO^-]}{[PhOH]} [H_2O]$$

As the amount of water in the system is in large excess over the other species, then the hydroxide concentration is proportional to the phenoxide/phenol ratio. A plot of k_{obs} versus this ratio was reasonably linear, with an intercept (corresponding to k_r for hydroxide addition) of $0{\cdot}75\ s^{-1}$. Thus it seems likely that in this solvent, hydroxide addition is responsible for the formation of the observed σ-adduct, and that the phenoxide ion is not sufficiently reactive (in comparison with hydroxide) for its reaction with TNB to be observed.

Table 7.3.

Rate and equilibrium data for 1,3,5-trinitrobenzene and sodium phenoxide in 50/50 (v/v) methanol/water

[TNB] (M)	[PhOH] (M)	[PhO^-] (M)	k_{obs} (s^{-1})	O.D.[a] 1st	2nd
5×10^{-5}	0·01	0·01	22·8	0·0117	0·0141
5×10^{-5}	0·02	0·02	20·3	0·0088	0·0102
5×10^{-5}	0·03	0·01	37·1	0·0058	0·0066

a. Optical densities (at 480 nm) for 2mm pathlength cell. 1st and 2nd refer to the ends of the two colour-forming processes.

Table 7.4.

Rate and equilibrium data for 1,3,5-trinitrobenzene and sodium phenoxide in 90/10 (v/v) DMSO/water.

[TNB] (M)	[PhOH] (M)	[PhO^-] (M)	k_{obs} (s^{-1})	O.D.[a] 480nm
$6·5 \times 10^{-5}$	0·025	0·05	3·07	0·019
$6·5 \times 10^{-5}$	0·05	0·05	2·01	0·019
$6·5 \times 10^{-5}$	0·10	0·05	1·31	0·018

a. Optical density at end of colour-forming process, for 2mm pathlength cell.

7.3.3. Potassium Cyanide.

The reaction of potassium cyanide with TNB was studied by stopped-flow spectrophotometry in a number of methanol-water mixtures. In all cases two processes were observed, a rapid colour-forming process followed by a slower fading process. The spectrum of the product of the colour-forming process, as measured using the stopped-flow instrument, showed two peaks in all solvent mixtures. In 50/50 (v/v) methanol/water the peaks were at 420nm and 525nm, whilst in 80% methanol they were found at 420nm and 510nm. The wavelength maxima reported for the TNB-cyanide complex in methanol are 428nm and 540nm[92].

A preliminary series of kinetic runs in 50/50 (v/v) methanol/water indicated that the value of k_r would be small. Accordingly, to obtain the most accurate value possible, sodium hydroxide (1×10^{-3} M) was added to suppress the formation of HCN in the solutions. Typical kinetic runs are in table 7.5, and the rate and equilibrium data are in tables 7.6-7.10.

In all cases, the concentration of cyanide was in large excess over that of TNB, and so equation 7.2 applies, with CN^- as Nu^-. Plots of k_{obs} versus cyanide concentration were reasonably linear in each case, although the intercept of the plot for the 30/70 (v/v) methanol/water mixture was subject to a large uncertainty. Values derived from the plots and the optical density data are in table 7.11.

The values of k_{obs}, and those of the equilibrium constant K, are not consistent with attack by either methoxide or hydroxide ions. The values of k_f and k_r increase with increasing methanol content up to 60% methanol

by volume, beyond which point the values appear constant. The magnitude of the change is somewhat lower than that observed for the variation of the same parameters for methoxide and sulphite additions to TNT with the DMSO content of the solvent (chapters three and five). These changes in k_f and k_r balance in such a way that the complex has similar stability in each of the solvent systems used.

Table 7.5.

Typical kinetic runs for the reaction of 1,3,5-trinitrobenzene and potassium cyanide in methanol-water mixtures.

5×10^{-5} M TNB

0·01 M KCN

(i) 60/40 (v/v) methanol/water

(ii) 80/20 (v/v) methanol/water

t (s)	(i) ΔV^a	(i) k^b (s^{-1})	(ii) ΔV^a	(ii) k^b (s^{-1})
1	4·30		5·05	
2	3·55	·19	4·10	·21
3	2·85	·22	3·30	·22
4	2·30	·21	2·60	·24
5	1·80	·25	2·05	·24
6	1·45	·22	1·60	·25
7	1·10	·28	1·20	·29
8	0·85	·26	0·90	·29
Mean		·23		·25

a. $\Delta V = V_t - V_\infty$

b. $k = \frac{1}{(t - t')} \ln \frac{\Delta V'}{\Delta V}$

Table 7.6.

Kinetic and equilibrium data for the reaction of 1,3,5-trinitrobenzene with potassium cyanide in 50/50 (v/v) methanol/water.

[KCN] (M)	k_{obs} (s^{-1})	O.D.[a] 500nm	K[b] (l $mole^{-1}$)
0·0023	0·055	0·0101	295
0·0025	0·076	0·0099	264
0·0046	0·088	0·0123	211
0·0092	0·148	0·0168	221
0·010	0·167	0·0193	339
0·0139	0·194	0·0192	238
0·0185	0·191	0·0213	311
0·020	0·257	0·0240	1200

a. Optical density at end of colour-forming process, for 2mm cell, $2·5 \times 10^{-5}$ M TNB.

b. Calculated from O.D. values and a value of 0·025 (Benesi-Hildebrand plot) for complete conversion.

Table 7.7.

Kinetic and equilibrium data for the reaction of 1,3,5-trinitrobenzene with potassium cyanide in 70/30 (v/v) methanol/water.

[KCN] (M)	k_{obs} (s^{-1})	O.D.[a] 500nm	K[b] (l $mole^{-1}$)
0·0025	9·21	0·0155	218
0·005	13·3	0·0224	207
0·010	22·2	0·0297	208
0·015	26·9	0·0370	352
0·020	36·0	0·0407	617

a. Optical density at end of colour-forming process, for 2mm cell, 5×10^{-5} M TNB.

b. Calculated from O.D. values and a value of 0·044 (Benesi-Hildebrand plot) for complete conversion.

Table 7.8.

Rate data for the reaction of 1,3,5-trinitrobenzene with potassium cyanide in 30/70 (v/v) methanol/water.

[KCN] (M)	k_{obs} (s^{-1})
0·0025	0·039
0·005	0·040
0·010	0·073
0·015	0·122
0·020	0·158

Table 7.9.

Rate and equilibrium data for the reaction of 1,3,5-trinitrobenzene with potassium cyanide in 60/40 (v/v) methanol/water.

[KCN] (M)	k_{obs} (s^{-1})	O.D.[a] 500nm	K[b] (l $mole^{-1}$)
0·0025	10·5	0·0124	170
0·005	13·9	0·0186	155
0·010	22·6	0·0254	140
0·015	29·9	0·0304	150
0·020	31·2	0·0336	160

a. Optical density at end of colour-forming reaction, for 2mm cell, 5×10^{-5} M TNB.

b. Calculated from O.D. values and a value of 0.053 (Benesi-Hildebrand plot) for complete conversion.

Table 7.10.

Rate and equilibrium data for the reaction of 1,3,5-trinitrobenzene with potassium cyanide in 80/20 (v/v) methanol/water.

[KCN] (M)	k_{obs} (s^{-1})	O.D.[a] 500nm	K[b] (l $mole^{-1}$)
0·0025	11·7	0·0192	227
0·005	15·6	0·0272	211
0·010	24·4	0·0363	217
0·015	30·1	0·0407	221
0·020	29·9	0·0473	415

a. Optical density at end of colour-forming reaction, for 2mm cell, 5×10^{-5} M TNB.

b. Calculated from O.D. values and a value of 0·053 (Benesi-Hildebrand plot) for complete conversion.

Table 7.11.

Variation of kinetic and equilibrium parameters with solvent composition, for the reaction of 1,3,5-trinitrobenzene and potassium cyanide.

MeOH:H_2O (v/v)	k_f (l $mole^{-1}s^{-1}$)	$10^2 k_r$ (s^{-1})	K^a (l $mole^{-1}$)	K^b (l $mole^{-1}$)
30:70	7·5 ± 1·0	1·5 ± 0·7	500 ± 250	
50:50	10·7 ± 0·5	4·6 ± 0·7	233 ± 26	268 ± 48
60:40	15·7 ± 0·8	6·4 ± 0·7	245 ± 13	155 ± 11
70:30	15·2 ± 0·8	5·8 ± 1·4	262 ± 50	246 ± 71
80:20	15·6 ± 1·0	7·8 ± 0·4	200 ± 3	219 ± 7

a. $K = k_f/k_r$

b. K from equilibrium measurements

7.3.4. Diethylmalonate.

The visible spectrum of a solution containing TNB (4×10^{-5} M), diethylmalonate (0·1 M) and sodium methoxide (0·01 M) in methanol showed two peaks, at 453nm and 540nm, the former being the more intense. The intensities of the two peaks increased with increasing diethylmalonate or methoxide concentration. The methylmalonate adduct of TNB has λ_{max} 455nm and 555nm[91], whereas the methoxide adduct has λ_{max} 425nm and 495nm[93]. Thus these spectra indicate the formation of a diethylmalonate-TNB adduct.

The diethylmalonate ion (DEM^-) is produced from the parent compound (DEM) by proton abstraction, according to the equilibrium in equation 7.4.

$$OMe^- + DEM \overset{K_a}{\rightleftharpoons} DEM^- + MeOH \qquad \text{Eq. 7.4}$$

Before any useful kinetic work could be done, the value of K_a was needed so that the concentration of DEM^- in the solutions could be calculated. Measurements of the optical density at 260nm (the absorbance maximum of the diethylmalonate ion) were made on a series of solutions containing diethylmalonate and sodium methoxide at various concentrations. The data are in table 7.12. Values for K_a were calculated assuming that conversion to anion was complete at the highest methoxide concentration used.

Variation in the value of K_a, in line with an acidity function dependence, would be expected at high methoxide concentrations. However, the variation observed here is too great, and occurs at too low concentrations, to be accounted for solely in this way. The probable cause is association between the diethylmalonate ions

Table 7.12

Optical densities at 260nm of diethylmalonate-methoxide mixtures in methanol at 25°C.

NaOMe (M)	DEM (M)	Optical density a	Optical density b	K_a ($l\ mole^{-1}$)
0·0218	$2·0 \times 10^{-3}$	0·217	0·011	0·230
0·0545	$1·0 \times 10^{-3}$	0·297	0·030	0·254
0·105	$3·8 \times 10^{-4}$	0·361	0·094	0·431
0·160	$2·0 \times 10^{-4}$	0·310	0·158	0·490
0·214	$2·0 \times 10^{-4}$	0·484	0·247	0·601
0·495	$1·0 \times 10^{-4}$	0·850	0·858	1·319
0·694	$7·9 \times 10^{-5}$	1·310	1·650	3·256
0·971	$2·9 \times 10^{-5}$	0·438	1·498	2·289
1·941	$2·9 \times 10^{-5}$	0·613	2·106	16·44
2·913	$2·9 \times 10^{-5}$	0·590	2·027	4·80
3·690	$2·9 \times 10^{-5}$	0·632	2·172	

a. As measured

b. For $[DEM]_{stoich} = 1 \times 10^{-4}$ M

and sodium ions, a chelation effect which has been shown to occur with a number of β-dicarbonyl compounds[94,95]. That this was the case here was demonstrated by the addition of solid sodium bromide to one of the solutions - this caused an increase in the optical density by a factor of two, showing the increased formation of the ion-pair.

In an attempt to remove this interaction, tetramethylammonium methoxide was used to generate the anion. However, here the formation of the anion appeared to take place at a reduced rate - with 0·1 M methoxide and 4×10^{-4} M DEM, the absorbance at 260nm took 6·5 minutes to reach a maximum value, and then decreased slowly. Accordingly, it was felt that this system would not be suitable for kinetic measurements on the TNB-malonate reaction.

A number of kinetic runs were performed using sodium methoxide to generate the diethylmalonate ion. In one series, the methoxide and diethylmalonate solutions were mixed together immediately before measurements and this solution put in one syringe with the TNB solution in the other. In the other series, one solution contained both TNB and DEM, with the methoxide solution kept separate until the solutions were mixed. In both cases only one (colour-forming) reaction was observed.

Where the methoxide and diethylmalonate were mixed before the reaction was started, the value of the observed rate coefficient, k_{obs}, increased with the length of time that the methoxide-DEM solution had been made up, until it reached a limiting value. An example is given in table 7.13. In the other case, where the methoxide was added to the other two reactants, the rate coefficient showed

Table 7.13

Variation of rate coefficient with time after mixing of methoxide[a] and diethylmalonate solutions in the reaction of this mixture with TNB[b].

Time (min)	Rate Coefficient[c] (s^{-1})
5	152
7	188
8·5	222
10	197
12	208
14	240
16	256
20	255
25	270
30	254
35	250
40	260
45	245

a. OMe^- = 0·01 M, DEM = 0·2 M, together in one syringe

b. TNB = 2×10^{-5} M.

c. Taken from only one oscilloscope trace.

no tendency to vary with time. The value obtained for the same concentrations as the above example was $128 \pm 6\ s^{-1}$, too low a value to be due to methoxide attack.

APPENDICES

APPENDIX ONE

Derivation of Rate Expressions

i. Formation of 1:1 complex

$$P + B \underset{k_{-1}}{\overset{k_1}{\rightleftharpoons}} C$$

$$\frac{d[C]}{dt} = k_1[P][B] - k_{-1}[C]$$

$$[P]_0 = [P] + [C]$$

Hence

$$\frac{d[C]}{dt} = k_1[P]_0[B] - k_1[C][B] - k_{-1}[C] \qquad (1)$$

At Equilibrium

$$\frac{d[C]}{dt} = 0 = k_1[P]_0[B] - k_{-1}[C]_e[B] - k_{-1}[C]_e \qquad (2)$$

Subtracting (2) from (1)

$$\frac{d[C]}{dt} = (k_1[B] + k_{-1})([C]_e - [C])$$

$$\text{Observed rate} = \frac{d\ OD}{dt} = k_{obs}(OD_e - OD)$$

To relate this to the change in concentration

$$OD = \varepsilon_c\ C \qquad (3)$$

At equilibrium

$$OD_e = \varepsilon_c\ C_e$$

Hence

$$OD_e - OD = \varepsilon_c([C]_e - [C])$$

Differentiating (3)

$$\frac{d\ OD}{dt} = \varepsilon_c \frac{d[C]}{dt}$$

Hence

$$\frac{d\ OD}{dt} \cdot \frac{1}{(OD_e - OD)} = \frac{d[C]}{dt} \cdot \frac{1}{([C]_e - [C])}$$

Hence

$$k_{obs} = k_1[B] + k_{-1}$$

ii. Formation of a 1:2 complex

$$C + B \underset{k_{-2}}{\overset{k_2}{\rightleftharpoons}} D$$

$$\frac{d\ D}{dt} = k_2[C][B] - k_{-2}[D]$$

For the pre-equilibrium

$$K_1 = \frac{[C]}{[P][B]}$$

Hence

$$\frac{d[D]}{dt} = k_2K_1[P][B]^2 - k_{-2}[D]$$

$$[P]_0 = [P] + [C] + [D]$$

Substituting

$$\frac{d[D]}{dt} = \frac{k_2K_1[B]^2}{1 + K_1[B]} ([P]_0 - [D]) - k_{-2}[D] \qquad (1)$$

At Equilibrium

$$\frac{d[D]}{dt} = 0 = \frac{k_2K_1[B]^2}{1 + K_1[B]} ([P]_0 - [D]_e) - k_{-2}[D]_e \qquad (2)$$

Subtracting (2) from (1)

$$\frac{d[D]}{dt} = \frac{(k_2K_1[B]^2)}{1 + K_1[B]} ([D]_e - [D]) + k_{-2} ([D]_e - [D])$$

By a similar method to that above it can be shown that

$$\frac{d\ OD}{dt} \cdot \frac{1}{(OD_e - OD)} = \frac{d[D]}{dt} \cdot \frac{1}{([D]_e - [D])}$$

Hence

$$k_{obs} = k_{-2} + \frac{k_2K_1[B]^2}{1 + K_1[B]}$$

iii. Proton abstraction by alkoxide ion following complex formation.

$$P + B^- \underset{k_{-p}}{\overset{k_p}{\rightleftharpoons}} P^- + B$$

B here is the solvent, and does not therefore appear in the rate expression.

$$\frac{d\ P}{dt} = k_p[P][B^-] - k_{-p}[P^-] \qquad (1)$$

$$[P]_0 = [P] + [C] + [P^-] \qquad (2)$$

For the pre-equilibrium

$$K_c = \frac{[C]}{[P][B^-]}$$

Substituting in (2)

$$[P]_0 = [P] + K_c[P][B^-] + [P^-]$$

and hence in (1)

$$\frac{d[P^-]}{dt} = \frac{k_p[B^-]}{1 + K_c[B^-]}([P]_0 - [P^-]) - k_{-p}[P^-] \qquad (3)$$

At equilibrium

$$0 = \frac{k_p[B^-]}{1 + K_c B^-}([P]_0 - [P^-]_e) - k_{-p}[P^-]_e \qquad (4)$$

Subtracting

$$\frac{d[P^-]}{dt} = \left(k_{-p} + \frac{k_p[B^-]}{1 + K_c[B^-]}\right)([P^-]_e - [P])$$

$$\frac{d[P^-]}{dt} \cdot \frac{1}{([P^-]_e - [P^-])} = \frac{d\ OD}{dt} \cdot \frac{1}{(OD_e - OD)}$$

Hence

$$k_{obs} = k_{-p} + \frac{k_p[B^-]}{1 + K_c[B^-]}$$

iv. Proton abstraction by amine following complex formation.

$$P + Am \underset{k_{-p}}{\overset{k_p}{\rightleftharpoons}} P^- + AmH^+$$

$$\frac{d[P^-]}{dt} = k_p[Am][P] - k_{-p}[P^-][AmH^+] \qquad (1)$$

$$[P]_0 = [P] + [C] + [P^-] \qquad (2)$$

For the pre-equilibrium

$$K_c = \frac{[C][AmH^+]}{[P][Am]^2}$$

Substituting in (2)

$$[P]_0 = [P] + K_c[P]\frac{[Am]^2}{[AmH^+]} + [P^-]$$

And hence in (1)

$$\frac{d[P^-]}{dt} = \frac{k_p[Am]([P]_0 - [P^-])}{1 + K_c\frac{[Am]^2}{[AmH^+]}} - k_{-p}[P^-][AmH^+] \qquad (3)$$

At equilibrium

$$0 = \frac{k_p[Am]([P]_0 - [P^-]_e)}{1 + K_c\frac{[Am]^2}{[AmH^+]}} - k_{-p}[P^-]_e[AmH^+] \qquad (4)$$

Subtracting

$$\frac{d[P^-]}{dt} = \left(k_{-p}[AmH^+] + \frac{k_p[Am]}{1 + K_c\frac{[Am]^2}{[AmH^+]}}\right)([P^-]_e - [P^-])$$

$$\frac{d[P^-]}{dt} \cdot \frac{1}{([P^-]_e - [P^-])} = \frac{d\ OD}{dt} \cdot \frac{1}{(OD_e - OD)}$$

Hence

$$k_{obs} = k_{-p}[AmH^+] + \frac{k_p[Am]}{1 + K_c\frac{[Am]^2}{[AmH^+]}}$$

APPENDIX TWO

a. Lectures and Seminars organised by the Department of Chemistry during the period 1978-1981.

(* denotes those attended)

15 September 1978

Professor W. Siebert (University of Marburg, West Germany), "Boron Heterocycles as Ligands in Transition Metal Chemistry".

22 September 1978

Professor T. Fehlner (University of Notre Dame, USA), "Ferraboranes : Syntheses and Photochemistry".

* 12 December 1978

Professor C.J.M. Stirling (University of Bangor) "'Parting is such sweet sorrow' - the Leaving Group in Organic Reactions".

14 February 1979

Professor B. Dunnell (University of British Columbia), "The Application of NMR to the study of Motions in Molecules".

16 February 1979

Dr. J. Tomkinson (Institute of Laue-Langevin,Grenoble), "Properties of Adsorbed Species".

14 March 1979

Dr. J.C. Walton (University of St. Andrews), "Pentadienyl Radicals".

20 March 1979

Dr. A. Reiser (Kodak Ltd.),
"Polymer Photography and Mechanism of Cross-link Formation in Solid Polymer Matrices".

25 March 1979

Dr. S. Larsson (University of Uppsala),
"Some Aspects of Photoionisation Phenomena in Inorganic Systems".

* 25 April 1979

Dr. C.R. Patrick (University of Birmingham),
"Chlorofluorocarbons and Stratospheric Ozone : An Appraisal of the Environmental Problem".

1 May 1979

Dr. G. Wyman (European Research Office, US Army),
"Excited State Chemistry in Indigoid Dyes".

* 2 May 1979

Dr. J.D. Hobson (University of Birmingham),
"Nitrogen-centred Reactive Intermediates".

8 May 1979

Professor A. Schmidpeter (Institute of Inorganic Chemistry, University of Munich),
"Five-membered Phosphorus Heterocycles Containing Dicoordinate Phosphorus".

* 9 May 1979

Dr. A.J. Kirby (University of Cambridge),
"Structure and Reactivity in Intramolecular and Enzymic Catalysis".

9 May 1979

Professor G. Maier (Lahn-Giessen),

"Tetra-tert-butyltetrahedrane".

* 10 May 1979

Professor G. Allen, F.R.S. (Science Research Council),

"Neutron Scattering Studies of Polymers".

16 May 1979

Dr. J.F. Nixon (University of Sussex),

"Spectroscopic Studies on Phosphines and their Coordination Complexes".

23 May 1979

Dr. B. Wakefield (University of Salford),

"Electron Transfer in Reactions of Metals and Organometallic Compounds with Polychloropyridine Derivatives".

13 June 1979

Dr. G. Heath (University of Edinburgh),

"Putting Electrochemistry into Mothballs - (Redox Processes of Metal Porphyrins and Phthalocyanines)".

* 14 June 1979

Professor I. Ugi (University of Munich),

"Synthetic Uses of Super Nucleophiles".

* 20 June 1979

Professor J.D. Corbett (Iowa State University, Ames, Iowa, USA),

"Zintl Ions: Synthesis and Structure of Homo-polyatomic Anions of the Post-Transition Elements".

27 June 1979

Dr. H. Fuess (University of Frankfurt),

"Study of Electron Distribution in Crystalline Solids by X-ray and Neutron Diffraction".

21 November 1979

Dr. J. Muller (University of Bergen),

"Photochemical Reactions of Ammonia".

* 28 November 1979

Dr. B. Cox (University of Stirling),

"Macrobicyclic Cryptate Complexes, Dynamics and Selectivity".

5 December 1979

Dr. G.C. Eastmond (University of Liverpool),

"Synthesis and Properties of some Multicomponent Polymers".

* 12 December 1979

Dr. C.I. Ratcliffe (University of London),

"Rotor Motions in Solids".

19 December 1979

Dr. K.E. Newman (University of Lausanne),

"High Pressure Multinuclear NMR in the Elucidation of the Mechanisms of Fast, Simple Reactions."

30 January 1980

Dr. M.J. Barrow (University of Edinburgh),

"The Structures of some Simple Inorganic Compounds of Silicon and Germanium - Pointers to Structural Trends in Group IV".

6 February 1980

Dr. J.M.E. Quirke (University of Durham),

"Degradation of Chlorophyll-a in Sediments".

23 April 1980

B. Grievson B.Sc., (University of Durham)

"Halogen Radiopharmaceuticals".

14 May 1980

Dr. R. Hutton (Waters Associates, USA),

"Recent Developments in Multi-milligram and Multi-gram Scale Preparative High Performance Liquid Chromatography".

* 21 May 1980

Dr. T.W. Bentley (University of Swansea),

"Medium and Structural Effects in Solvolytic Reactions".

10 July 1980

Professor P. des Marteau (University of Heidelburg),

"New Developments in Organonitrogen Fluorine Chemistry".

7 October 1980

Professor T. Felhner (Notre-Dame University, USA),

"Metalloboranes - Cages or Coordination Compounds ? ".

* 15 October 1980

Dr. R. Adler (University of Bristol),

"Doing Chemistry Inside Cages - Medium Ring Bicyclic Molecules".

12 November 1980

Dr. M. Gerloch (University of Cambridge),

"Magnetochemistry is about Chemistry".

* 19 November 1980

Dr. T. Gilchrist (University of Liverpool),

"Nitroso Olefins as Synthetic Intermediates".

3 December 1980

Dr. J.A. Connor (University of Manchester),

"Thermochemistry of Transition Metal Complexes".

* 18 December 1980

Dr. R. Evans (University of Brisbane, Australia),
"Some Recent Communications to the Editor of the Australian Journal of Failed Chemistry".

* 18 February 1981

Professor J.F.A. Kettle (University of East Anglia),
"Variations in the Molecular Dance at the Crystal Ball".

* 25 February 1981

Dr. K. Pounden (University of Sussex),
"The Transmission of Polar Effects of Substituents".

4 March 1981

Dr. S. Craddock (University of Edinburgh),
"Pseudo-linear Pseudohalides".

11 March 1981

Dr. J.F. Stoddart (I.C.I. Ltd./University of Sheffield),
"Stereochemical Principles in the Design and Function of Synthetic Molecular Receptors".

17 March 1981

Professor W. Jencks (Brandeis University, Massachusetts),
"When is an Intermediate not an Intermediate ? ".

18 March 1981

Dr. P.J. Smith (International Tin Research Institute),
"Organotin Compounds - A Versatile Class of Organo-metallic Compounds".

9 April 1981

Dr. W.H. Meyer (RCA /urich),
" Properties of Aligned Polyacetylene".

* 6 May 1981

Professor M. Szware, F.R.S.,

"Ions and Ion Pairs"

10 June 1981

Dr. J. Rose (I.C.I. Plastics Division),

"New Engineering Plastics".

17 June 1981

Dr. P. Moreau (University of Montpellier),

"Recent Results in Perfluoroorganometallic Chemistry".

b. Conferences attended during the period 1978-1981

i. Annual Congress of the Chemical Society and the Royal Institute of Chemistry, Durham University, April 1980.

c. First year induction course (October-November 1978)

A series of one hour presentations on the services available in the department.

i. Departmental organisation

ii. Safety matters

iii. Electrical appliances

iv. Chromatography and microanalysis

v. Library facilities

vi. Atomic absorption and inorganic analysis

vii. Mass spectrometry

viii. Nuclear magnetic resonance spectroscopy

ix. Glassblowing technique

REFERENCES

1. C.A. Lobry de Bruyn, Rec. Trav. Chim., 1890, 9, 180, 208.
2. V. Meyer, Ber., 1894, 27, 3153.
3. A. Hantzsch and H. Kissel, Ber., 1899, 32, 3137.
4. C.L. Jackson and F.H. Gazzolo, Amer. Chem. J., 1900, 23, 376.
5. J. Meisenheimer, Ann., 1902, 323, 205.
6. M.R. Crampton and V. Gold, J. Chem. Soc., 1964, 4293.
7. H. Wennerstrom and O. Wennerstrom, Acta. Chem. Scand., 1972, 26, 2883.
8. G.A. Olah and H. Mayr, J. Org. Chem., 1976, 41, 3448.
9. D.E. Klinge, H.C. van der Plas and A. van Veldhuizen, Rec. Trav. Chim., 1976, 95, 21.
10. C.A. Fyfe, M. Cocivera and S.W.H. Damji, Accounts Chem. Res., 1978, 11, 277.
11. R. Destro, C.M. Gramaccioli and M. Simonetta, Acta. Cryst., 1968, B24, 1369.
12. H.A. Benesi and J.H. Hildebrand, J. Amer. Chem. Soc., 1949, 71, 2703.
13. R. Foster and C.A. Fyfe, Tetrahedron, 1965, 21, 3363.
14. C.A. Fyfe, M.I. Foreman and R. Foster, Tetrahedron Letters, 1969, 1521.
15. C.F. Bernasconi and R.G. Bergstrom, J. Amer. Chem. Soc., 1974, 96, 2397.
16. M.R.Crampton and B. Gibson, J. Chem. Soc. Perkin Trans. 2, 1979, 648.
17. C.F. Bernasconi, J. Amer. Chem. Soc., 1971, 93, 6975.
18. K.L. Servis, J. Amer. Chem. Soc., 1967, 89, 1508.
19. M.R. Crampton, J. Chem. Soc. Perkin Trans. 2, 1977, 1442.
20. A.D.A. Al Aruri and M.R. Crampton, J. Chem. Res. 1980, (s) 140, (m) 2157.
21. M.R.Crampton, B. Gibson and F.W. Gilmore, J. Chem. Soc. Perkin Trans. 2, 1979, 91.

22. M.R. Crampton and V. Gold, J. Chem. Soc. Chem. Commun., 1965, 549.

23. M.R. Crampton and V. Gold, J. Chem. Soc. (B), 1967, 23.

24. C.F. Bernasconi, J. Phys. Chem., 1971, 75, 3636.

25. J.A. Chudek and R. Foster, J. Chem. Soc. Perkin Trans. 2, 1979, 628.

26. P. Caveng and H. Zollinger, Helv. Chim. Acta., 1967, 50, 261.

27. J.V. Janovsky and L. Erb, Ber., 1886, 19, 2155.

28. M.J. Strauss, Accounts Chem. Res., 1974, 7, 181.

29. E. Buncel, A.R. Norris and W. Proudlock, Canad. J. Chem., 1968, 46, 2759.

30. A.R. Norris, Canad. J. Chem., 1969, 47, 2895.

31. R.P. Taylor, J. Org. Chem., 1970, 35, 3578.

32. M.J. Strauss, Chemical Reviews, 1970, 70, 667.

33. M. Marendic and A.R. Norris, Canad. J. Chem., 1973, 51, 3927.

34. C.F. Bernasconi and R.G. Bergstrom, J. Amer. Chem. Soc., 1973, 95, 3603.

35. M.J. Strauss and S.P.B. Taylor, J. Amer. Chem. Soc., 1973, 95, 3813.

36. M.R. Crampton and M.J. Willison, J. Chem. Soc. Chem. Commun., 1973, 215.

37. M.R. Crampton, J. Chem. Soc. (B), 1968, 1208.

38. M.R. Crampton and M.A. El Ghariani, J. Chem. Soc. (B), 1971, 1043.

39. J. Miller, "Aromatic Nucleophilic Substitution", Elsevier, Amsterdam, 1968.

40. J.H. Fendler, E.J. Fendler and C.E. Griffin, J. Org. Chem., 1969, 34, 689.

41. J.H. Fendler, E.J. Fendler, C.E. Griffin and J.W. Larsen, J. Org. Chem., 1970, 35, 287.

42. J.F. Bunnett, Quarterly Rev., 1958, 12, 1.

43. M.R. Crampton, Adv. in Phys. Org. Chem., 1969, 7, 211.

44. C.F. Bernasconi, J. Amer. Chem. Soc., 1970, 92, 4682.

45. M.R. Crampton and H.A. Khan, J. Chem. Soc. Perkin Trans. 2, 1972, 2286, 1973, 1103.

46. J.H. Fendler, E.J. Fendler and M.V. Merritt, J. Org. Chem., 1971, 36, 2172.

47. Ryan and O'Riordan, Proc. Irish Acad., 1919, 34B, 175.

48. E.F. Caldin and G. Long, Proc. Roy. Soc., Ser. A, 1955, 226, 263.

49. E. Buncel, A.R. Norris, K.E. Russell and R. Tucker, J. Amer. Chem. Soc., 1972, 94, 1646.

50. C.F. Bernasconi, J. Org. Chem., 1971, 36, 1671.

51. C.A. Fyfe, C.D. Malkiewich, S.W.H. Damji and A.R. Norris, J. Amer. Chem. Soc., 1976, 98, 6983.

52. E. Buncel, A.R. Norris, K.E. Russell, P. Sheridan and H. Wilson, Canad. J. Chem., 1974, 52, 1750.

53. E. Buncel, A.R. Norris, K.E. Russell and H. Wilson, Canad. J. Chem., 1974, 52, 2306.

54. A.R. Norris, Canad. J. Chem., 1980, 58, 2178.

55. H. Muraour, Bull. Soc. Chim. France, 1924, 35, 367.

56. A.R. Norris, Canad. J. Chem., 1967, 45, 175.

57. L.H. Gan and A.R. Norris, Canad. J. Chem., 1974, 52, 8.

58. A. Ya Kaminskii, S.S. Gitis, L.I. Khaborova, V. Sh Golubchik and E.G. Kaminskaya, Tezisy Vses. Simp. Org. Sint. : Benzoidnye Aromat. Soedin., 1st, 1974, 12. Chem. Abs., 87 , 39042m.

59. M.J. Strauss and S.P.B. Taylor, J. Org. Chem., 1973, 38, 1330.

60. R.E. Miller and W.F.K. Wynne-Jones, J. Chem. Soc., 1959, 2375.

61. W. Waclawek and K. Poblocka, Bull. Acad. Pol. Sci., Ser. Sci. Chem., 1978, 86, 141. Chem. Abs., 89, 107681n.

62. R. Foster and T.J. Thomson, Trans. Farad. Soc., 1963, 59, 1059.

63. M.J. Strauss, S.P.B. Taylor and A. Reznick, J. Org. Chem., 1972, 37, 3076.

64. Y. Okamoto and J.Y. Wang, J. Org. Chem., 1977, 42, 1261.

65. G. Corfield, Report to PERME, Waltham Abbey, 1977.

66. P. Barth, Analysenmethoden Treib-Explosivst., Int. Jahrestag., Inst. Chem. Treib-Explosivst. Fraunhofer-Ges, 1977, 283. Chem. Abs., 89, 156958s

67. E. Buckley, J.E. Everard and C.H.J. Wells, J. Chem. Soc. Perkin Trans. 2, 1980, 132.

68. K.G. Shipp and L.A. Kaplan, J. Org. Chem., 1966, 31, 857.

69. K.G. Shipp, J. Org. Chem., 1964, 29, 2620.

70. K.G. Shipp, L.A. Kaplan and M.E. Sitzmann, J. Org. Chem., 1972, 37, 1966.

71. "Dictionary of Organic Compounds", 4th Edn., London, Eyre and Spottiswoode, 1965.

72. A. Mc Gookin, S.R. Swift and E. Tittensor, J. Soc. Chem. Ind., 1940, 59, 92.

73. M.R. Crampton, J. Chem. Soc. (B), 1967, 1341.

74. W.L. Hinze, L.J. Liu and J.H. Fendler, J. Chem. Soc. Perkin Trans. 2, 1975, 1751.

75. M.R. Crampton and H.A. Khan, J. Chem. Soc. Perkin Trans.2, 1973, 710.

76. M.R. Crampton and M.J. Willison, J. Chem. Soc. Perkin Trans. 2, 1976, 160.

77. E. Buncel, A.R. Norris, K.E. Russell and P.J. Sheridan, Canad. J. Chem., 1974, 52, 25.

78. D.N. Brooke and M.R. Crampton, J. Chem. Res., 1980, (s) 340, (m) 4401.

79. J. Barthel, R. Wachter and M. Knerr, Electrochim. Acta., 1971, 16, 273.

80. A.P. Chatrousse, F. Terrier, F.M. Fouad and P.G. Farrell, J. Chem. Soc. Perkin Trans. 2, 1979, 1243.

81. C.F. Bernasconi and R.G. Bergstrom, J. Org. Chem., 1971, 36, 1325.

82. M.R. Crampton and B. Gibson, J. Chem. Soc. Perkin Trans. 2, 1981, 523.

83. M.R. Crampton, B. Gibson, and R.S. Mathews, Org. Mag. Res., 1980, 13, 455.

84. D.D. Perrin, "Dissociation Constants of Organic Bases In Aqueous Solution", I.U.P.A.C., Supplemement, 1972

85. A. Mucci, R. Domain, and R.L. Benoit, Canad. J. Chem., 1980, 58, 953.

86. F. Cuta and E. Beranek, Coll. Czech. Chem. Commun., 1968, 23, 1501.

87. E. Buncel and J.G.K. Webb, J. Amer. Chem. Soc., 1973, 95, 8470.

88. E. Buncel, A. Jonczyk and J.G.K. Webb, Canad. J. Chem., 1975, 53, 3761.

89. C.F. Bernasconi and M.C. Muller, J. Amer. Chem. Soc., 1978, 100, 5530.

90. A.R. Norris, J. Org. Chem., 1969, 34, 1486.

91. I. Kolb, V. Machacek and V. Sterba, Coll. Czech. Chem. Commun., 1976, 41, 590.

92. E. Buncel, A.R. Norris, W. Proudlock and K.E. Russell, Canad. J. Chem., 1969, 47, 4129.

93. V. Gold and C.H. Rochester, J. Chem. Soc., 1964, 1692.

94. D. Midgley, Chem. Soc. Reviews, 1975, 4, No. 4.

95. J. Kavalek, V. Machacek, A. Lycka and V. Sterba, Coll. Czech. Chem. Commun., 1976, 41, 590.